A Simplified Method for Estimating the Load-Shortening Behavior of Damaged Tubular Columns

by

Joseph A. Padula

Presented to the Graduate Committee

of Lehigh University

in Candidacy for the Degree of

Doctor of Philosophy

in

Civil Engineering

Lehigh University

May 1999

Approved and recommended for acceptance as a dissertation in partial fulfillment of the requirements for the degree of Doctor of Philosophy.

April 15, 1999
Date

Dr. Alexis Ostapenko
Dissertation Advisor

April 15, 1999
Accepted Date

Special Committee directing the doctoral work of Mr. Joseph A. Padula

Dr. Celal N. Kostem
Committee Chairman

Dr. George C. Driscoll

Dr. Arturs Kalnins

Dr. Ben T. Yen

Dr. Arup SenGupta
Chairman, Department of Civil Engineering

Acknowledgments

The author extends his sincerest gratitude to Dr. Alexis Ostapenko for his support during the course of this work. His untiring efforts in guiding and teaching the student are deeply appreciated. Sincere thanks are also extended to each member of the committee directing the doctoral work, Drs. Celal N. Kostem, Committee Chair, George C. Driscoll, Arturs Kalnins and Ben T. Yen. The support of Dr. N. Radhakrishnan, Director, Information Technology Laboratory, U.S. Army Engineer Waterways Experiment Station, in encouraging the completion of this work while the author was employed at the Waterways Experiment Station is acknowledged and greatly appreciated.

Finally, the author is thankful to all of those who provided support on a personal level over many years. These include, above all, his dear aunt, Ms. Edith Hunnisett and the memory of his mother Mrs. Helen A. Padula.

Table of Contents

List of Tables

List of Figures

Abstract

A simple "engineering" method was formulated for computing the axial load vs. axial shortening relationship of pin-ended tubular members damaged by a dent and/or out-of-straightness. The method predicts the pre- and post-ultimate load-shortening response, and can be used in analyzing the strength and behavior of offshore platform frames containing damaged members. The method was developed from a parametric study and regression analysis of a database containing load-shortening data from published tests results on damaged columns and data generated from a finite element analysis.

The effects of geometric nonlinearity and elasto-plastic material properties were included in the finite element analysis of the pre- and post-ultimate response of damaged tubular columns. Prior to generating data for the parametric study and regression analysis, the finite element model was verified by comparing calculated (finite element) load-shortening responses with experimental data.

The regression model used as a basis for the simplified engineering method, was developed by considering the geometry of the load vs. axial shortening curves for a wide range of column geometries and yield strengths. A parametric study was

conducted to determine the influence of each independent variable on the axial behavior of damaged members. The object of the study was to select the shortest suitable approximating function for each independent variable. The variables considered were: column slenderness, D/t ratio, dent-depth to diameter ratio, out-of-straightness, yield stress, and axial shortening. The regression analysis of the load-shortening relationships in the database resulted in a set of 80 constants which is reduced to a five-term approximating function for the load-shortening response, once specific values are given for the member geometry, material and damage. The procedure is illustrated with an example and comparisons with test results. Implementation of the method only requires computational resources for matrix multiplication and basic function evaluation typically within the capability of a handheld calculator. The method is valid for member geometries and material properties typically found in fixed offshore platforms.

1 Introduction

The design of offshore structures must include considerations of strength, stability, and serviceability while providing for safe and reliable resistance to applied loads over the life of the structure. From monitoring and inspection of in-service platforms, it has become increasingly apparent that these basic requirements must be met for the structure in a deteriorated or damaged condition. The circular tubular members that typically are used for framing of steel offshore structures are susceptible to damage from accidental impact with supply vessels or falling objects. Overload of a structure can also result in damage in the form of member out-of-straightness or local buckling. Consequently, these structures must be designed with some degree of damage tolerance. "Damage-tolerance may especially be crucial for deep-water fixed platforms, where inspection and maintenance of the deeply submerged parts of the structure may be difficult, if not impossible."[1] Minimum requirements for damage tolerance are derived from consideration of the consequences of structural failure: loss of human life, of the structure, and/or environmental pollution. These dictate that operational and environmental loads must not result in collapse or progressive failure of the structure, particularly as a result of slight or undetected damage. Furthermore,

the economy of operation/maintenance of a platform requires that a structure should have the capacity to withstand some minimal damage without the need for costly repairs.

Although some degree of damage tolerance is implicit in any redundant structure, quantification of the residual strength of a damaged member(s) and of the whole structure is needed for a rational approach to efficient, cost-effective design and maintenance. Consequently, the research described herein was directed at the assessment of the effect of accidental damage on member behavior. It is applicable for the analysis of a hypothetical case of damage that is anticipated in the design process or a real consequence of an accidental overload or impact on an actual platform in-service.

1.1 Problem Definition

The scope of this research was to develop a simplified engineering method for estimating the axial load vs. axial shortening of an accidentally damaged round tubular steel column. For the purpose of this report, accidental damage is defined as dents and/or out-of-straightness. Cumulative fatigue damage, tearing or fracture of members are not considered. Common causes of accidental damage are impacts from supply or work boats servicing the platform or from dropped or mishandled crane loads. Overloads from severe storms or operational loads may also cause accidental damage. The problem is schematically illustrated in Fig. 1.1.

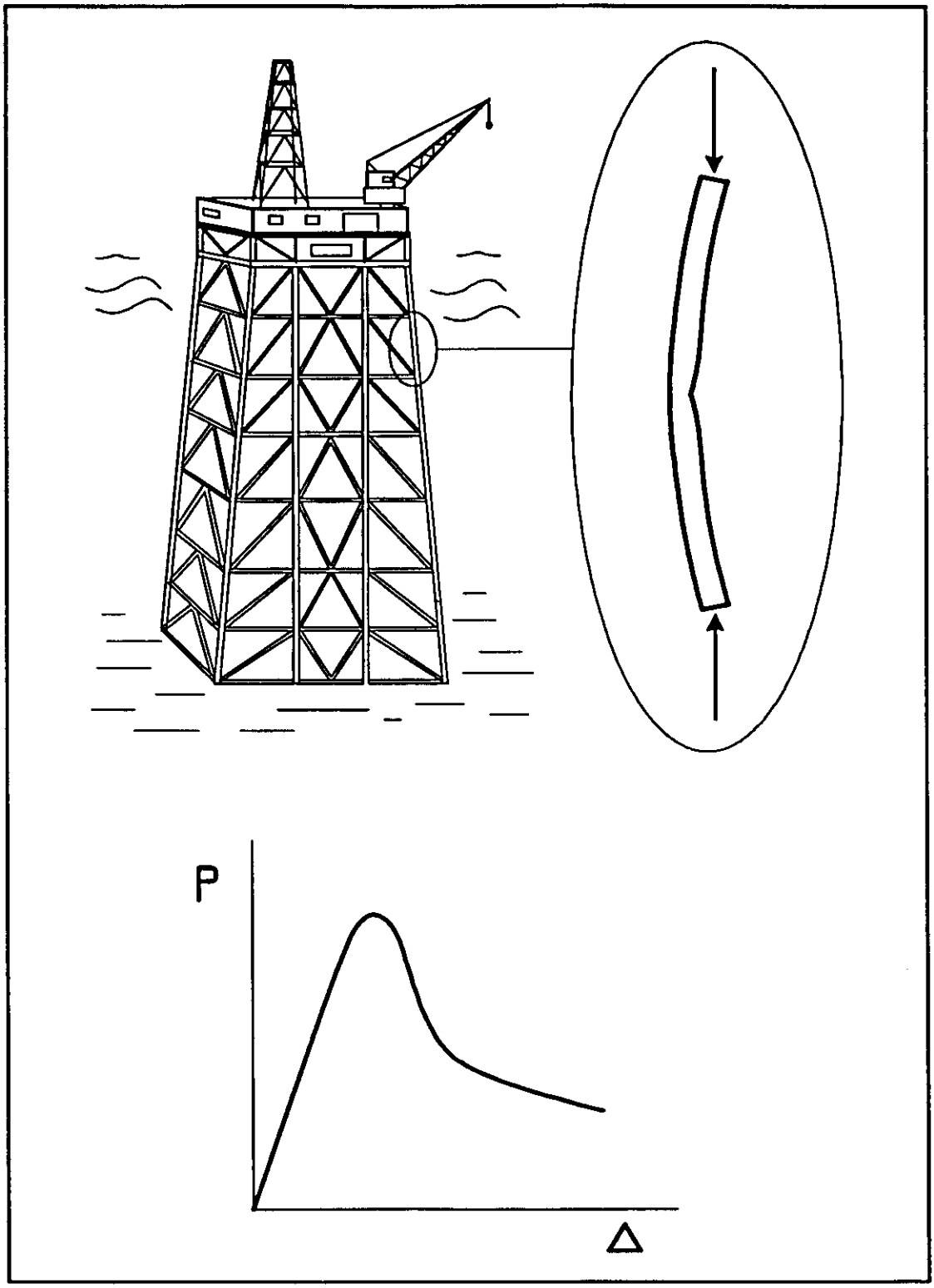

Figure 1.1. Schematic illustration of damaged tubular column behavior

Typically the effect of dents and/or out-of-straightness of a tubular column results in a reduction of the stiffness and/or capacity of the member which may significantly affect the strength and/or serviceability of the structure. The behavior and residual strength of the structure is dependent on the pre- and post-ultimate behavior of the damaged member since it is possible that service loads will lead to non-linear response of the damaged member as illustrated in the hypothetical load-shortening plot in Fig. 1.1. When the damaged member response is non-linear, the reduction of stiffness and non-linear behavior will result in a redistribution of forces in the structure. Consequently, the response of the damaged member must be known or estimated in order to assess the effect of damage on the structure.

In general, prediction of the pre- and post-ultimate load-shortening response of a damaged tubular column requires an analysis of the member that includes the effects of large deformations and material nonlinearity. This includes considering the tube wall as a shell, as opposed to a beam-column analysis. While it is possible to predict, with reasonable accuracy, the response of a damaged member by a finite element analysis using shell elements and including material non-linearity and large deformations, such an analysis is impractical in terms of cost, computer resources needed, and, perhaps most importantly, the time required to formulate a reliable model. Furthermore, analysis of an entire platform or even a sub-frame containing a damaged member with such a model would be even more impractical. Even if a non-linear finite element analysis could be performed efficiently, the results should, in some fashion, be

independently verified. Consequently, there is a need for a simplified yet reasonably accurate "engineering method" for predicting the behavior of damaged members.

1.2 Previous Research

Since 1979, there has been much research devoted to developing approximate methods for estimating the ultimate load and load-shortening response of damaged tubular columns. Some of the major efforts are listed here.

In one of the first reported efforts to quantify the effects of damage in tubular members, Smith conducted a parametric study of data from finite element analyses of initially crooked tubular columns and experiments on small-scale specimens to develop a simplified analysis procedure.[2] This procedure was based on a beam-column analysis and good correlation was obtained for columns with out-of-straightness damage. In a later attempt to include the effect of dent damage, it was suggested that the effect of dents may be included in the analysis, not by modeling the geometry of the dent, but by retaining the circular cross section of the member and modifying the stress-strain relationship for the material in the dent-affected area.[3] A reduction or "knock-down" factor applied to the modulus of elasticity and yield stress was suggested based on empirical data from small-scale tests. The same reduction factor was determined from a least squares fit to experimental data of a four term function which was linear in diameter-to-thickness ratio, relative dent-depth and the inverse of the yield strain.

In a series of papers, Taby presented an analytical method which estimates the load-deformation response of dented and/or initially crooked, simply supported columns.[4,5,6,7,8] This approach is based on a simplified physical model of the dent in a damaged column. The equilibrium formulated on the simplified dent geometry and an amplification factor based on Euler buckling loads for the lateral displacement of the column are used for calculation of the column response up to first yield. Empirical data from 109 small-scale tests were used to determine correction factors for the effect of geometric assumptions on which the model is based, the effects of local buckling at high diameter-to-thickness ratios and plastification at the dent. After first yield, the lateral deflection of the column is incremented until the ultimate load is reached. In the post-ultimate range, the response is calculated based on a plastic hinge analysis. Effects of local buckling and ovalisation (a flattening of the originally circular cross section resulting from axial stress) are incorporated with parameters derived from regression analysis of experimental data from small-scale tests. The computer program DENTA, developed by Taby, is based on this method and provides the load-shortening response of pin-ended tubular columns with dents and/or out-of-straightness.[9] The program DENTA II incorporates the ability to analyze fixed-ended and elastically restrained columns and lateral loading.[10]

An analysis procedure for damaged tubulars that could be readily incorporated into a finite element program for analyzing frames was proposed by van Aanhold and Taby.[11] The undamaged portions of the member are modeled with beam-column

elements. The dented portion of the member is also modeled with a beam-column element, but with a reduced diameter and thickness and is connected to the adjacent elements (modeling the undamaged portion of the tube) with some eccentricty. The reduced equivalent diameter and thickness and the element eccentricity for modeling the damaged section of the tube are determined from an analysis based on the simplified model of a dent suggested by Taby (See, for example, Refs. 5,6,8.). The principal advantage of this method is that it can be readily incorporated into a non-linear frame analysis using existing finite element programs.

Ellinas quantified the effect of dent-damage with a lower bound prediction of the ultimate strength of a damaged tubular based on a simplified beam-column model.[12] The effect of dent damage was modeled by assuming that once plastification resulting from bending at the dent occurs, the axial load is carried primarily by the undamaged portion of the circumference. Overall bending damage was considered by the use of an amplification factor. The ultimate load is then calculated based on a first yield criterion resulting in a lower bound estimate for ultimate strength.

In their experimental work Taby and Smith carried out a number of tests on damaged (dented and crooked) small-scale specimens made from drawn tubing or cold-rolled plate.[2,3,4,7,8] From the tests of two large-scale members removed from an offshore platform retired from service and of two comparable small-scale specimens, Smith concluded that small-scale tests were adequate to predict the behavior of full-size damaged members.[13] However, the results of these tests

showed that the small-scale specimens underestimated the ultimate strength by as much as 15% and the post-ultimate strength by as much as 30%. Smith attributed the discrepancy in the post-ultimate range to the effect of different load vs. displacement control in the tests for the large- and small-scale specimens.

Another method for estimating the load-shortening response for damaged columns was presented by Richards and Andronicou.[14] The basic method is an iterative numerical integration procedure in which the column is subdivided into a number of elements along its length. The initial slope of an end element and axial load are assumed and the moment-thrust-curvature relationship for each element is used to determine the displacements along the length. This is a displacement control procedure in that the applied axial load is varied during the iterations until the numerical integration results in displacements that satisfy the boundary conditions. The moment-thrust-curvature-axial strain relationship for the dented section of the tube is derived from the assumption of linear variation of axial strain across the cross-section, elastic perfectly plastic material behavior, and a reduction of the modulus of elasticity and yield strength for the material at the dent. These reductions in material stiffness and strength are the same as proposed by Smith.[3] The method includes the ability to analyze columns with dents anywhere along its length and accommodate various column boundary conditions.

In a more recent effort, Kim developed a method for predicting the load-shortening behavior (including post-ultimate response) of accidentally damaged tubular columns

based on a numerical integration procedure.[15] This numerical integration procedure is similar to that used by Richards and Andronicou[14] and can incorporate the effect of column end restraint. The column is divided into a number of elements along its length and the moment-thrust-curvature relationship for each segment is used in the integration to determine the displacements along the length of the column. This is an iterative procedure where the axial load of the member is varied for each iteration until the displacement boundary conditions are satisfied. The moment-thrust-curvature-axial strain relationship for the dented segment was determined from a regression analysis of data generated by finite element analysis of dented tube segments. The finite element analysis included the effects of large deformations and elastic-plastic material behavior. Kim also developed a regression model for estimating the ultimate strength of a damaged tubular column based on data generated from his method for predicting the load-shortening response.[15]

A number of tests on damaged tubular columns were conducted by Ricles, et al, to investigate the effectiveness of a repair scheme.[16, 17] Column load-shortening behavior was provided for both unrepaired and grout-repaired near-full-scale test specimens.

As with any simplified approximate method, each of the approaches discussed above incorporates certain assumptions or ignores complexities that affect the behavior of the column. For example, Ellinas' method for predicting ultimate strength[12] tends to be fairly conservative as a lower bound because of the assumption that the dented

portion of the tube wall is ineffective due to the bending stress in the tube wall causing yielding at fairly low levels of axial load.

The method proposed by van Aanhold and Taby[11] is based on modeling the behavior of the dented segment of the column with an equivalent undamaged beam-column element with reduced section properties. Obviously this approach will not be able to capture the effects of increased deformation of the cross section, particularly amplification or growth of the dent under axial load, which can significantly affect the post-ultimate response of the column.[8] The same criticism would apply to the numerical integration procedure used by Richards and Andronicou[14] since the moment-thrust-curvature-axial strain relationship for the dented segment is based on a cross section with constant geometry.

Smith's model also neglects the effect of additional distortion of the cross section, and the proposed reduction in modulus of elasticity and yield stress is based on a limited number of tests on small scale tubes.

Taby's method (DENTA and DENTA2) includes the effect of cross-sectional distortion and estimates the load-shortening response in the pre- and post-ultimate ranges. However, these are based on a simplified beam-column model that was tuned to experimental results from small-scale tests on manufactured tubes.

Kim's method also takes into account the deformation of the cross section under axial load since the axial load-moment-curvature-axial shortening relationships for the

dented segment are based on results from finite element analyses which included large deformations.

Of all the proposed methods, only Taby's and Kim's take into account the growth of the dent under axial load. None of the methods addresses the effects of residual stresses from cold rolling and welding. However, the behavior of an accidentally damaged column is likely to be dominated by the effects of the dent and out-of-straightness.

1.3 Objective and Methodology

The objective of this research was to produce a relatively simple yet reasonably accurate engineering method for predicting axial load as a function of axial shortening of damaged, pin-ended, tubular steel columns in the pre- and post-ultimate ranges. The procedure outlined here is straightforward to implement and requires no special computational software other than the ability to perform matrix multiplications and computation of some simple functions.

The simplified method presented here is based on a regression model formulated from a parametric study of column load-shortening data. This approach has been used successfully in the past to predict the pre- and post-ultimate response to in-plane loading of plates and stiffened plates, the load-indentation response of circular tubes, and the axial load-moment-rotation relationship for a damaged tubular column segment.[15, 18, 19, 20]

The development of the proposed simplified method consisted of two major tasks; the development of a database including experimental and analytical (finite element) load-shortening data, and the development of a regression model. The application of the resulting engineering method is demonstrated in an example. The accuracy of the method is illustrated by comparison of the load-shortening relationships generated by the method and test data.

The basic approach to the problem consisted of the following steps:

1. Collection and generation of experimental and analytical data on the load-shortening behavior of damaged columns.
    a. Literature search and collection of published experimental data.
    b. Finite element analysis to generate additional data.
        i. Development of a model and verification with experimental results.
        ii. Generation of analytical data.
2. Development of a model for the simplified method.
    a. Parametric study of the data and selection of suitable approximation functions for the regression model.
    b. Regression analysis and refinement of the model (an iterative procedure).

Details of these tasks are described in the following chapters.

2 Database of Column Behavior

The development of the simplified method for predicting the load-shortening response of damaged tubular columns was based on a regression model of analytical and experimental load-shortening relationships. Experimental data collected from available literature and analytical data generated from finite element analyses were incorporated into a database. (The finite element analysis is described in Chapter 3.)

2.1 Database Management and Structure

In order to develop the regression model a database of load-shortening data was required. The SAS[1] software system was used because it provided a relational database with capabilities for graphical representation of data. SAS also includes extensive statistical analysis capabilities which were used for the regression analysis. Initially, the SAS software was used on a Digital Equipment Corporation VAX 8530. Later in the course of the work, the database was moved to a personal computer based version of SAS.

[1]SAS Institute, Cary, N.C.

For each experiment or finite element analysis, the database included the basic data on column geometry (diameter, thickness, length, dent-depth, initial out-of-straightness), material yield stress, and pairs of load vs. shortening coordinates. For the experimental data, the database also contained information on the location and shape of the dent when it was available. The database was separated into two datasets (separate files containing different data), one containing the column geometry and material data and the other with the load vs. shortening data. The two files were related through a tag or name assigned to each column and contained in both datasets.

The load-shortening responses of 130 columns comprised of 3077 pairs of axial load and axial shortening coordinates were included in the database. Thirty-seven of the column responses were from published experimental data and 93 were from finite element analyses. An average of 31 and 21 points per curve defined the column response for the experimental and analytical data, respectively.

2.2 Included Data

Published experimental load-shortening relationships were available from the empirical work done in this area by other researchers. Data was taken from Smith [2,13,3], Taby [5,6,7,8] and Ostapenko[30]. Although, in Taby's research, over 100 tubes had been tested with a variety of end conditions, only a representative sampling of load-shortening curves was published, all of which (pin-ended tests) were included in the database.

Analytical data generated by finite element analysis (See Ch. 3) were also incorporated into the database to expand it over a broader range of column geometry and damage. The number of load-shortening curves included in the database from each source and the range of geometrical parameters, yield strength and damage are shown in Table 2.1.

Table 2.1 Source and description of columns included in database

Source	Quantity	λ	D/t	d/D	δ/l ($\times 10^3$)	σ_y (MPa)
Ref. [2]	8	0.66-1.06	29-86	0-8%	0.0-5.5	198-477
Ref. [13]	4	0.67-0.84	30-41	0-13%	3.2-5.0	274-293
Ref. [3]	12	0.45-1.10	26-46	9-18%	0.5-3.7	334-479
Ref. [5]	3	0.62-0.82	41-60	2-10%	0.7-1.8	204-465
Ref. [6]	1	0.66	78	5%	0.7	383
Ref. [7]	1	0.65	91	14%	2.4	295
Ref. [8]	2	0.65-0.72	88-99	8-12%	0.8-0.9	295-312
Ref. [30]	6	0.68-1.1	29-95	5-16%	0.0-2.6	303-409
F.E. Analysis	93	0.4-1.2	20-100	5-30%	0.0-20	250-500

Data on each of the 130 columns included in the database is given in Appendix A.

3 Finite Element Analysis

In order to effectively study the behavior of damaged tubular columns, additional data were needed to supplement the limited number of published experimental load-shortening curves. Due to the complexity of the behavior of a damaged tubular member and the need to generate data on the pre- and post-ultimate response including large deformations and material nonlinearity, a finite element analysis was used. The finite element software ADINA[1] was selected because of its capabilities for nonlinear analysis and automatic load incrementation and its availability. The analyses were performed on a Control Data Corporation Cyber 850 Model 180 running the NOS/VE operating system.

3.1 Damaged Column Model

The basic concepts employed in the finite element modeling of a damaged tubular column are illustrated in Fig. 3.1. A damaged tubular member with initial crookedness

[1]ADINA R & D Inc., Watertown, MA

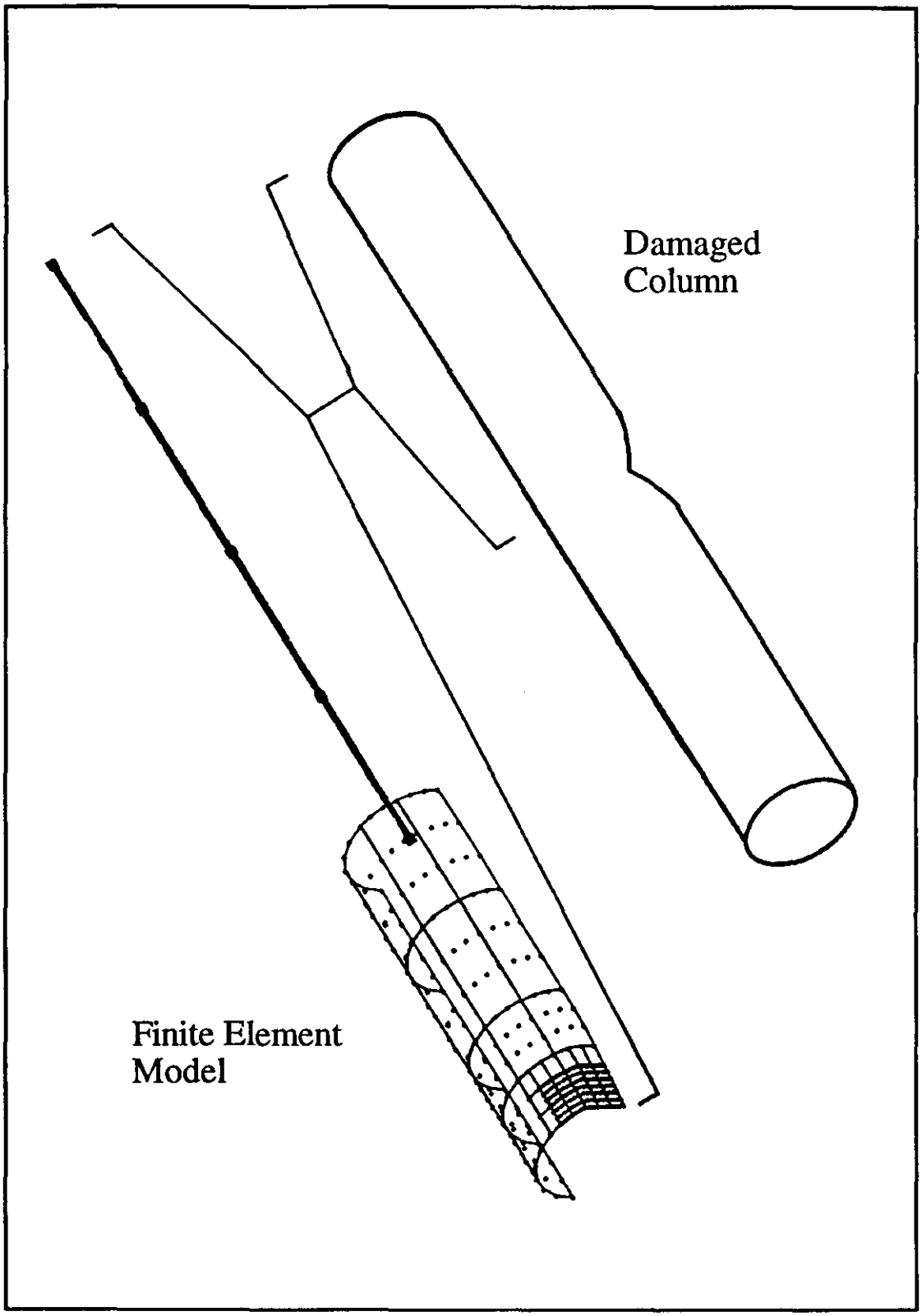

Figure 3.1 Basic concept of finite element model

and a dent at mid-length has two planes of symmetry, one longitudinal and one at the dent perpendicular to the longitudinal axis, assuming that the dented cross section is symmetrical about the longitudinal plane of symmetry. This is a reasonable assumption if the dent and out-of-straightness were caused by the same accident. (The idealized dent geometry and out-of-straightness used in the model are discussed in the following section.) Due to the double symmetry of the problem, it was necessary to model only one-quarter of the tube as indicated in Fig. 3.1. In addition to the symmetry of the problem, further simplifying assumptions were made based on the behavior of the column. For pin-ended boundary conditions, a portion of the column some distance away from the dent behaves as an elastic beam-column with no distortion of the cross section. The region near the dent is subjected to bending of the tube wall leading to distortion of the cross section and plastic deformations. These considerations are reflected in the model where the region near and including the dent is modeled with shell elements while the remainder of the column with beam-column (line) elements.

The length of the portion of the column modeled with shell elements was taken to be one-half the length of the dent, l_d, as determined from Eq. 3.4 plus twice the column diameter. Considering the well known solution for axisymmetric edge loading of a cylindrical shell,[21] the effect of an applied axisymmetric edge moment, the exponential decay of the loading effect for a steel cylinder (Poisson's ratio, $\nu = 0.3$) at a distance of two diameters from the edge is given by

$$e^{-\sqrt[4]{3(1-\nu^2)}\frac{x}{\sqrt{\frac{D}{2}t}}} = e^{-1.29\frac{1}{\sqrt{\frac{t}{8D}}}} = 8.2 \cdot (10)^{-8} \qquad (3.1)$$

where ν is Poisson's ratio, x is the longitudinal distance from the edge, and D and t are the diameter and thickness of the cylinder. For a cylinder with a diameter to thickness ratio (D/t) of 20 (the smallest considered in this study and most critical in this consideration), the edge loading effect is reduced by 7 orders of magnitude at a distance of 2 diameters. Although the bending of the tube wall at the dent in a tubular column is not axisymmetric and is not elastic, this provides some indication that the segment length of two diameters beyond the dented region should be sufficient to model the effects of deformation of the cross section.

An elastic-plastic material model was used for the shell elements and a linear elastic model was used for the beam-column elements. The elastic-plastic model was based on the von Mises yield criterion. A large displacement (geometrically nonlinear) formulation was used for all elements. A rectangular cross section was used for the beam elements with the area and moment of inertia equal to those of the undamaged (circular) cross section.

3.2 Idealized Dent Geometry

In the development of the finite element model, certain assumptions were made about the location and geometry of the dent damage and the initial out-of-straightness. The assumption of transverse and longitudinal planes of symmetry dictates that the

dent is located at midlength, the out-of-straightness is symmetric about the midlength of the column and the dented cross section is symmetric about the longitudinal plane of symmetry. In addition, the idealized geometry used in the model contained assumptions pertaining to the shape of the dent and out-of-straightness. These assumptions permitted description of the damage in terms of only two parameters: dent depth d, and the magnitude of the initial out-of-straightness δ.

Although dent damage and initial crookedness may occur with arbitrary geometries in damaged columns, the longitudinal location of the dent and variations in the shape of the dent and out-of-straightness have been found by other researchers to have little effect on the behavior. For example, Smith concluded that "Comparison of test results ... indicates radical variations in the position of a dent and associated bending damage do not substantially change the damage effect"[3], and "Test results also support previous theoretical findings that loss of strength is insensitive to the shape and location of dents and to the shape of bending deformation."[3] Further verification comes from Taby, who concluded "The sensitivity to dent shape and location is, however, insignificant ...".[6] Consequently, a single damage model based on an assumed dent geometry and location and shape of initial crookedness was used in the analysis.

As shown in Fig. 3.2, the longitudinal axis defining the initial crookedness of the damaged member was assumed to be of sinusoidal shape. With the origin at midlength, the initial crookedness is given by

$$z = \delta \cos \frac{\pi}{L} x \tag{3.2}$$

where, as shown in Fig. 3.2, x is the longitudinal distance from mid-length of the column, δ is the magnitude of maximum initial lateral out-of-straightness (occurs at midlength), and z is the lateral deflection of the longitudinal axis of the tube. Thus, the initial crookedness is defined by a single parameter, δ.

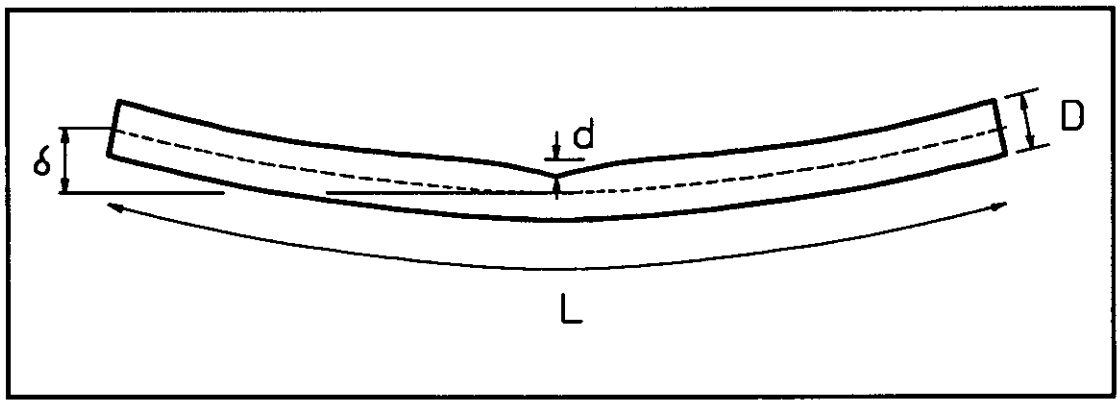

Figure 3.2. Damaged column geometry

The dent was assumed to be a sharp "vee" as if produced by a "knife-edge" loading perpendicular to the longitudinal axis. The geometry of the dent was defined in terms of the dent depth, d, as shown in Fig. 3.3. The longitudinal profile of the dent is defined by ζ, the deviation of the top fiber in the longitudinal plane of symmetry (see Fig. 3.3) from the sinusoidal shape given by Eq. 3.2.

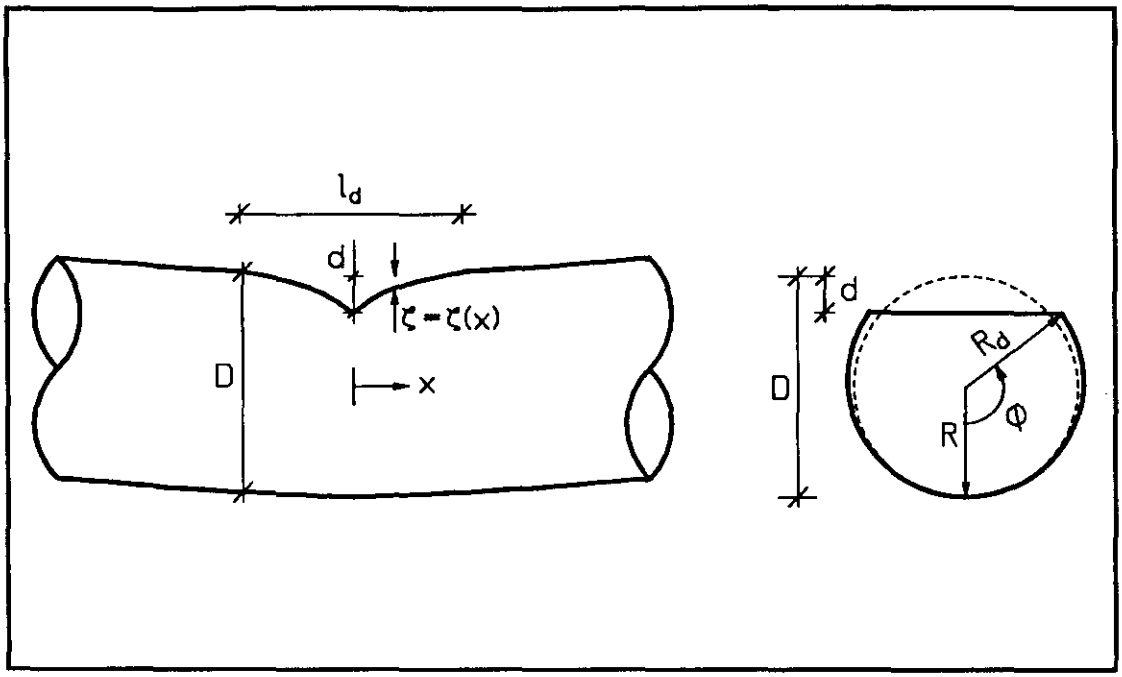

Figure 3.3. Dent geometry

The bottom fiber (opposite the dent) is assumed to be parallel to the sinusoid defined by Eq. 3.2. The dent profile, ζ, as a function of the distance x from the center of the dent at the midlength of the column ($\zeta = \zeta(x)$) is given by

$$\zeta = d\left(1 - \frac{2x}{l_d}\right)^2 \qquad 0 < x < \frac{l_d}{2} \tag{3.3}$$

and the length of the dent, l_d, is given by

$$l_d = D\sqrt{\frac{\pi d}{4t}} \tag{3.4}$$

where D is the diameter (measured to mid thickness of the tube wall), d is the dent depth, and t is the tube wall thickness.

The expressions for ζ and l_d were taken from an analytically derived relationship for a tube supported along its length with no end restraint and subjected to a "knife-edge" lateral loading.[22] The expression for l_d (Eq. 3.4) is in good agreement with dent profiles published by Smith.[3]

The cross-sectional geometry of the dent is based on empirical observations and is composed of a flattened and a curved segment. As shown in Fig. 3.3, the curved segment is defined by the radius which varies linearly as a function of the angle ϕ. The radius increases from R (the radius to midthickness of the undamaged tube) to R_d at the intersection of the curved and flattened segments. R_d is determined from the requirement that the circumferential length of the dented and circular cross sections must be equal.

$$\pi R = \frac{R + R_d}{2} + R_d \sin\phi \tag{3.5}$$

Or,

$$\pi R = \frac{R + R_d}{2} \cos^{-1}\left(\frac{d - R}{R_d}\right) + \sqrt{R_d^2 - (R - d)^2} \qquad (3.6)$$

which gives R_d, although not explicitly, in terms of R and d. The discontinuous slope at the intersection of the flattened and curved segments, as shown in Fig. 3.3, corresponds to the plastic hinge formed during indentation.

3.3 Finite Element Discretization

Prior to using the finite element model (Fig. 3.1) to generate data, the accuracy of the model was verified by analyzing test specimens for which published experimental data were available and comparing the calculated and empirical responses. In the course of this process three different models were developed. The models differed primarily in the pattern of discretization and the type and number of shell elements used in modeling the portion of the column near the dent. The finite element model ultimately used to generate load-shortening data included in the database was the last of the three models developed.

The first model, Model 1, was found to be inadequate for predicting the response of columns with diameter to thickness (D/t) ratios greater than 60 and had limited flexibility for modeling different magnitudes of dent depth. Model 2 (the second in the series) was much more accurate but was extremely costly in terms of CPU time.

Model 3 exhibited good correlation with experimental data and was much more economical than Model 2 and therefore was selected for generating data included in the database.

The discretization of the portion of the tube modeled with shell elements for Model 1 is shown in Fig. 3.4. Eighteen 16-node quadrilateral and four 9-node triangular isoparametric shell elements were used. Reasonable results were obtained with this model when compared to experimental data for tubes with a D/t ratio less than 60.

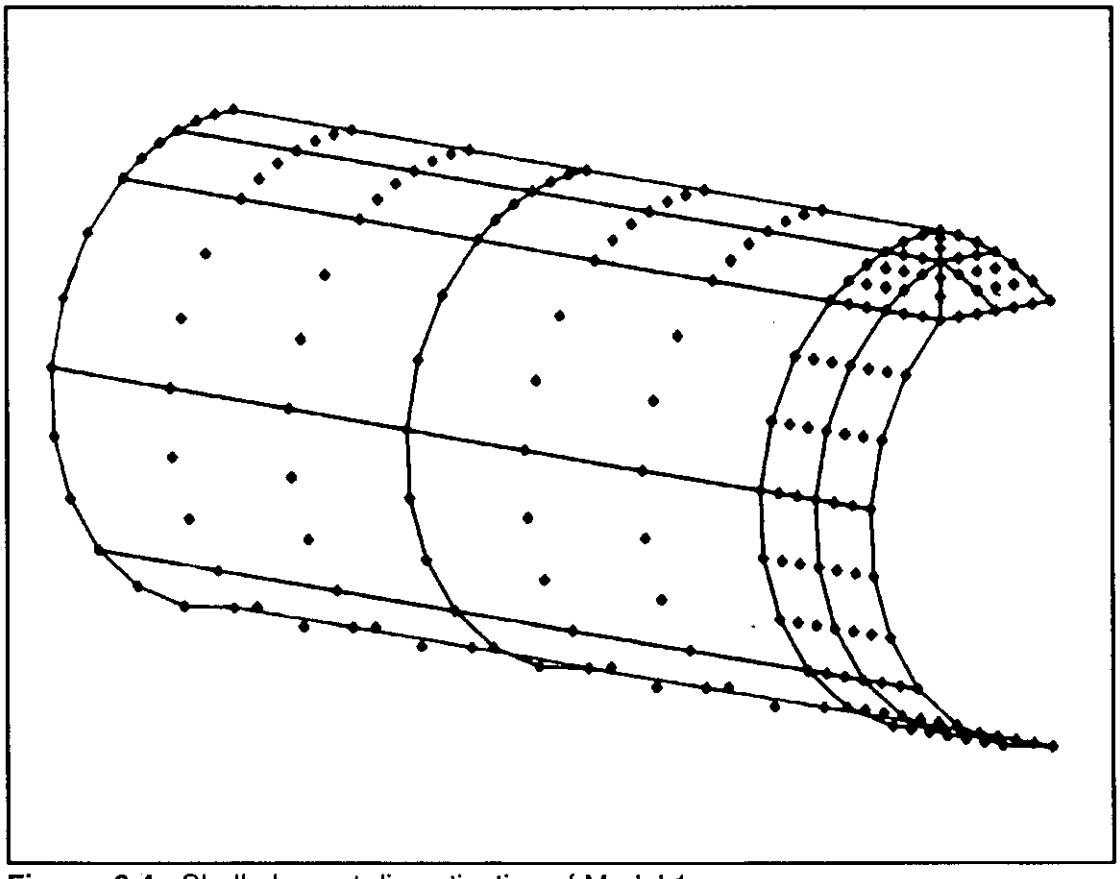

Figure 3.4. Shell element discretization of Model 1

For D/t greater than 60, the model significantly overestimated the strength with the difference between the calculated and empirical responses increasing approximately linearly with the D/t ratio. This was due to the inability of the model to simulate the growth of the dent that coincides with attainment of the ultimate load for tubes with larger D/t ratios. The relatively coarse mesh overestimated the flexural stiffness of the tube wall and could not capture the complex deformation at the dent resulting in overestimation of the ultimate and post-ultimate strength for columns with larger D/t ratio.

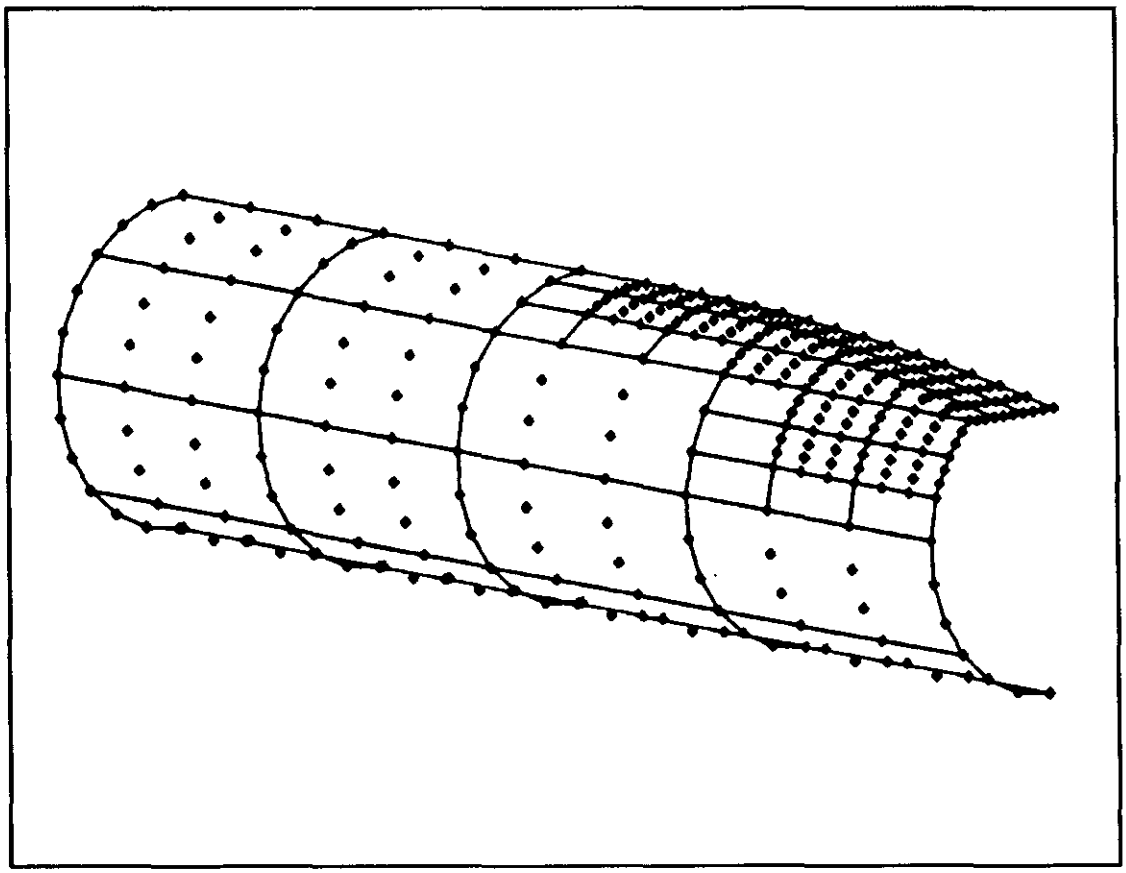

Figure 3.5. Shell element discretization of Model 2

In order to improve the predictions of Model 1, a finer discretization of the dented area was used for Model 2, and 16-node elements were incorporated as shown in Fig. 3.5. Model 2 resulted in much improved agreement with experimental data for columns with larger D/t. However, the model was extremely expensive in terms of CPU time. This led to the development of Model 3.

The discretization of Model 3 is shown in Fig. 3.6 and it resulted in a much more economical computer usage than Model 2 while producing reasonable agreement with experimental data. Consequently, Model 3 was selected for generating data for the database.

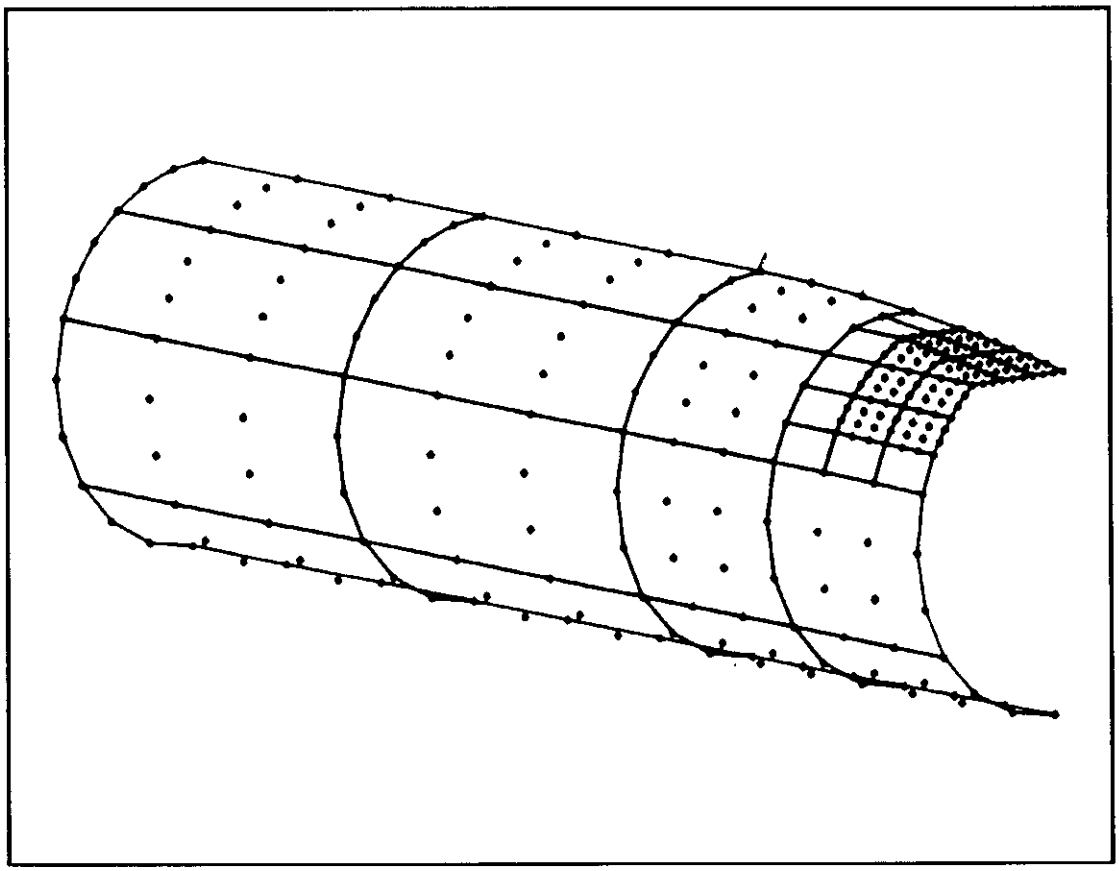

Figure 3.6. Shell element discretization of Model 3

Model 3 is composed of 32 shell elements, 4 beam elements, 268 nodes, and has 1162 degrees of freedom. The shell elements were either 16-node elements or a variation of these with 4 or 6 nodes needed for transition from the finer mesh at the dent to a coarser mesh outside the dent.

The appropriate boundary conditions were imposed on the nodes at the edges of the shell elements lying in the two planes of symmetry. Nodes lying in a plane of symmetry are allowed to displace and rotate only within the plane. All other degrees of freedom for nodes in the planes of symmetry are inhibited. In the cross-sectional plane at the interface of the beam and shell elements, the displacements of the shell element nodes were constrained to the beam element node so that a section through the model remained plane. The rotations and the transverse displacements of the shell element nodes were constrained to be equal to the rotation and displacement of the beam element node. The longitudinal displacements were constrained to be the sum of the displacement of the beam element node and the rotation of the beam node multiplied by the distance to the shell node from the axis of rotation.

The loading was applied to the model by imposing a displacement in the longitudinal direction to the end node of the beam element at the opposite end of the model from the shell elements. The automatic load incrementation procedure available in ADINA was used. This capability was extremely effective since the response of the model is not known before the analysis and, consequently, appropriate displacement increments could not always be determined in advance.

3.4 Verification of the Model

A comparison of the predicted responses from the three finite element models and experimental data from one column test, is shown in Fig. 3.7. (Comparisons are shown for several other columns in reference 25.) The column analyzed (test specimen 1CDC from reference 7) had D/t=91, λ=0.65 d/D=0,141 and δ/L=0.0024. The predicted response from Model 1 overestimated the ultimate and post-ultimate force in the column. The coarse mesh at the dent was unable to accurately simulate the bending of the tube wall at the dent for large D/t ratio columns. (Model 1 had produced better agreement with experimental data for columns with lower D/t ratio.) The calculated response for Model 2 and Model 3 are essentially identical and agree reasonably well with the experimental data. This indicates that the discretization of Model 2 is likely to be sufficiently fine since further refinement of the mesh does not produce different results. The D/t ratio for this column is at the upper extreme of the range of interest in this study and a finer mesh is not needed. In general, the finite element analysis (Model 3) accurately predicted the ultimate load of the test specimen. With a few exceptions, the calculated responses in the post-ultimate range generally underestimated the load compared to the experimental data (See Fig. 3.7 and reference 25).

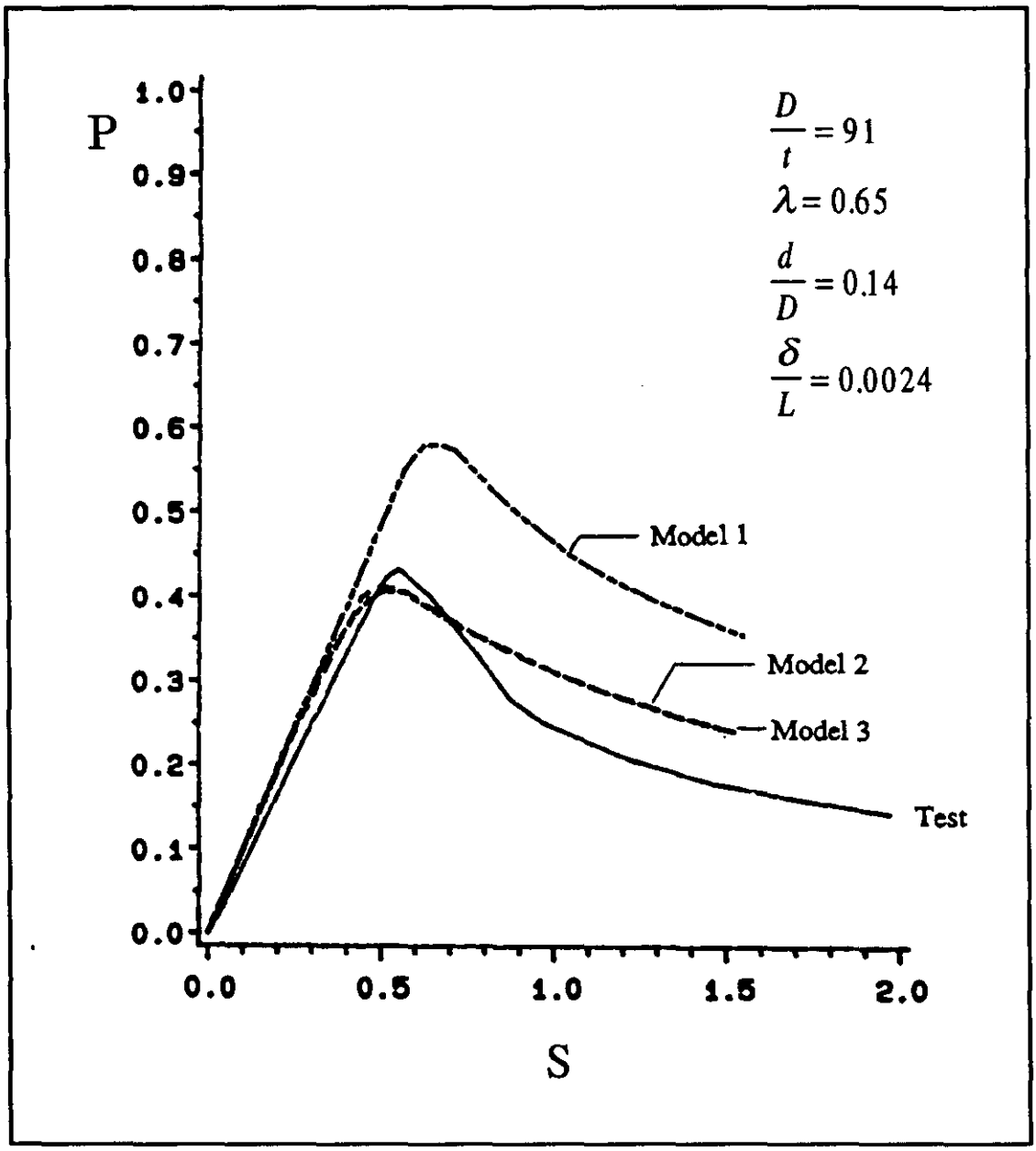

Figure 3.7 Comparison of experimental response with Models 1, 2 and 3

4 Approximation with Linear Regression Models

The simplified method for predicting the load-shortening behavior of damaged tubular columns developed here is based on a regression analysis. A brief overview of linear regression, the product formulation used, and specifics with respect to the analysis of the load-shortening behavior are given in this chapter. Ultimately a nonlinear regression model was used as described in Chapter 5.

4.1 Regression Analysis

Due to the dependence of column behavior on geometrical and material properties, a multiple regression model was required to approximate the load-shortening response from the data in the database. In this context, the term multiple refers to a single independent variable as a function of more than one independent variable. As an introduction, a brief overview of multiple regression analysis and the concept of the direct product in forming the regression model is provided since this explains much of the basis for the regression model.

4.1.1 Multiple Linear Regression

In a linear regression analysis, the known values of the dependent variable are approximated by a continuous function that is linear in terms of a set of regression coefficients. These coefficients are determined by the method of least squares. The known values of the dependent variables (for l data points) are arranged in a column matrix, F.

$$F = \begin{bmatrix} f_1 \\ \vdots \\ f_i \\ \vdots \\ f_l \end{bmatrix} \tag{4.1}$$

For each value, f_i, of the dependent variable there is a set, $(x_{1i}, ..., x_{ki}, ..., x_{ni})$, of corresponding values of the n independent variables. The approximation, f (a continuous function), to the data, F, is taken to be in the form of a linear series.

$$f = \sum_{j=1}^{m} a_j q_j = a_1 q_1 + ... + a_j q_j + ... + a_m q_m \tag{4.2}$$

where a_j are the regression coefficients and q_j are the regressors. Each regressor q_j is a function of one or more of the independent variable(s). In matrix notation, Eq. 4.2 can also be expressed by the product

$$f = QA \tag{4.3}$$

where Q is a $1 \times m$ row matrix of regressors q_j and A is a $m \times 1$ column matrix of the coefficients, a_j.

The approximation f_i to an individual data point f_i is given by evaluating Eq. 4.3 with the corresponding values of the independent variables. The data can then be represented as an approximation plus some (unknown) residual, ϵ

$$f_i = f_i + \epsilon_i = Q_i A + \epsilon_i \tag{4.4}$$

where Q_i is the row matrix Q evaluated at the i^{th} value of each of the independent variables. Analogous to Eq. 4.4, the vector of known values of the dependent variable, F, is given by

$$F = B A + E \tag{4.5}$$

where each i^{th} row of the $l \times m$ matrix B is the row matrix Q_i, and E is a column matrix of the corresponding values of ϵ_i.

The coefficients **A** are determined by enforcing the least squares criterion, which minimizes the sum of the squares of the residuals. Defining the error function, e, as

$$e = \sum_{i=1}^{l} \epsilon_i^2 \tag{4.6}$$

the least squares criterion (minimization of the sum of the squares of the residuals) is given by setting the derivatives of the error function with respect to the coefficients, a, equal to zero.

$$\frac{\partial e}{\partial a_j} = \{ 0 \} \tag{4.7}$$

This results in the following well-known set of simultaneous equations for the m regression coefficients **A**.

$$B^T B \ A = B^T F \tag{4.8}$$

B is a $l \times m$ matrix and the product $\mathbf{B}^{\mathrm{T}}\mathbf{B}$ is a $m \times m$ matrix, sometimes referred to as the crossproduct matrix. The approximation is given by solving Eq. 4.8 for the coefficients, **A**. Although ill-conditioning can be a problem in solving least squares equations, the greater challenge in performing a linear regression analysis is not in determining the coefficients, but in selecting appropriate regressors.

4.1.2 Product Formulation for Multiple Regression Models

In multiple regression analysis it is often convenient to examine the relationships between the dependent variable and each independent variable individually. Approximating functions can then be selected for each independent variable. Each of these approximating or "coordinate" functions is simply a function of a single independent variable chosen to approximate the relationship between that independent variable and the dependent variable for constant values of all other independent variables. The regression model can be formed as the product of the individual coordinate functions.

For clarity, the definition of the subscripts used in describing this formulation are provided in Table 4.1.

Table 4.1 Subscript definitions

	Data Points	Regressors	Independent Variables	Terms of the Coordinate Function for the k^{th} Independent Variable
Total Number	l	m	n	m_k
Index	i	j	k	j_k

For each independent variable, a coordinate function can be formulated as a linear combination of terms, each of which is a function of the independent variable. Analogous to the row matrix **Q** in Eq. 4.3, a coordinate function, $\mathbf{G_k}$, for the k^{th} independent variable, x_k, can be expressed as

$$G_k = \left[g_{k1}(x_k) \ \cdots \ g_{kj_k}(x_k) \ \cdots \ g_{km_k}(x_k) \right] \tag{4.9}$$

where each element of $\mathbf{G_k}$ is a function of x_k and m_k is the number of elements or terms in the coordinate function for the k^{th} independent variable.

The regressors Q for the model can then be formed as the product of the individual coordinate functions. Forming the regression model as a product allows the effect of each independent variable to be examined separately and facilitates the process of selecting suitable coordinate functions for the individual independent variables.

For a model with n independent variables and with each k^{th} independent variable having a coordinate function with m_k terms (or elements), the total number of regressors in the model, m, is given by

$$m = \prod_{k=1}^{n} m_k \tag{4.10}$$

In order to express the product as a matrix operation, the "direct product" is adopted. The direct product, sometimes referred to as the Kronecker product or Zehfuss product, is a matrix product of two matrices that includes all possible products of the elements of each matrix. For an m×n matrix **A** and a p×q matrix **B**, the direct product, indicated by the symbol ⊗, is defined by

$$A \otimes B = \begin{bmatrix} a_{11}B & \cdots & a_{1n}B \\ \vdots & & \vdots \\ a_{m1}B & \cdots & a_{mn}B \end{bmatrix} \tag{4.11}$$

where a_{ij} is the i^{th} row and j^{th} column element of **A**.[23] The right hand side of Eq. 4.11 is an $(m \cdot p) \times (n \cdot q)$ matrix.

In the matrix formulation the regression model, the regressors, **Q**, can be expressed as the direct product of the regressors of the individual coordinate functions

$$Q = G_1 \otimes \cdots \otimes G_k \otimes \cdots \otimes G_n \tag{4.12}$$

(Note that the direct product operation is associative, but not commutative.) The elements, q_j, of the row matrix **Q** resulting from the direct product formulation are given by

$$q_j = \prod_{k=1}^{n} g_{k\,j_k}(x_k) \tag{4.13}$$

where the j_k is given by,

$$j_k = \text{int}\left[\frac{\text{mod}\left(j-1, \prod_{h=k}^{n} m_h\right)}{\frac{\prod_{h=k}^{n} m_h}{m_k}}\right] + 1 \tag{4.14}$$

The function **int** is defined as the integer portion of the argument and **mod** is defined as

$$\text{mod}\,(x,y) = x - \text{int}\left(\frac{x}{y}\right) \cdot y \tag{4.15}$$

The matrix product **QA** defines the regression model as indicated in Eq. 4.3. This process facilitates selection of an appropriate regression model when there are several independent variables.

4.1.3 Selection of Coordinate Functions

In developing a regression model as described above, the effects of each independent variable can be studied independently. This is accomplished by observing the relationship between the dependent variable and an independent variable while all other independent variables are kept constant. By observing the nature of the relationship for various values of the other independent variables an appropriate coordinate function can be chosen to approximate the relationship.

After coordinate functions are selected for each independent variable, it is assumed that regressors q_j which define the approximation, f as a function of all the independent variables in Eq. 4.2 are formed as a product of the coordinate functions for the individual independent variables. The m coefficients A are then determined by solving Eq. 4.8 and the approximation function for the given data is given by Eq. 4.3.

4.1.4 Consolidation of Independent Variables

One advantage of this formulation by the direct product procedure is that, after the coefficients A are determined, the dependent variable expressed as a function of the m regressors and coefficients can be systematically reduced to a function with fewer (or a single) independent variables by setting selected variables to constant values and thus consolidating them into the coefficients of the remaining regressors in the regression model. Often the ultimate goal of a multiple regression analysis is to express the dependent variable as a function of a single independent variable. For example in this

study, the load versus displacement relationship for a given column is desired but in general the load is also a function of material and geometrical parameters.

By separating the independent variables into two groups, those that are to be retained as variables in the model and those that are to be consolidated into coefficients of the remaining regressors, two row matrices can be defined consisting of the direct product of the coordinate functions for the independent variables in each group. The direct product of the coordinate functions for the variables to be retained is defined as $\mathbf{Q_R}$ and consists of m_R elements. Typically this will be the coordinate function for a single independent variable. Likewise, $\mathbf{Q_C}$ is defined as the direct product of the coordinate functions of the variables to be consolidated and consists of m_C elements. Obviously, the relationship between the total number of regressors in the model, m, and m_R and m_C is given by

$$m = m_R \cdot m_C \tag{4.16}$$

Then the approximation, f, as given in Eq. 4.3 may be rewritten as

$$f = Q_R \, A^* \, Q_C^T \tag{4.17}$$

where $\mathbf{A^*}$ is a $m_r \times m_c$ rectangular matrix that consists of a rearrangement of the coefficients, $\mathbf{A}$.

The rearrangement of the elements of **A** to form $\mathbf{A}^*$ is based on the direct product formulation of $\mathbf{Q_R}$ and $\mathbf{Q_C}$. Each element, a^*_{rs} of $\mathbf{A}^*$ is based on the product of the r^{th} element of $\mathbf{Q_R}$, q_{Rr}, and the s^{th} element of $\mathbf{Q_C}$, q_{Cs}. The product of any q_{Rr} and q_{Cs} is equivalent to one of the regressors, q_j, since both ($q_{Rr} \cdot q_{Cs}$ and q_j) consist of the product of one element from each of the coordinate functions for the n independent variables (See Eq. 4.13.). Defining the regressor that corresponds to the product, $q_{Rr} \cdot q_{Cs}$, as $q_{j(r,s)}$, the element, a^*_{rs} of $\mathbf{A}^*$, is then the coefficient, $a_{j(r,s)}$, of the regressor $q_{j(r,s)}$. For example,

$$a^*_{rs} = a_{j(r,s)} \tag{4.18}$$

where

$$j(r,s) = \sum_{k=1}^{n-1}\left[\left(j_k - 1\right)\prod_{k^*=k+1}^{n} m_{k^*}\right] + j_n \tag{4.19}$$

and each j_k in Eq. 4.19 is the counter of the coordinate function for the k^{th} independent variable in the product, $q_{Rr} \cdot q_{Cs}$.

With the coefficients, **A**, known and the elements of $\mathbf{Q_C}$ also being constants by virtue of each independent variable being set to a constant value, Eq. 4.17 can be simplified to

$$f = Q_R A_R \tag{4.20}$$

where

$$A_R = A^* \, Q_C \tag{4.21}$$

Thus the approximation, f, is reduced to a linear combination of m_r terms.

4.2 A Linear Model for Column Load-Shortening

As expected in developing a predictive regression model, many models were tried, analyzed and assessed for accuracy and effectiveness. The final model presented here evolved out of first attempting to develop a conventional linear regression model. The development of a linear model is described in the following section to illustrate the formulation and to provide background for the development of the nonlinear model described in the subsequent section. This particular model is described in more detail in Reference 24 and is also presented in Reference 25.

4.2.1 Parametric Study

The complete load-shortening relationship, including the post-ultimate behavior, of a damaged tubular column is obviously non-linear and dependent on the geometry of the column and the amount of damage (dent depth and out-of-straightness).

Obviously, the regressors would be nonlinear functions of the independent variables, x_k. One of the first steps in developing a regression model is to conduct a parametric study to determine the appropriate predictor or dependent variables and the response or independent variable. The parametric study is discussed here, as it is applicable to both the linear regression model presented in References 24 and 25, as well as the nonlinear regression model.

In conducting a parametric study, the data should be examined to determine appropriate predictor and response variables for the regression model. It is often advantageous to formulate the predictor and response variables as nondimensional parameters.

In addition, the response and predictor variables should be selected so as to minimize the amount of scatter in the data, thus providing an improved basis for the regression model. To illustrate, consider a simple example where the object is to predict the response of steel stub column from data on a number of specimens with differing cross-sectional areas and yield stresses. Plots of the raw data in the form of the load versus axial deformation would exhibit considerable scatter. Obviously, more appropriate variables for a regression model would be obtained by nondimensionalizing the load and axial deformation with respect to the squash load (cross-sectional area multiplied by the yield stress) and length, respectively. In more complex problems appropriate nondimensionalized parameters are not obvious and must be determined from a study of the data.

In this study, the axial load, P, was assumed to be a function of diameter, thickness, length, yield strain, dent depth, out-of-straightness and axial shortening as indicated in Eq. 4.22

$$P = P(D,\ t,\ L,\ \epsilon_y,\ d,\ \delta,\ \Delta) \tag{4.22}$$

Since only steel columns were considered in this study, the modulus of elasticity was not included as a variable.

In previous work (references 24 and 25), the parametric study resulted in a linear regression model of the form

$$\mathrm{P} = \frac{P}{P_y} = \mathrm{P}\left(\frac{D}{t},\ \lambda,\ \frac{d}{D},\ \frac{\delta}{L},\ S\right) \tag{4.23}$$

where

$$\lambda = \frac{L}{\pi r}\sqrt{\epsilon_y} \tag{4.24}$$

and

$$S = \frac{\Delta}{L\,\epsilon_y} \tag{4.25}$$

For the regression model presented in the following chapter, variations of the five nondimensionalized parameters shown on the right hand side of Equation 4.23 were used. These parameters were selected to minimize the error of the least squares regression and are described in the following chapter.

5 Piecewise Approximation of the Load - Shortening Behavior

The preceding chapter described some fundamental concepts pertaining to multiple linear regression, and the direct product formulation of a linear regression. This chapter presents the application of a regression analysis to the load-shortening behavior of damaged tubular columns.

Linear regression models, as indicated by Eq. 4.3, can represent or approximate a wide variety of relationships and present a mathematically tractable problem of determining the regression coefficients. However, there are cases where a nonlinear model may be more appropriate. For example, the form of the actual relationship between the dependent and independent variables may be known and may not be able to be expressed in the form of Eq. 4.3. Or, the nature of the relationship between dependent and independent variables and the benefit of a concise approximation function with as few terms as practical may be more readily realized with a model that is nonlinear.

In developing a regression model to predict the axial load as a function of axial shortening, it was difficult to obtain accurate approximations over the reasonably wide range of geometrical and damage parameters considered in this study. This was due to the variations in the characteristics of the load-shortening relationship as a function of geometry and damage.

References 24 and 25 describe a linear regression model that was developed for a limited range of column geometries, out-of-straightness and dent depth. Many attempts were made to improve and broaden the scope of this model and to develop a more general model. However, these efforts were generally unsuccessful. During this work, it was realized that it was not practical to expect that a linear combination of a small number of coordinate functions for the axial displacement parameter could approximate the wide range of shapes of the load - shortening curves.

5.1 The Load-Shortening Relationship

Over the range of column geometries, material properties, dent depth and out-of-straightness considered in this study, there is considerable variation in the characteristics of the load versus shortening relationships. In general, the range of load-shortening behavior is illustrated by the three curves depicted in Fig. 5.1. For columns with a relatively small amount of damage (dent damage and initial crookedness) and large D/t ratios, the behavior was characterized by an essentially

linear response up to the ultimate load followed by very rapid decrease in load as illustrated by curve A in Fig 5.1. This response was also observed to be a function of the slenderness λ of the column. For columns with greater damage, the load-shortening response was smoother, with a more gradual approach to the ultimate load and a more gradual reduction in load in the post-ultimate range as illustrated by curve B in Fig 5.1. The curve labeled C has a short initial linear range followed by gradual reduction in stiffness up to the ultimate load and then a relatively flat unloading curve, typical of a column with a relatively large amount of damage.

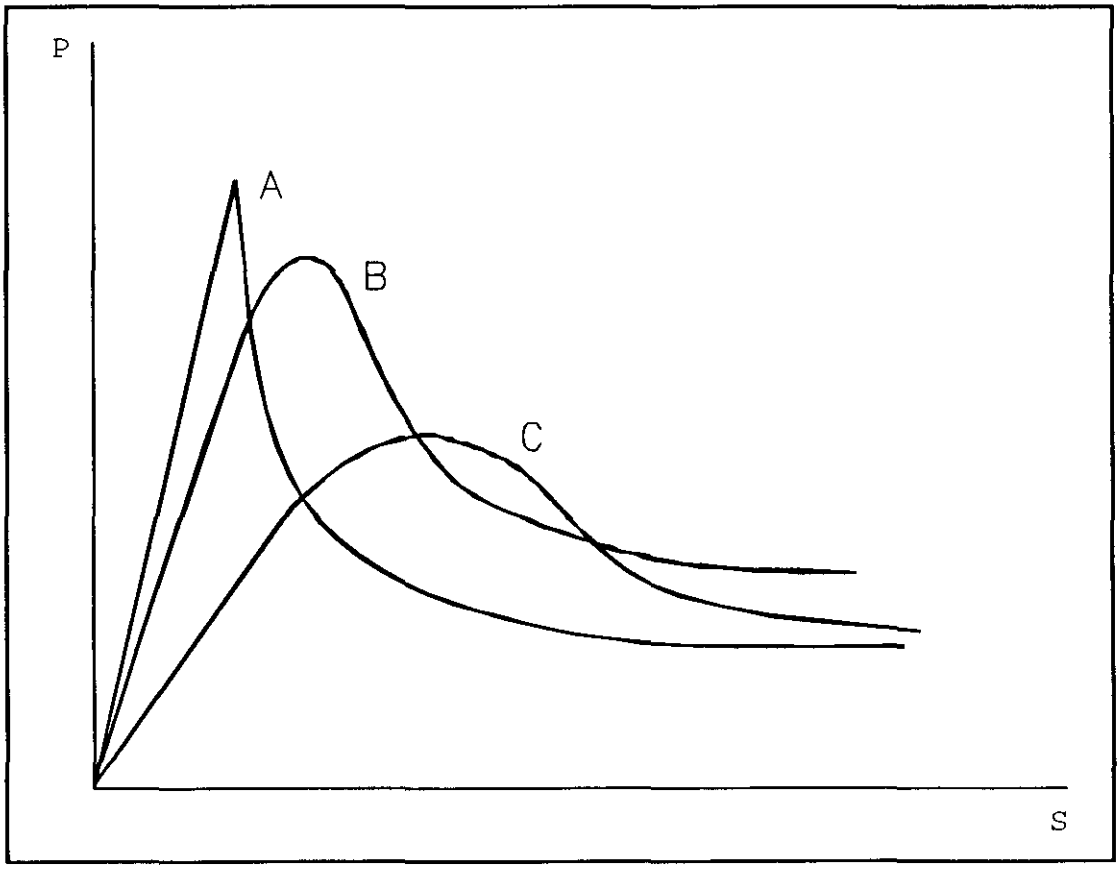

Figure 5.1 General characterization of load-shortening behavior.

Although curves A, B and C illustrate the overall character of the load shortening relationship, it should be noted that for each type of response there is a broad range in values determining the actual curve. For example, columns with type A response can vary widely in the maximum value of the nondimensionalized load, P. Also, the value of the nondimensionalized axial shortening, S at which the maximum load occurs varies significantly for each of the three types of column response.

The difficulty in modeling the column behavior with a linear regression model is largely due to the variation in the shape of the load - shortening relationships shown in Fig. 5.1. A linear model has to be of the form of Eq. 4.3 and can be reduced to a simple linear combination of the individual terms of the coordinate function for a single variable as discussed in Section 4.1.4. Although the discussion in Section 4.1.4 specifically applies to a model formed as a Kronecker, Zehfuss or direct product of the coordinate functions, any linear multiple regression model can be so reduced to a function of a single variable. The model in its reduced form, i.e., the load as a function of the axial shortening, is simply a linear combination of the terms of the coordinate function for axial shortening. With five independent variables in this study, three to five terms in the coordinate function for axial shortening was considered reasonable in order to keep the total number of regressors in the model manageable and to provide a compact procedure for the simplified method.

The lack of success from application of traditional linear regression modeling and an examination of the nature of the load shortening relationship led to the adoption of a piecewise approximation.

Although markedly different in the structural behavior they represent, the curves in Fig 5.1 have similar characteristics. As shown for the hypothetical load-shortening curve in Fig. 5.2, each curve has an initial linear segment. This is followed by the ultimate load segment that includes the maximum value of load and has nonpositive curvature (nonpositive second derivative, $\frac{d^2P}{dS^2} \leq 0$). The post-ultimate segment of each curve is always positive, has negative slope (negative first derivative, $\frac{dP}{dS} < 0$) and nonnegative curvature. The point labeled S_L in Fig. 5.2. represents the maximum value of nondimensionalized axial shortening S of the linear segment and marks the transition from the linear segment to the ultimate load segment. S_I is the value of S at the inflection point between the ultimate load and post-ultimate segments. Thus, these two points along with the origin define the domain of the "linear segment", the "ultimate load segment" and the initial point of the "post-ultimate segment". Any of the curves of type A, B, or C can be divided into these three segments. Obviously for a curve of type A, the difference or distance between S_I and S_L will be very small.

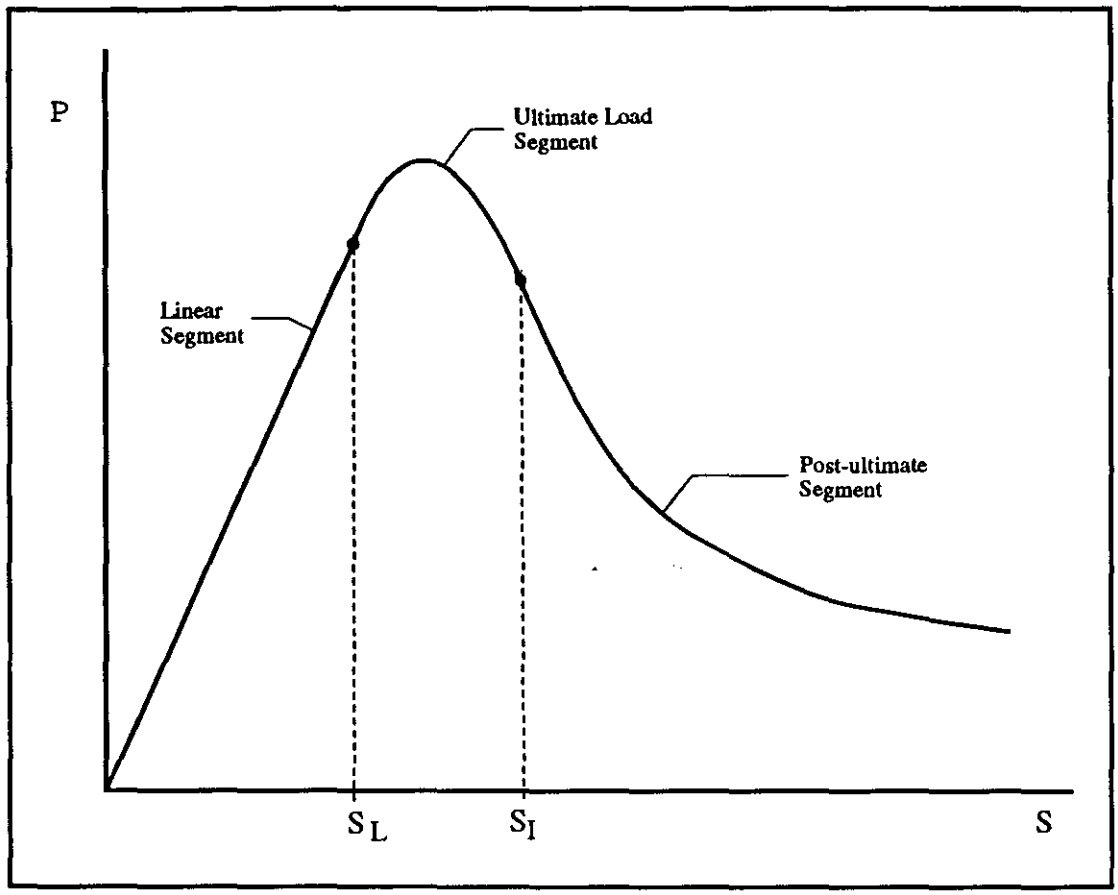

Figure 5.2 Piecewise description of the load - shortening response

This piecewise description of the load - shortening curves provides the basis for the development of the regression model. For each segment a simple function can be used to describe the curve. These functions along with the values of S_L and S_I are used to approximate the load - shortening curve. This is described in detail in the following sections.

5.2 General Description of the Piecewise Approximation

The regression model for approximating the load shortening behavior of tubular columns is unique in the formulation of the coordinate function for the axial shortening S. A general description of the approximation of P as a function of S is given here.

The nature of the three segments that comprise the load - shortening relationship implies that simple functions could be used to approximate each segment. For example, it is clear that the simple linear relationship in Eq. 5.1 is appropriate for the linear segment.

$$P = P(S) = \frac{c_{SI}}{S_L} S \qquad for \quad 0 \le S \le S_L \qquad (5.1)$$

Note that c_{SI} is magnitude of the load when $S = S_L$.

The characteristics of the ultimate load segment of a load shortening curve is that it is curvilinear and its second derivative is nonpositive.. Continuity between the segments is also a requirement for the coordinate function. At a minimum, continuity of the function, sometimes referred to as C^0 continuity, and of its first derivative or C^1 continuity are required. In order to enforce the required continuity, a third order polynomial was selected to approximate the ultimate load segment.

The formulation of the coordinate function is based on Hermitian interpolation where the ordinates and slopes are matched at the end points. For the ultimate load segment, the coordinate function for S is determined from the third order polynomial given by

$$c_1 + c_2(S - S_L) + c_3(S - S_L)^2 + c_4(S - S_L)^3 \tag{5.2}$$

and the values of the ordinate and slope at the ends of the segment. The relationship between the constants, c and the ordinates and slope at $S = S_L$ and $S = S_I$ is then given by

$$\begin{bmatrix} G_S(S_L) \\ \dfrac{\mathrm{d}\,G_S(S_L)}{\mathrm{d}\,S} \\ G_S(S_I) \\ \dfrac{\mathrm{d}\,G_S(S_I)}{\mathrm{d}\,S} \end{bmatrix} = \begin{bmatrix} 1 & 0 & 0 & 0 \\ 0 & 1 & 0 & 0 \\ 1 & S_{IL} & S_{IL}^2 & S_{IL}^3 \\ 0 & 1 & 2S_{IL} & 3S_{IL}^2 \end{bmatrix} \begin{bmatrix} c_1 \\ c_2 \\ c_3 \\ c_4 \end{bmatrix} \tag{5.3}$$

where,

$$S_{IL} = S_I - S_L \tag{5.4}$$

By inverting the matrix in Eq. 5.3, the polynomial in Eq. 5.2 is expressed in terms of the ordinate and slopes at the endpoints of the ultimate load segment.

$$\left[1 \quad (S-S_L) \quad (S-S_L)^2 \quad (S-S_L)^3\right]\begin{bmatrix} 1 & 0 & 0 & 0 \\ 0 & 1 & 0 & 0 \\ \frac{-3}{S_{IL}^2} & \frac{-2}{S_{IL}} & \frac{3}{S_{IL}^2} & \frac{-1}{S_{IL}} \\ \frac{2}{S_{IL}^3} & \frac{1}{S_{IL}^2} & \frac{-2}{S_{IL}^3} & \frac{1}{S_{IL}^2} \end{bmatrix}\begin{bmatrix} G_S(S_L) \\ \frac{\mathrm{d}\,G_S(S_L)}{\mathrm{d}\,S} \\ G_S(S_I) \\ \frac{\mathrm{d}\,G_S(S_I)}{\mathrm{d}\,S} \end{bmatrix} \tag{5.5}$$

The slope at $S = S_L$ is defined by the value of the function since it must match the slope of the linear segment given by Eq. 5.1. Imposing the requirement that

$$\frac{\mathrm{d}\,G_S(S_L)}{\mathrm{d}S} = \frac{G_S(S_L)}{S_L} \tag{5.6}$$

results in the three term coordinate function for S over the ultimate load segment given in Eq. 5.7.

$$g_{S1} = 1 + \frac{(S - S_L)}{S_L} - \frac{2S_{IL} + 3S_L}{S_L S_{IL}^2}(S - S_L)^2 + \frac{S_{IL} + 2S_L}{S_L S_{IL}^3}(S - S_L)^3$$

$$g_{S2} = \frac{3}{S_{IL}^2}(S - S_L)^2 - \frac{2}{S_{IL}^3}(S - S_L)^3 \qquad \textbf{(5.7)}$$

$$g_{S3} = \frac{-1}{S_{IL}}(S - S_L)^2 + \frac{1}{S_{IL}^2}(S - S_L)^3$$

The subscript, S is used for clarity to indicate the coordinate function for S in lieu of a numerical subscript indicating the k^{th} coordinate function as given in the notation used in Eqs. 4.9 and ?.

$$G_S = \begin{bmatrix} g_{S1} & g_{S2} & g_{S3} \end{bmatrix} \qquad \textbf{(5.8)}$$

The three components of the coordinate function G_s over the ultimate load segment is shown graphically in Fig. 5.3. The linear segment is also shown to illustrate the continuity between the linear and ultimate load segments.

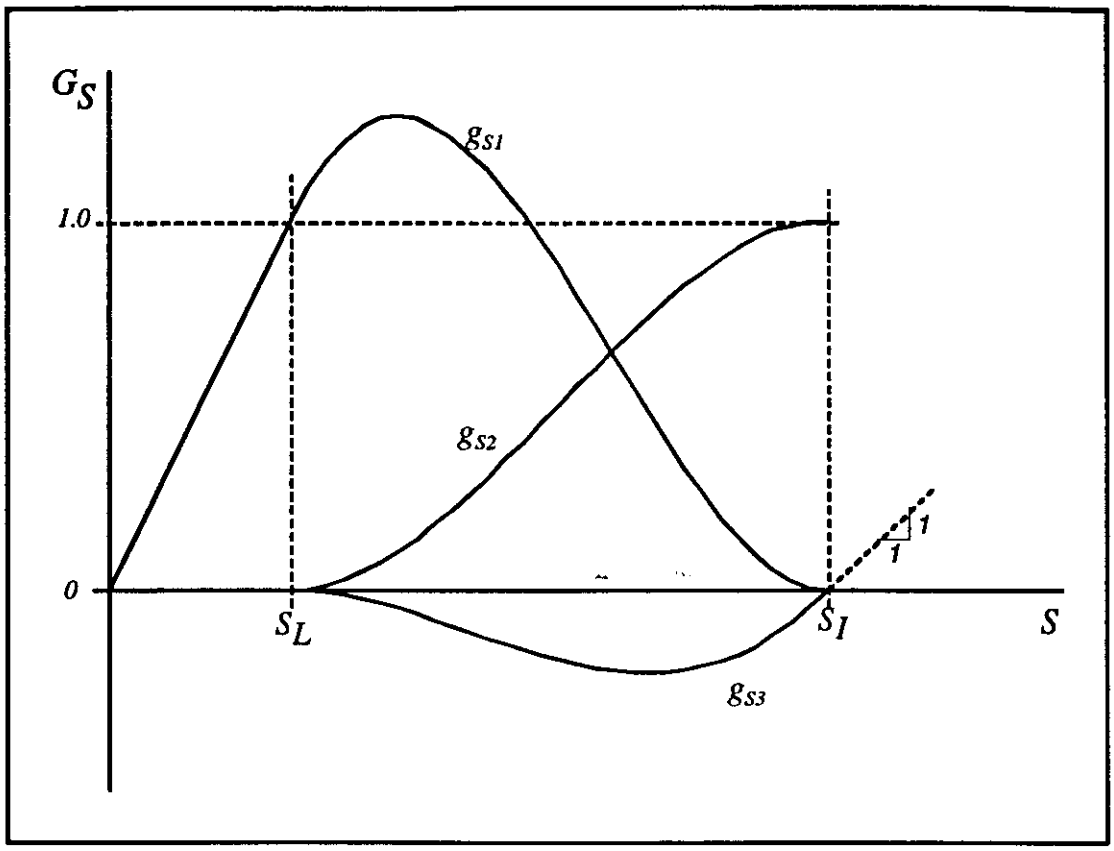

Figure 5.3 Coordinate function G_S for $S < S_I$

Note that the ordinates of g_{S1} and g_{S2} have values of 1 and 0 and 0 and 1 at $S = S_L$ and $S = S_I$, respectively. The first derivative of g_{S1} has values of $\frac{1}{S_L}$ at $S = S_L$ and 0 at $S = S_I$. Similarly, the first derivative of g_{S2} is 0 at both end points of the ultimate load segment. The third term of the coordinate function, g_{S3}, has slopes of 0 and 1 at $S = S_L$ and $S = S_I$, respectively. Thus, a linear combination of these terms of the coordinate function provides the approximation for the ultimate load segment where the coefficients of each term of the coordinate function represent the values of the function at $S = S_L$ and $S = S_I$ and the slope at $S = S_I$.

The post-ultimate segment has the following characteristics that are important in selecting an approximating function. As listed previously, these are 1) positive value of the function, 2) negative first derivative and 3) positive second derivative over the domain of $S \geq S_1$. It can be advantageous if the desired characteristics are inherent in the approximating function. This will preclude the possibility of the resulting regression model producing spurious results such as negative values or positive slopes for the post-ultimate segment of the load shortening curves.

The characteristics of the post-ultimate segment listed above proved to be unamenable to approximation by a linear combination of functions of S. In a regression analysis, the coefficients are independent variables and as such, do not preclude the violation of the above characteristics of the post-ultimate segment. For example, a linear combination of functions, each having positive curvature, would not necessarily have positive curvature or be a positive valued function.

These considerations led to the use of a nonlinear regression function for approximating the post-ultimate segment. The approximating function is given by

$$P = \frac{c_{S2}}{1 - \frac{c_{S3}}{c_{S2}}\left(S - S_1\right)} = \frac{P(S_1)}{1 - \frac{P'(S_1)}{P(S_1)}\left(S - S_1\right)} \qquad \textbf{(5.9)}$$

This function maintains C^0 and C^1 continuity between the ultimate and post-ultimate segments and, assuming that c_{S2} and c_{S3} representing the ordinate and slope

at $S = S_1$ are positive and negative, respectively, exhibits the desired characteristics of the approximating function as described above. The approximating function for the post-ultimate segment, with the above assumptions, is illustrated in Fig. 5.4.

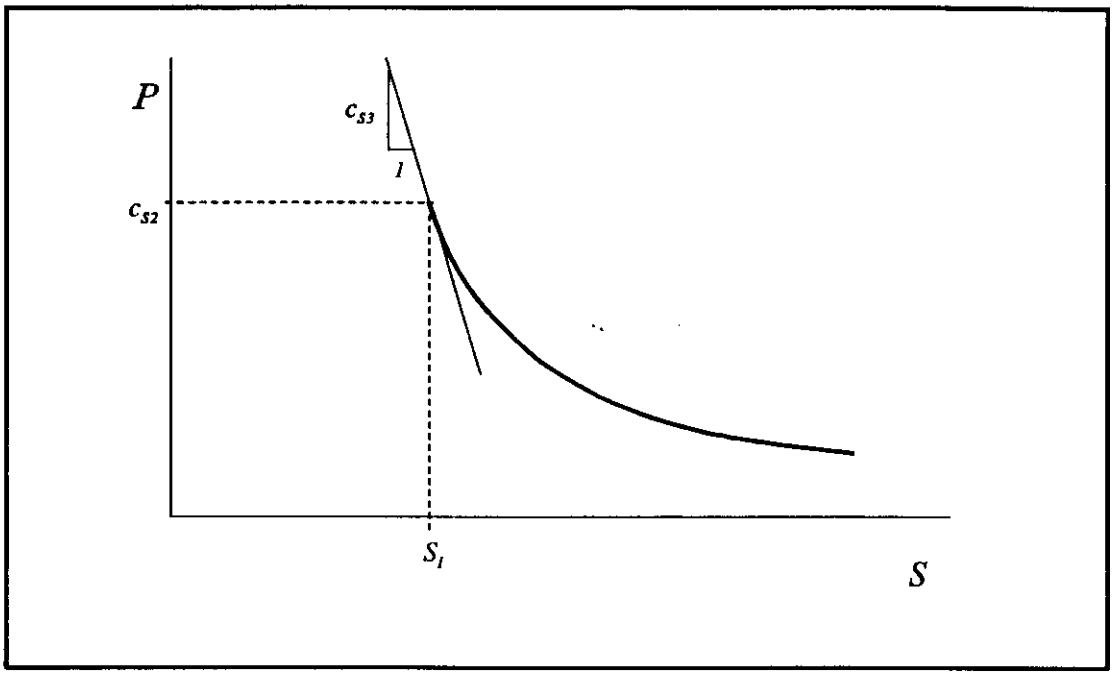

Figure 5.4 Coordinate function for the post-ultimate segment.

From Eqs. 5.1, 5.7, 5.8 and 5.9, the complete approximating function for the load as a function of the axial shortening is given by Eq. 5.10.

for $0 \le S \le S_L$

$$P(S) = \frac{c_{S1}}{S_L} S$$

for $S_L \le S \le S_I$

$$P(S) = c_{S1}\left[1 + \frac{(S - S_L)}{S_L} - \frac{2S_{IL} + 3S_L}{S_L S_{IL}^2}(S - S_L)^2 + \frac{S_{IL} + 2S_L}{S_L S_{IL}^3}(S - S_L)^3\right]$$

$$+ c_{S2}\left[\frac{3}{S_{IL}^2}(S - S_L)^2 - \frac{2}{S_{IL}^3}(S - S_L)^3\right] \qquad \textbf{(5.10)}$$

$$+ c_{S3}\left[\frac{-1}{S_{IL}}(S - S_L)^2 + \frac{1}{S_{IL}^2}(S - S_L)^3\right]$$

for $S \ge S_I$

$$P(S) = \frac{c_{S2}}{1 - \frac{c_{S3}}{c_{S2}}(S - S_I)}$$

5.3 Segmentation of the Load-Shortening Response

From Eq. 5.10, it is obvious that in addition to the three coefficients, c_{S1}, c_{S2} and c_{S3}, the points S_L and S_I are required to describe the piecewise approximation. Since predictive capability was the primary reason for developing the regression model, it

was necessary to be able to predict S_L and S_I for a damaged column. The basis for predicting or estimating S_L and S_I was, not surprisingly, a regression model. In order to develop the regression model, it was necessary to determine the values of S_L and S_I for each load-shortening relationship in the database. Because of the method by which these points were determined, the inflection point between the ultimate load segment and the post-ultimate segment, S_I was determined prior to S_L , and is presented first.

5.3.1 Determination of S_I

S_I is an inflection point and was determined by estimating the point where the second derivative of the load-shortening relationship is equal to zero. Since the load-shortening relationships in the database are defined by discrete points, the second derivative at a point was estimated by the finite difference calculation given in Eq. 5.11

$$\frac{d^2P}{dS^2} \approx \frac{2\left(\Delta P_R \Delta S_L - \Delta P_L \Delta S_R\right)}{\Delta S_R \Delta S_L \left(\Delta S_R + \Delta S_L\right)} \tag{5.11}$$

and illustrated conceptually in Fig. 5.5.

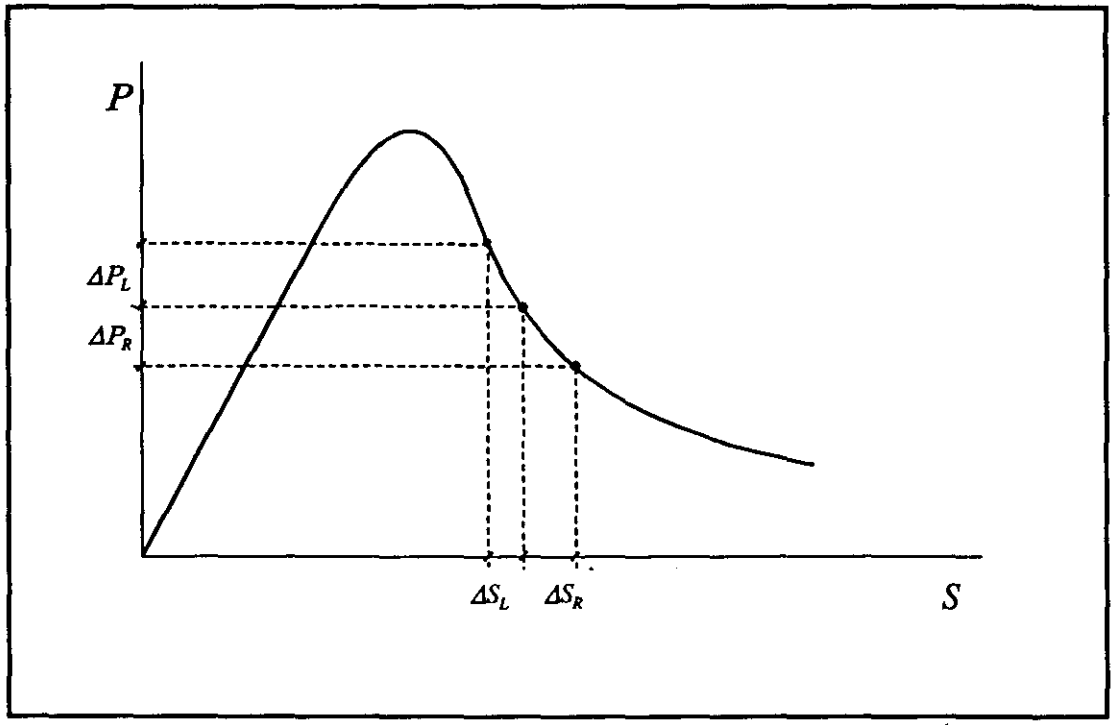

Figure 5.5 Illustration of quantities for finite difference calculation of 2nd derivative

For each load-shortening relationship in the database, a search for the two points where the second derivative changes sign from negative to positive was performed by calculating the second derivative at successive points until the change of sign was found as illustrated in Fig. 5.6. The abscissa and the ordinate of the inflection point, S_I and $P(S_I)$ were then determined by linear interpolation between the positive and negative values of the second derivative.

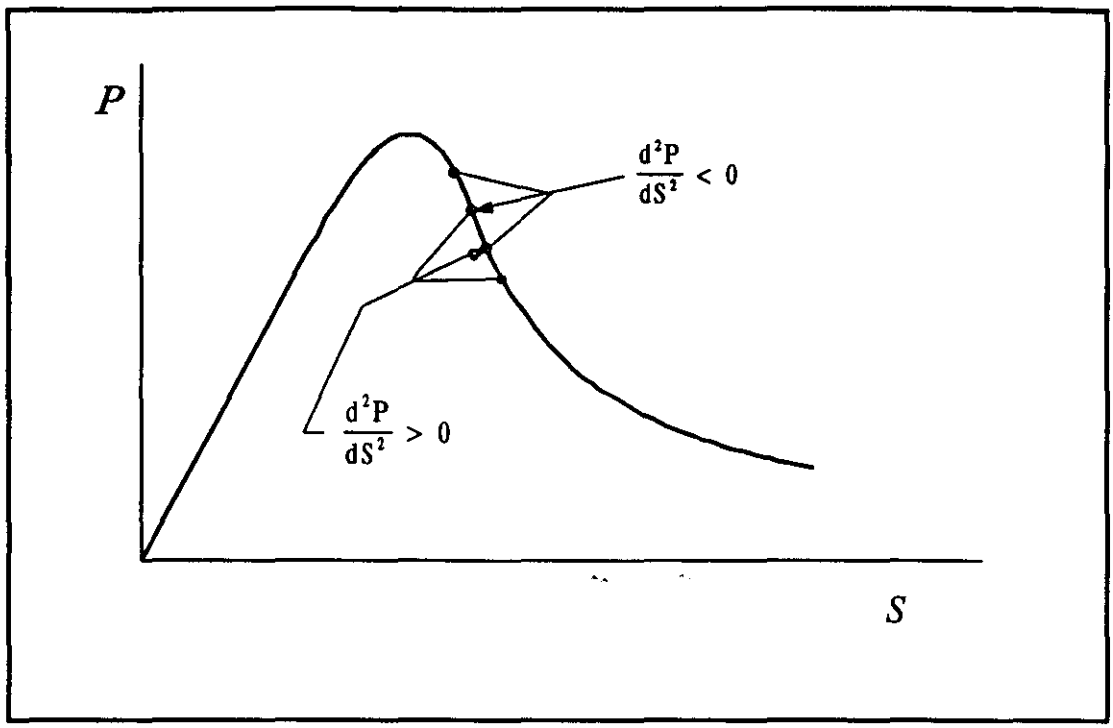

Figure 5.6 Sequential search for inflection point

After S_I and $P(S_I)$ were determined for each load-shortening relationship, the results were incorporated into the database. As discussed above, the values of S_I formed the basis for the regression model to predict S_I. The values of $P(S_I)$ were used to facilitate the selection of coordinate functions but were not directly used in the regression analysis of the load-shortening data as discussed in Section 5.5.

5.3.2 Determination of S_L

In the context of a series of discrete points that represent a load-shortening relationship in the database, the value of S_L is not as readily determined as an inflection point. Attempts to develop an automated numerical procedure to locate the end of the

linear segment were not completely successful. Procedures based on numerical calculation of the second derivative were used but generally met with inconsistent results. Selecting a small "trigger" value of curvature to indicate the end of the linear segment produced varying results that did not appear to be consistently valid when graphically observed. Also, small amounts of "noise" in the data would produce inaccurate results.

The difficulties in determining S_L from a numerical calculation of curvature led to the use of another regression procedure. For each load-shortening relationship in the database, S_L was determined from an individual regression analysis of each curve with S_L as one of the regression coefficients. The approximating function for load as a function of shortening used in the regression analyses for S_L was the same as described above in Eq. 5.10 and used in the complete model for the load as a function of column geometry, dent damage, out-of-straightness and axial shortening. Consequently, a nonlinear regression analysis was required to determine the values of S_L. The regression model is defined by Eq. 5.10 where c_{S1}, c_{S2}, c_{S3} and S_L are the regression coefficients. For each load-shortening relationship, S_I is known from the procedure described in Section 5.3.1.

A modified Gauss-Newton technique included in the SAS software was used to perform the nonlinear regression analysis. This method requires initial approximate values for each of the regression coefficients and derivatives of the approximating function with respect to the regression coefficients. The initial values of the regression

coefficients for each of the load-shortening curves were determined graphically by visual examination of the curves. The derivatives of the approximating function (Eq. 5.10) are given in Eq. 5.12.

for $0 \le S \le S_L$

$$\frac{\partial P}{\partial c_{S1}} = \frac{S}{S_L}, \qquad \frac{\partial P}{\partial c_{S2}} = 0, \qquad \frac{\partial P}{\partial c_{S3}} = 0, \qquad \frac{\partial P}{\partial S_L} = -c_{S1}\frac{S}{S_L^2}$$

for $S_L \le S \le S_I$

$$\frac{\partial P}{\partial c_{S1}} = c_{S1}, \quad \frac{\partial P}{\partial c_{S2}} = c_{S2}, \quad \frac{\partial P}{\partial c_{S3}} = c_{s3}$$

$$\frac{\partial P}{\partial S_L} = \frac{c_{S1}}{S_L^2 S_{IL}^4}\left[\left(-2S_L^2 S_I^3 - 4S_L^3 S_I^2\right) + \left(4S_L S_I^3 + 7S_L^2 S_I^2 + 8S_L^3 S_I - S_I^4\right)S + \left(2S_I^3 - 8S_L S_I^2 - 8S_L^2 S_I - 4S_L^3\right)S^2 + \left(-S_I^2 + 4S_L S_I + 3S_L^2\right)S^3\right] \tag{5.12}$$

for $S \ge S_I$

$$\frac{\partial P}{\partial c_{S1}} = 0, \quad \frac{\partial P}{\partial c_{S2}} = c_{S2}\frac{c_{S2} - 2c_{S3}(S - S_I)}{\left[c_{S2} - c_{S3}(S - S_I)\right]^2},$$

$$\frac{\partial P}{\partial c_{S3}} = \frac{S - S_I}{\left[1 - \frac{c_{s3}}{c_{S2}}(S - S_I)\right]^2}, \quad \frac{\partial P}{\partial S_L} = 0$$

The values of S_L determined from the regression analysis were verified graphically and added to the database. The values of $P(S_I)$ were then determined for each column in the database from linear interpolation of the load-shortening data. At this point, the database includes the geometry, material yield strength, dent-depth and out-of-straightness, the values of S_L, $P(S_L)$, S_I and $P(S_I)$, and load-shortening data for each column.

5.4 Approximation of S_L and S_I

In addition to values for c_{S1}, c_{S2}, and c_{S3}, the piecewise approximation described above requires values of S_L and S_I to define a load-shortening relationship. Two linear regression models, one each for S_L and S_I, were developed to predict their values as functions of the column geometry and damage.

5.4.1 Regression Model for S_L

As with all of the regression models, the model for S_L as a function of column geometry and damage was based on the physical phenomenon and the goodness of fit to the data. The coordinate functions for S_L as a function of column slenderness λ, D/t ratio, relative dent depth d/D, and out-of-straightness δ/L are given in Eqs. 5.13, 5.14, 5.15 and 5.16 where the superscript S_L is used to indicate that the coordinate function approximates S_L and not the nondimensionalized load, P. (By default the coordinate functions for P do not have superscripts.)

$$G_{\lambda}^{S_L} = \begin{bmatrix} 1 & \lambda^2 \end{bmatrix} \tag{5.13}$$

(The slenderness, λ is defined in Eq. 4.24 as $\frac{L}{\pi r}\sqrt{\epsilon_y}$ where r is the radius of gyration.)

$$G_{D/t}^{S_L} = \begin{bmatrix} 1 & \frac{1}{10}\frac{D}{t} \end{bmatrix} \tag{5.14}$$

$$G_{d/D}^{S_L} = \begin{bmatrix} 1 & \frac{1}{1+\frac{d}{D}} \end{bmatrix} \tag{5.15}$$

$$G_{\delta/L}^{S_L} = \begin{bmatrix} 1 & \sqrt{\frac{\delta}{L}} \end{bmatrix} \tag{5.16}$$

The factor of 10 in Eq. 5.14 was included to force each of the regressors to be of the same order of magnitude and various powers of 10 are used in other coordinate functions for the same purpose.

To illustrate the rationale for selecting the coordinate functions and a comparison between the data and the approximation for S_L , the coordinate function for S_L as a function of λ is shown in Fig. 5.7. The data and coordinate function in Fig. 5.7 represent constant values of D/t = 40, d/D = 0.10 and δ/L = 0. A curvilinear relationship is indicated by the data and a good fit is provided by the two term parabolic coordinate function given in Eq. 5.13. Note that the coordinate function shown in Fig. 5.7 is not the result of a least squares fit to the nine data points shown, but is the result of the fit to all 130 values of S_L in the database.

The process of selecting coordinate functions is a two step process. First the data are examined as a function of an individual parameter, e.g. λ as in Fig. 5.7, and a coordinate function is selected based on the trend exhibited by the data. The evaluation of the fit of individual coordinate functions is performed after the regression coefficients have been determined and the reduced coefficients for the coordinate function are determined for various values of the other remaining variables (in this case D/t, d/D and δ/L).

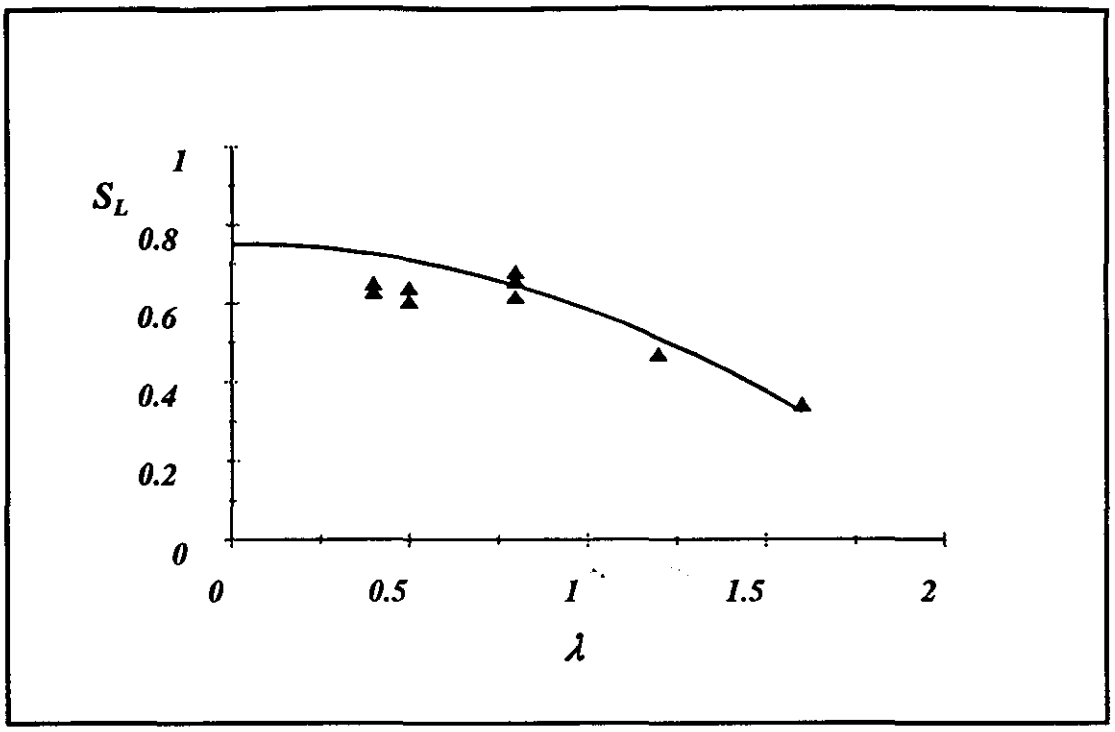

Figure 5.7 Example data and coordinate function for S_L as a function of λ.

The row matrix of regressors **Q** that defines the regression model for S_L is given by the direct product of the coordinate functions as shown in Eq. 5.17.

$$Q_{S_L} = G_{\delta/L}^{S_L} \otimes G_{d/D}^{S_L} \otimes G_{D/t}^{S_L} \otimes G_{\lambda}^{S_L} \tag{5.17}$$

5.4.2 Regression Model for S_{IL}

The segmentation of the load-shortening relationship was defined by the points S_L and S_I. However, it was observed that the length of the ultimate load segment, S_{IL} (defined in Eq. 5.3), was more directly related to the column geometry and damage parameters. Considering the load-shortening relationships in Fig. 5.1, it is apparent that the nature of the relationship is defined by the length of the ultimate load segment S_{IL} and not directly by the value of S_I. For example, two columns with significantly different geometries and damage would be expected to have differing load-shortening responses, but could have the same value of S_I as shown in Fig. 5.8. The differences between these two columns in geometry, damage and their consequent behavior is reflected in S_{IL} ($S_{IL} = S_I - S_L$, Eq. 5.3) rather than S_I. Consequently, S_{IL} was the dependent variable in the regression analysis to determine the location of the inflection point between the ultimate load and post-ultimate segments.

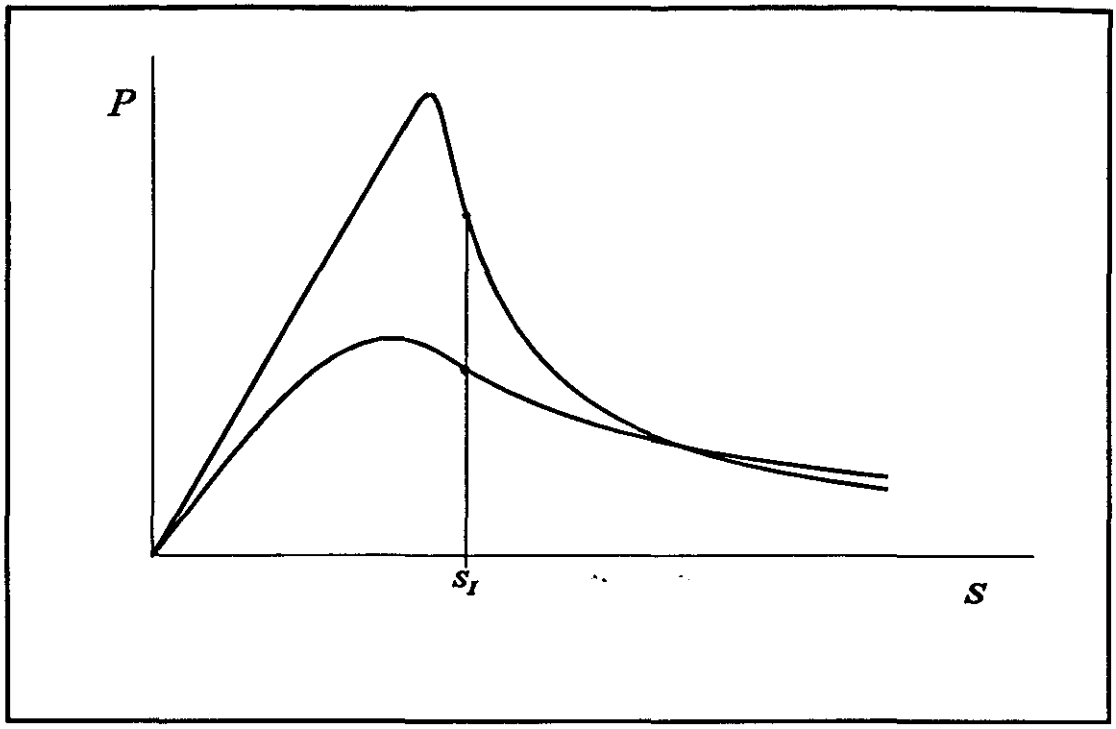

Figure 5.8 Two characteristically different column responses with equal S_I

The coordinate functions used in the regression analysis for S_{IL} are given in Eqs. 5.18, 5.19, 5.20 and 5.21.

$$G_{\lambda}^{S_{IL}} = \left[1 \qquad 10\sqrt{\epsilon_y}\,\frac{1}{\lambda} \right] \tag{5.18}$$

$$G_{D/t}^{S_{IL}} = \left[1 \qquad \frac{1}{10}\sqrt{\frac{D}{t}} \right] \tag{5.19}$$

$$G_{\frac{d}{D}}^{S_{IL}} = \left[1 \qquad \frac{1}{\sqrt{\epsilon_y}}\left(\frac{d}{D}\right)^2\right] \tag{5.20}$$

$$G_{\delta/L}^{S_{IL}} = \left[1 \qquad 100\,\frac{\delta}{L}\right] \tag{5.21}$$

The row matrix **Q** that defines the regression model for S_{IL} is then given by the direct product of the coordinate functions as shown in Eq. 5.22.

$$Q_{S_{IL}} = G_{\delta/L}^{S_{IL}} \otimes G_{d/D}^{S_{IL}} \otimes G_{D/t}^{S_{IL}} \otimes G_{\lambda}^{S_{IL}} \tag{5.22}$$

5.5 Formulation of the Complete Regression Model

The complete regression model consists of two components. First the abscissa S_L and the projected length along the S axis of the ultimate load segment S_{IL} are given by Eq. 5.23

$$\begin{Bmatrix} S_L \\ S_{IL} \end{Bmatrix} = \begin{Bmatrix} Q_{S_L} A_{S_L} \\ Q_{S_{IL}} A_{S_{IL}} \end{Bmatrix} \tag{5.23}$$

where, analogous to Eq. 4.3, the subscripted Q's and A's are the regressors and regression coefficients for the regression models for S_L and S_{IL}, respectively. Then the load-shortening relationship is calculated from regression model for P based on Eq. 5.10 and further developed in this section.

The initial development of the regression model for the axial load was based on a linear model and the final model presented in this section is largely based on the direct product formulation described in Chapter 4. The coordinate functions for load as a function of the nondimensional geometrical variables, D/t and λ, and the damage variables, d/D and δ/L, are linear functions with respect to the regression variables. The nonlinearity of the regression model is represented by the coordinate function for axial shortening as described by Eq. 5.10. The description of the model is facilitated by introducing the following notation for the linear portion of the model,

$$Q = G_{\delta/L} \otimes G_{d/D} \otimes G_{D/t} \otimes G_{\lambda} \tag{5.24}$$

where the subscripted Gs are the coordinate functions for axial load as a function of λ, D/t, d/D and δ/L. The coordinate function for S given by Eq. 5.10 is combined with Eq. 5.24 to complete the model as shown in Eq. 5.25 where the subcripted As are column vectors of regression coefficients.

$$
\begin{aligned}
&\textit{For} \quad S < S_L \\
&\qquad P = Q \cdot A_1 \, g_{S1} \\
&\textit{For} \quad S_L \le S \le S_I \\
&\qquad P = Q \cdot A_1 \, g_{S1} + Q \cdot A_2 \, g_{S2} + Q \cdot A_3 \, g_{S3} \\
&\textit{For} \quad S \ge S_I \\
&\qquad P = \frac{Q \cdot A_2}{1 - \dfrac{Q \cdot A_3}{Q \cdot A_2}\left(S - S_I\right)}
\end{aligned}
\tag{5.25}
$$

From Eq. 5.10, the terms of the coordinate function G_S in Eq. 5.25 are given by

for $S \le S_L$

$$g_{S1} = \frac{S}{S_L} \qquad g_{S2} = 0 \qquad g_{S3} = 0$$

for $S_L \le S \le S_I$

(5.26)

$$g_{S1} = 1 + \frac{(S - S_L)}{S_L} - \frac{2S_{IL} + 3S_L}{S_L S_{IL}^2}(S - S_L)^2 + \frac{S_{IL} + 2S_L}{S_L S_{IL}^3}(S - S_L)$$

$$g_{S2} = \frac{3}{S_{IL}^2}(S - S_L)^2 - \frac{2}{S_{IL}^3}(S - S_L)^3$$

$$g_{S3} = \frac{-1}{S_{IL}}(S - S_L)^2 + \frac{1}{S_{IL}^2}(S - S_L)^3$$

The final regression model included one additional refinement to the model given in Eq. 5.25. It was noted that the coefficients c_{S1}, c_{S2} and c_{S3} in Eq. 5.10 are succinctly represented by the product of the row and column matrices, Q and A where the subscript of A corresponds to the second subscript of c. Consequently, these coefficients, which represent the ordinate at S_L and the ordinate and slope at S_I, differ only by the regression coefficients A_1, A_2 and A_3. From Eq. 5.25, it was evident that some additional accuracy could be gained by allowing the use of unique coordinate functions in the direct product formulations for each Q corresponding to c_{S1}, c_{S2} and c_{S3}.

The final formulation for the regression model is given in Eq. 5.27

For $S < S_L$

$$P = Q_1 \cdot A_1 \, g_{S1}$$

For $S_L \leq S \leq S_I$

$$P = Q_1 \cdot A_1 \, g_{S1} + Q_2 \cdot A_2 \, g_{S2} + Q_3 \cdot A_3 \, g_{S3} \tag{5.27}$$

For $S \geq S_I$

$$P = \frac{Q_2 \cdot A_2}{1 - \frac{Q_3 \cdot A_3}{Q_2 \cdot A_2}(S - S_I)}$$

where each Q is defined by Eq. 5.28.

$$Q_1 = G_\lambda^{P(S_L)} \otimes G_{D/t}^{P(S_L)} \otimes G_{d/D}^{P(S_L)} \otimes G_{\delta/L}^{P(S_L)}$$

$$Q_2 = G_\lambda^{P(S_I)} \otimes G_{D/t}^{P(S_I)} \otimes G_{d/D}^{P(S_I)} \otimes G_{\delta/L}^{P(S_I)} \tag{5.28}$$

$$Q_3 = G_\lambda^{P'(S_I)} \otimes G_{D/t}^{P'(S_I)} \otimes G_{d/D}^{P'(S_I)} \otimes G_{\delta/L}^{P'(S_I)}$$

Since the products $Q_1 \cdot A_1$, $Q_2 \cdot A_2$ and $Q_3 \cdot A_3$, are coefficients of g_{s1}, g_{s2} and g_{s3} (from Eq. 5.27) and represent the ordinate of the nondimensionalized load-shortening relationship at S_L and the ordinate and slope at S_I, respectively, the superscripts, $P(S_L)$, $P(S_I)$ and $P'(S_I)$ are used to differentiate between the coordinate functions G that comprise the row matrices, Q_1, Q_2 and Q_3. The regression model is now completed with the definitions of the coordinate functions for λ, D/t, d/D and δ/L as given in the following sections.

Coordinate functions were selected based on the trends suggested from the relationships between the values of $P(S_L)$, $P(S_I)$ and $P'(S_I)$ as functions of λ, D/t, d/D and δ/L. While the coordinate functions G that comprise Q_1, Q_2, and Q_3 and the regression coefficients, A_1, A_2 and A_3 represent the least squares approximation to the entire database of load-shortening relationships, it is sometimes convenient to observe the coordinate functions in relation to the actual values of $P(S_L)$, $P(S_I)$ and $P'(S_I)$ included in the database. This approach was useful in selecting coordinate functions as described in the following sections.

5.5.1 Coordinate Functions for λ

The coordinate function selected to represent $P(S_L)$ as a function of λ is given by Eq. 5.29.

$$G_{\lambda}^{P(S_L)} = \left[\frac{1}{1.5 + \lambda} \qquad \operatorname{sech}\left(\frac{\lambda^2}{2} \right) \right] \tag{5.29}$$

The general shape of each term of the coordinate function is shown in Fig. 5.9 for values of λ ranging from 0.4 to 1.2. This serves to illustrate the characteristics of the selected coordinate function as it pertains to the relationship indicated by the data as described in the next paragraph.

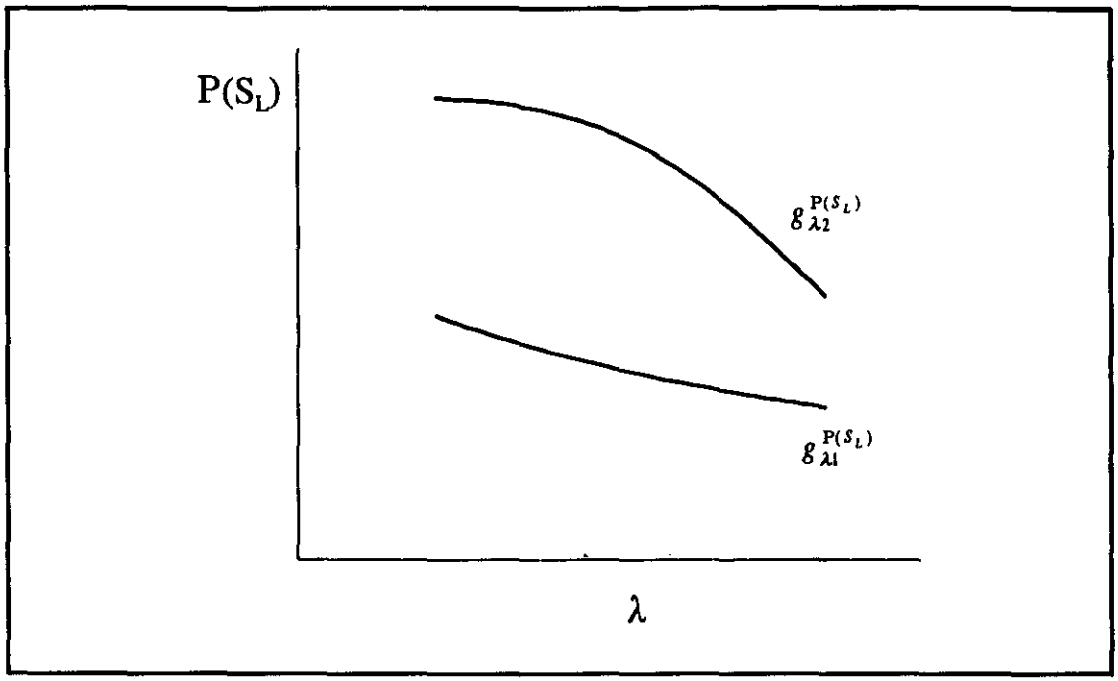

Figure 5.9 Two term coordinate function representing $P(S_L)$ as a function of λ.

The general basis for selecting this coordinate function is illustrated by observing values of $P(S_L)$ as a function of λ for constant values of D/t, d/D and δ/L. For example, the discrete data points shown in Fig. 5.10 are values of $P(S_L)$ for D/t≈40, d/D≈0.10 and δ/L≈0.0. By observing this relationship and the relationships for other values of D/t, d/D and δ/L, the desired characteristics of the coordinate function representing $P(S_L)$ as function of λ were determined. One of these characteristics was a generally decreasing function asymptotically approaching zero for large values of λ. Also, for decreasingly small values of λ the observed slope of the data varied considerably from zero to some finite (negative) value. These observations followed by an iterative procedure of "tweaking" the coordinate functions to minimize the least

squares residual led to the selection of the coordinate function given by Eq. 5.29 and shown in Fig. 5.9.

The continuous function shown in Fig. 5.10 is a linear combination of the two terms of the coordinate function for λ given by Eq. 5.29 and was calculated from the actual regression coefficients given in Chapter 6 and the specific values of D/t, d/D and δ/L by the procedure described in Section 4.1.4. This specific relationship illustrates the nature of the coordinate function with an example of the data used in selection process. Good correlation between the coordinate function and the values of $P(S_L)$ is observed.

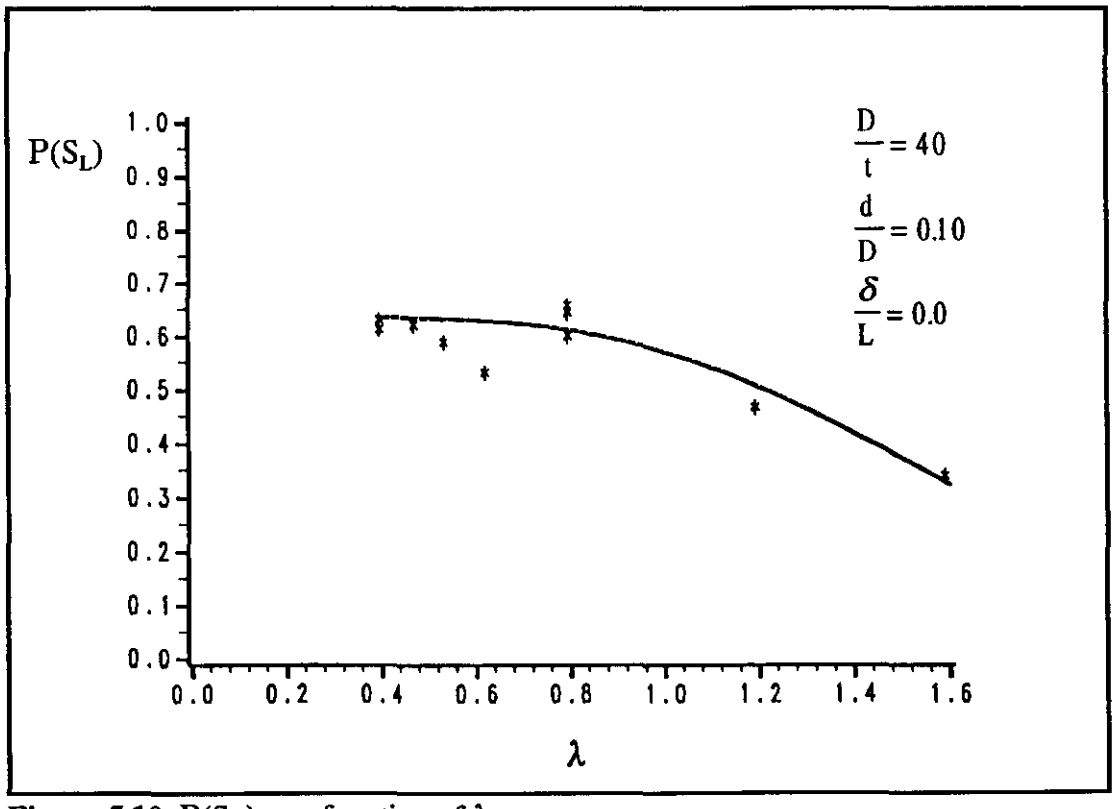

Figure 5.10 $P(S_L)$ as a function of λ.

The values of $P(S_I)$ as a function of λ exhibited characteristic shape similar to that for $P(S_L)$. The coordinate function selected for $P(S_I)$ as a function of λ is given by Eq. 5.30.

$$G_{\lambda}^{P(S_I)} = \left[e^{-\lambda} \quad \operatorname{sech}(2\lambda^2) \right] \tag{5.30}$$

The general shape of each term of the coordinate function is shown in Fig. 5.11 for values of λ ranging from 0.4 to 1.2. Selection of these two terms is based on the characteristics suggested by the data.

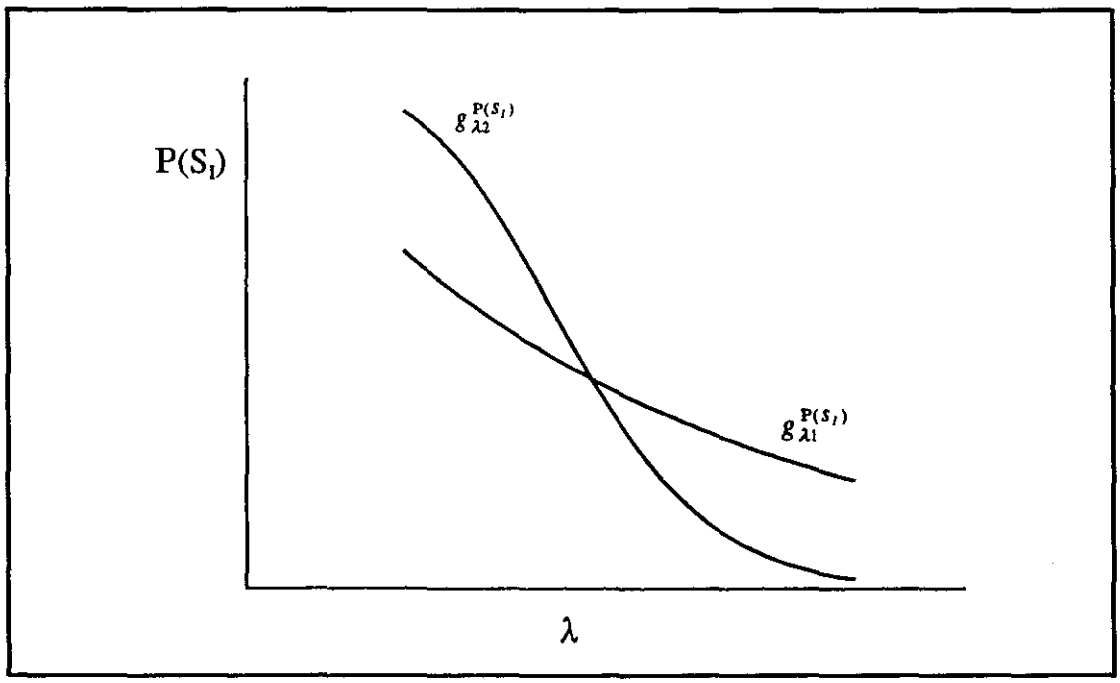

Figure 5.11 Two term coordinate function representing $P(S_I)$ as a function of λ.

For example, the data for specific values of the remaining parameters ($D/t \approx 40$, $d/D \approx 0.10$ and $\delta/L \approx 0.0$) and the linear combination of the two terms of the coordinate function determined from the actual regression coefficients are shown in Fig. 5.12. Again, good correlation is observed between the values of $P(S_I)$ from the database and the coordinate function.

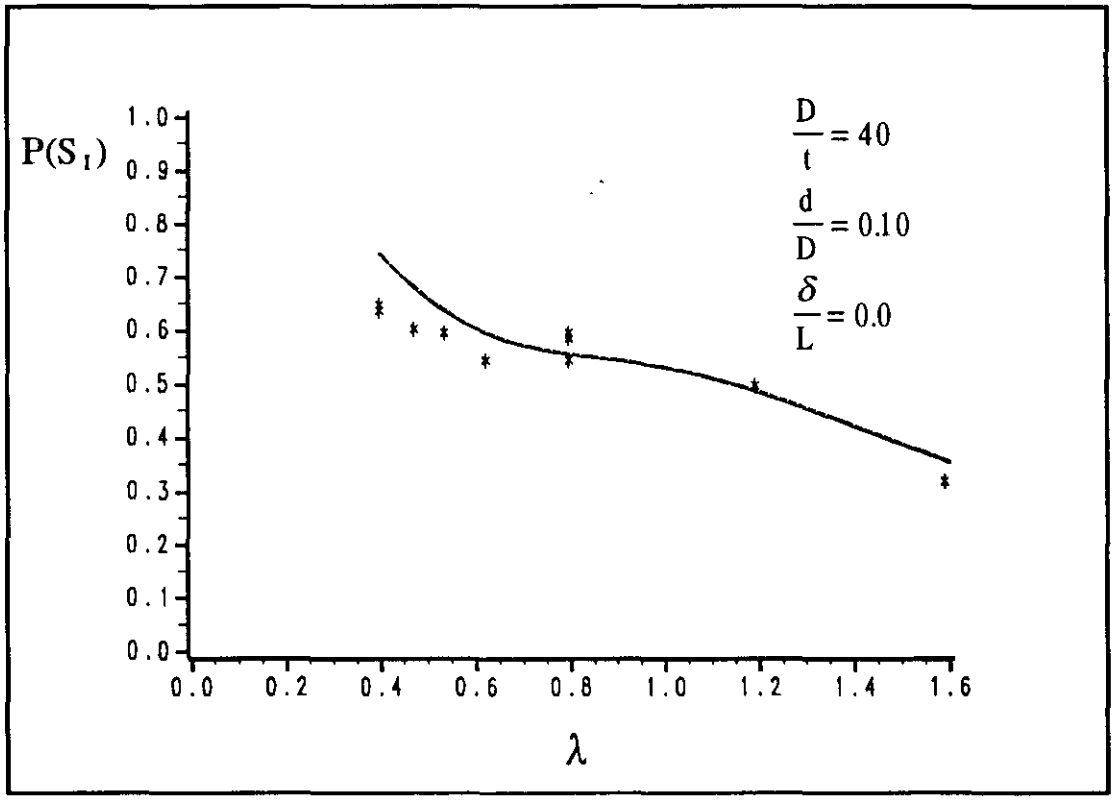

Figure 5.12 $P(S_I)$ as a function of λ.

The coordinate function selected for $P'(S_I)$ is given by Eq. 5.31

$$G_{\lambda}^{P'(S_I)} = \left[\lambda e^{-\lambda} \quad \lambda^3 e^{-\lambda^2}\right] \tag{5.31}$$

Each term of the coordinate function is graphically illustrated in Fig. 5.13 for values of λ ranging from 0.4 to 1.2 .

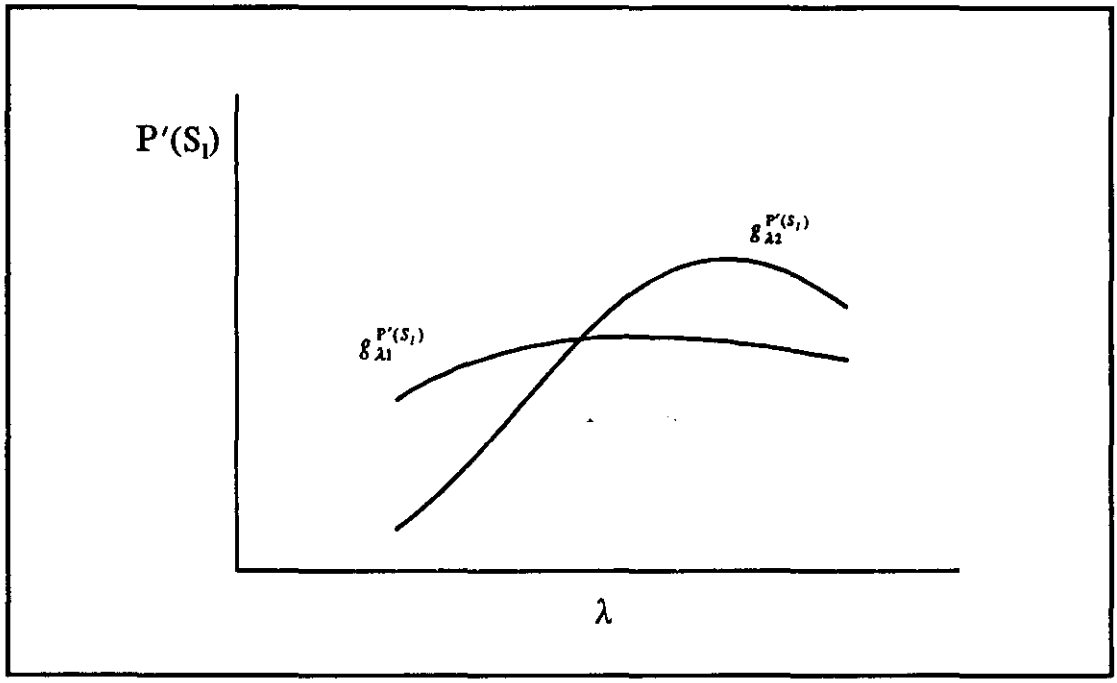

Figure 5.13 Two term coordinate function representing $P'(S_I)$ as a function of λ.

The nature of the relationship between the slope of the load-shortening curve at S_I, $P'(S_I)$, as a function of λ had significantly different characteristic shapes compared to the monotonically decreasing relationships for $P(S_L)$ and $P(S_I)$. As shown in Fig. 5.14, the data indicate a function whose value decreases from a maximum value for increasing and decreasing values of λ. This behavior was observed for columns with slight to moderate damage (dent depth and out-of-straightness). This may be explained by considering the behavior of a column as its slenderness approaches small and large extremes. As a column becomes less slender its response will tend toward that of a stub column where the behavior reflects the material properties (and residual

stress effects). Thus for mild structural steel the response would tend toward a flat post-ultimate curve. Conversely, as λ increases beyond a certain value, the column will tend toward elastic post-buckling behavior and the column will have some capacity to resist the applied load effects resulting in a "flatter" load-shortening response in the post-ultimate range. For columns with greater damage, the absolute value of $P'(S_1)$ tends to be relatively small and does not vary significantly as a function of λ. This occurs because the effects of bending (both localized in the vicinity of the dent and overall member bending from the effects of the initial out-of-straightness) tend to dominate the member response.

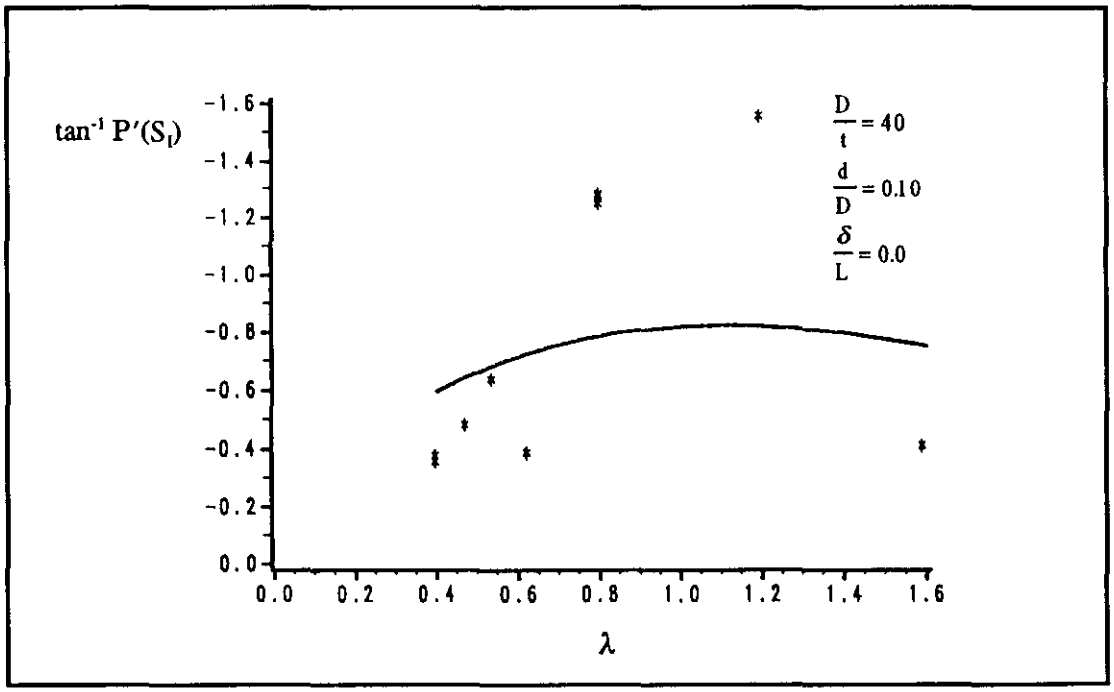

Figure 5.14 Inverse tangent of $P'(S_1)$ as a function of λ.

The relationship between $P'(S_I)$ and λ is shown in Fig. 5.14 as the inverse tangent of $P'(S_I)$ as a function of λ. The inverse tangent of $P'(S_I)$ is the angle from the horizontal of the tangent to the load-shortening curve at $P(S_I)$ and was convenient for plotting because of the finite range of the inverse tangent function (0 to $-\pi/2$ for non-positive arguments) compared to the infinite range of the slope $P'(S_I)$.

The agreement, or lack of, between the data and the values predicted by the regression model shown in Fig. 5.14 deserve comment considering the very good agreement between the regression model and the data for $P(S_L)$ and $P(S_I)$ shown in Figs. 5.10 and 5.12. Obviously, the coordinate function shown in Fig. 5.14 is the result of the least squares fit of the complete model to the load-shortening data in the database and not the result of fitting the coordinate function $G_{\lambda}^{P'(S_I)}$ to the data in the figure. For load shortening curves with steep unloading curves, the hyperbola that constitutes G_S for $S>S_I$ given in Eq. 5.27 tends to provide good fit in the post-ultimate range for smaller values of the slope at $S = S_I$ than those depicted by the data in Fig. 5.14. This is illustrated by comparing the predicted and actual load-shortening relationships for the column represented by the data point ($\lambda = 1.2$, $\tan^{-1} = -1.56$). This column represents a large discrepancy between the actual and predicted values of $P'(S_I)$ yet, there is good agreement between the actual and predicted load-shortening curve as shown in Fig. 6.5 (Comparisons between predicted and actual load-shortening curves are shown in Chapter 6). This is explained in part by the fact that the

regression procedure minimizes the least squares error between the data and the approximating function and agreement between the slope of the data and the slope of the approximating function should not be expected to be as good.

5.5.2 Coordinate Functions for D/t

Over the range considered in this study, the effect of D/t on the column response as quantified by $P(S_L)$ and $P(S_I)$ was not as significant as the slenderness. A slight to moderate monotonically decreasing trend for $P(S_L)$ and $P(S_I)$ with increasing D/t ratio was observed. The coordinate functions representing $P(S_L)$ and $P(S_I)$ as a function of D/t are given in the following equations.

$$G_{D/t}^{P(S_L)} = \left[1 \qquad \log_{10}\frac{D}{t} \right] \tag{5.32}$$

$$G_{D/t}^{P(S_I)} = \left[1 \qquad \log_{10}\frac{D}{t} \right] \tag{5.33}$$

Note that a monotonically decreasing function is realized if the coefficient for the logarithmic term in these coordinate functions is negative. The general shape of each term of the coordinate function is illustrated in Fig. 5.15.

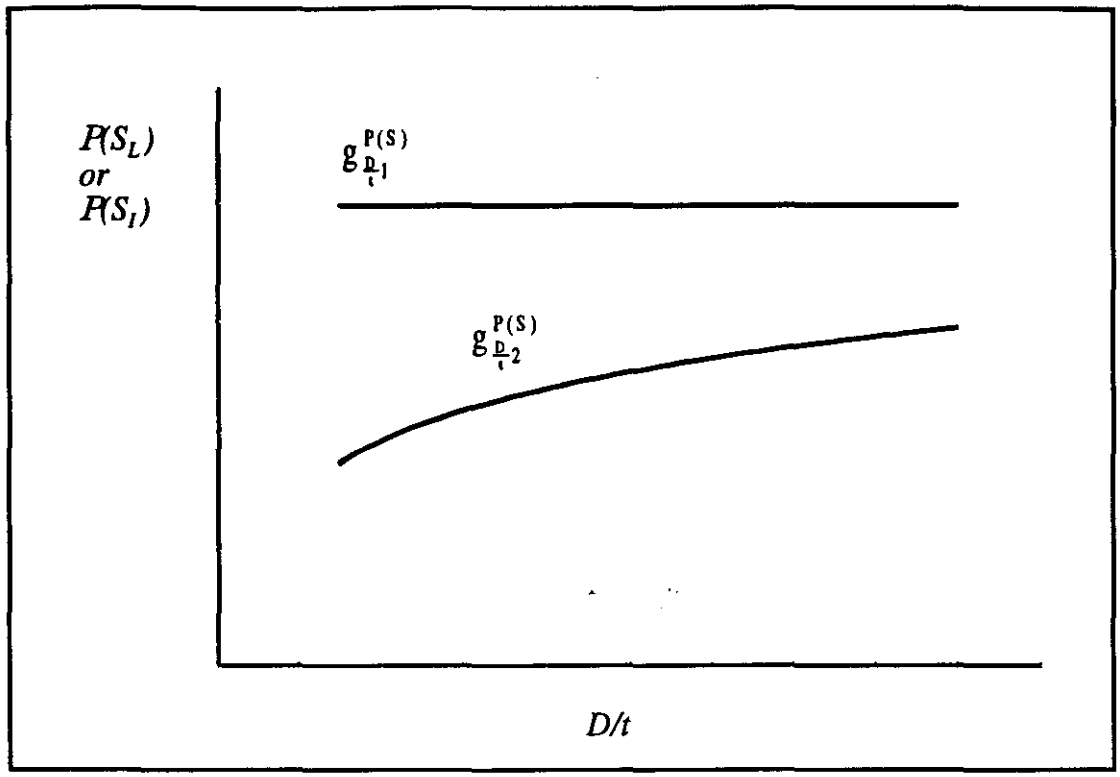

Figure 5.15 Two term coordinate function representing $P(S_L)$ or $P(S_I)$ as a function of D/t.

Examples of the relationship between $P(S_L)$ and $P(S_I)$ as a function of D/t are given by the discrete data points plotted in Figs. 5.16 and 5.17 for the indicated values of λ, d/D and δ/L. The continuous functions shown are the actual coordinate functions given by the products $Q_1 \cdot A_1$ and $Q_2 \cdot A_2$, respectively. Very good agreement is observed between the coordinate functions derived from the complete model and the data.

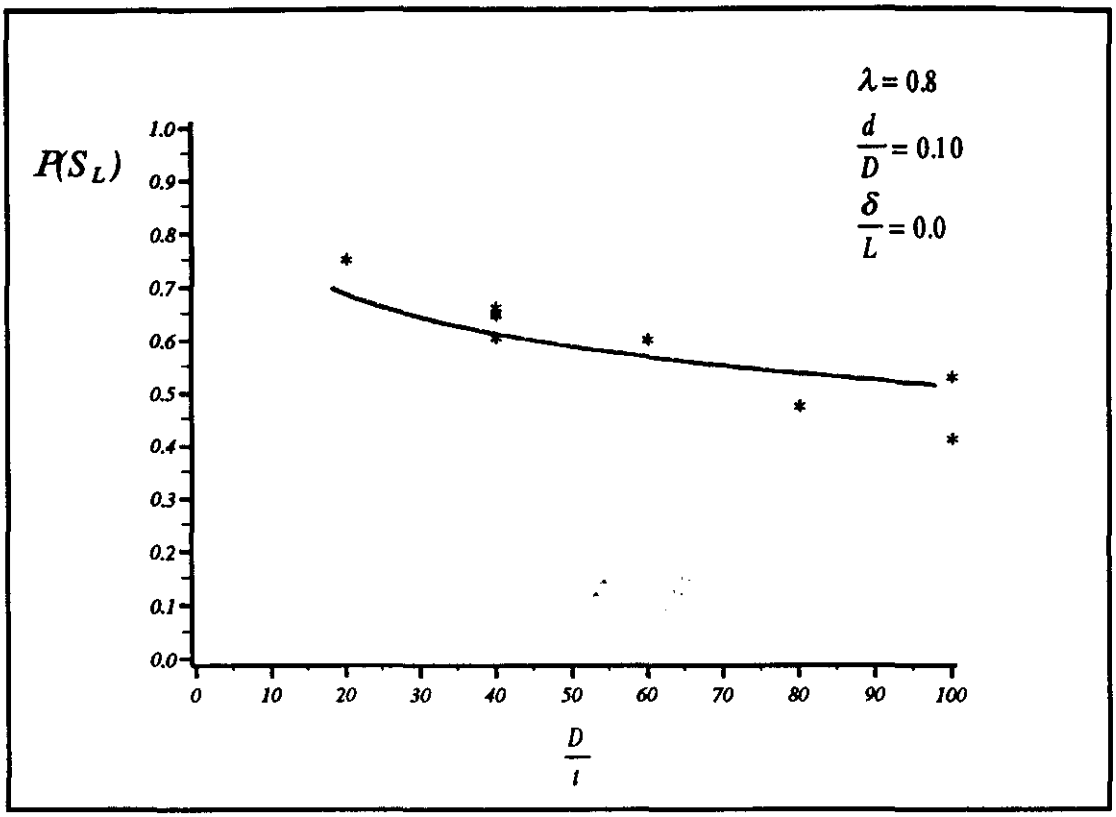

Figure 5.16 $P(S_L)$ as a function of D/t.

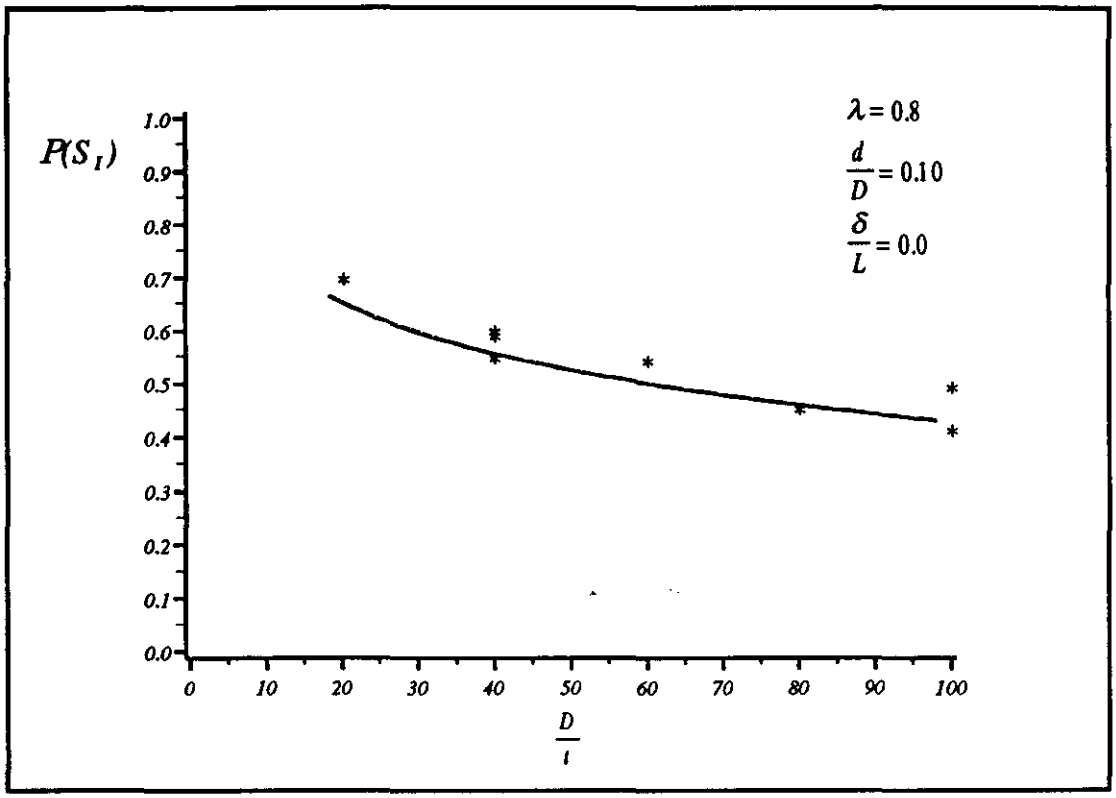

Figure 5.17 $P(S_I)$ as a function of D/t.

The effect of D/t on the slope at $S = S_I$, that is $P'(S_I)$, was more slightly more pronounced for columns with relatively small amounts of damage. For columns with greater damage the effect of D/t was not as great. In all cases, the general trend was a monotonically decreasing function with positive curvature. A reciprocal function of D/t and a constant term were selected as the coordinate function for $P'(S_I)$ as a function of D/t as given in Eq. 5.34 and shown in Fig. 5.18.

$$G_{D/t}^{P'(S_I)} = \left[1 \quad \left(\frac{D}{t}\right)^{-1} \right] \tag{5.34}$$

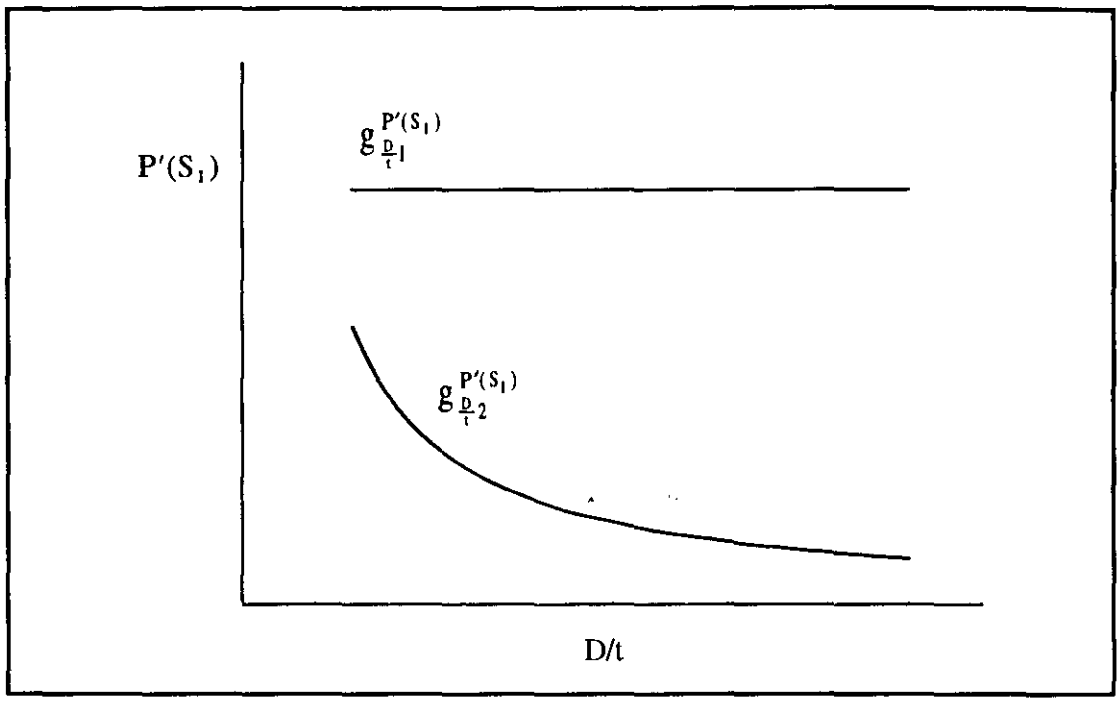

Figure 5.18 Two term coordinate function representing $P'(S_1)$ as a function of D/t.

An example of the relationship between $P'(S_1)$ and D/t is given by the discrete data points plotted in Fig. 5.19 for the indicated values of λ, d/D and δ/L. For consistency of scale in the plots the inverse tangent of $P'(S_1)$ is plotted as a function of D/t. The continuous function shown is the actual coordinate functions given by the product $Q_3 \cdot A_3$. The coordinate function calculated from the regression on the complete model and matches the decreasing trend indicated by the data although the predicted values of the slope at $S = S_1$ are smaller than the actual values. Again, this is due to the nature of the hyperbola used to approximate the post-ultimate range of the load-shortening relationship.

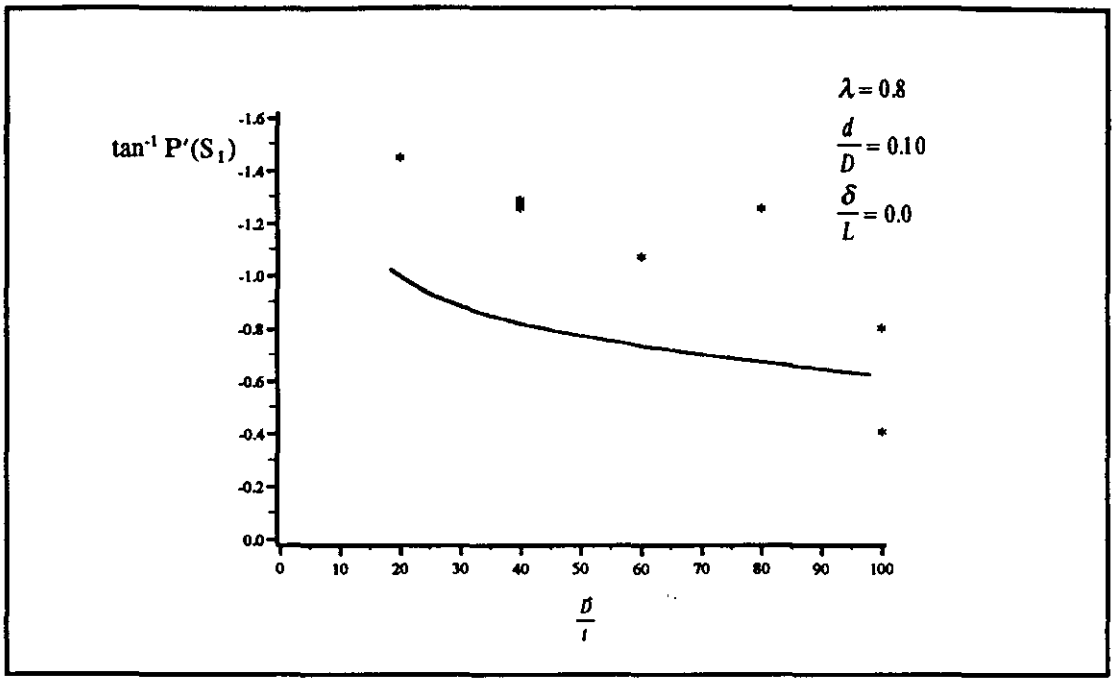

Figure 5.19 Inverse tangent of $P'(S_I)$ as a function of D/t.

5.5.3 Coordinate Functions for d/D

The relationships between $P(S_L)$ or $P(S_I)$ and d/D would be expected to be a monotonically decreasing function. It was also observed from the data that $P(S_L)$ and $P(S_I)$ asymptotically approached zero with increasing dent depth. Given that d/D has a maximum value of 1.0 and the reasonable assumption that $P(S_L)$ and $P(S_I)$ would equal zero at that point, the coordinate functions for d/D could be so constrained. A cubic parabola with its slope and magnitude constrained to zero at d/D=1.0 was selected for $P(S_L)$ and $P(S_I)$ as a function of d/D. The coordinate

functions are given by the following two equations and illustrated in Fig. 5.20 for $0 \le d/D \le 0.35$.

$$G_{d/D}^{P(S_L)} = \left[\frac{d}{D} - 2\left(\frac{d}{D}\right)^2 + \left(\frac{d}{D}\right)^3 \quad 1 - 3\left(\frac{d}{D}\right)^2 + 2\left(\frac{d}{D}\right)^3 \right] \tag{5.35}$$

$$G_{d/D}^{P(S_I)} = \left[\frac{d}{D} - 2\left(\frac{d}{D}\right)^2 + \left(\frac{d}{D}\right)^3 \quad 1 - 3\left(\frac{d}{D}\right)^2 + 2\left(\frac{d}{D}\right)^3 \right] \tag{5.36}$$

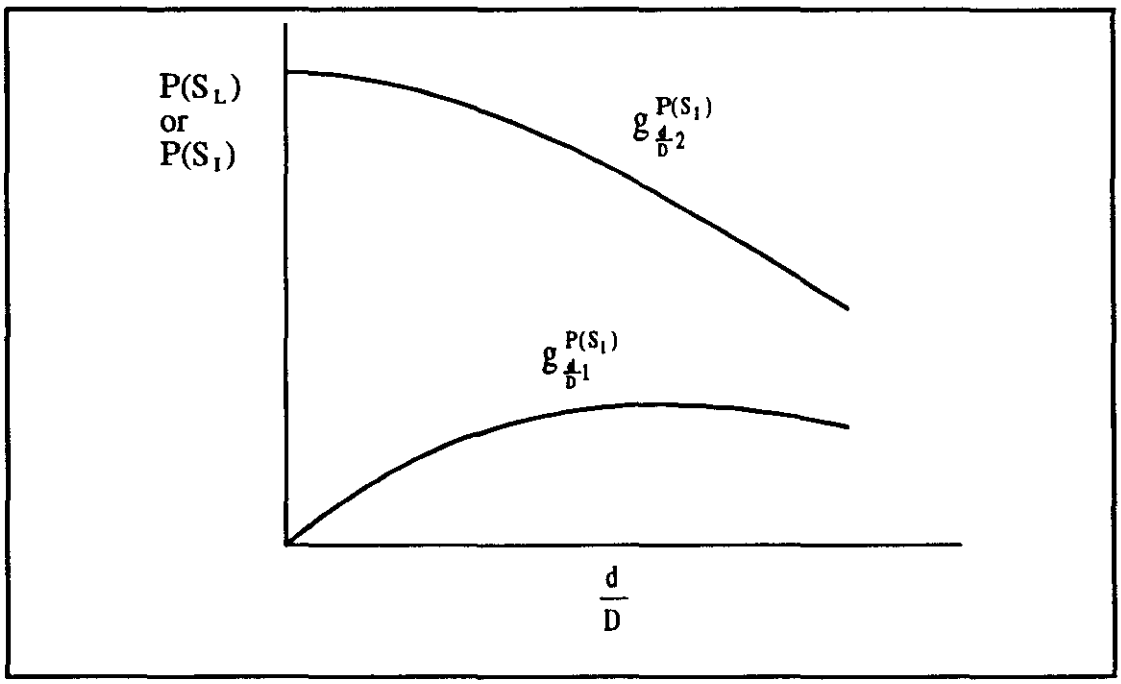

Figure 5.20 Two term coordinate function representing $P(S_L)$ or $P(S_I)$ as a function of d/D.

An example of the relationships between $P(S_L)$, $P(S_I)$ and d/D as provided by the data are shown in Figs. 5.21 and 5.22. Very good agreement between the data and the coordinate function calculated from Eq. 5.28 and the regression coefficients given in Chapter 6 validate the selected coordinate functions.

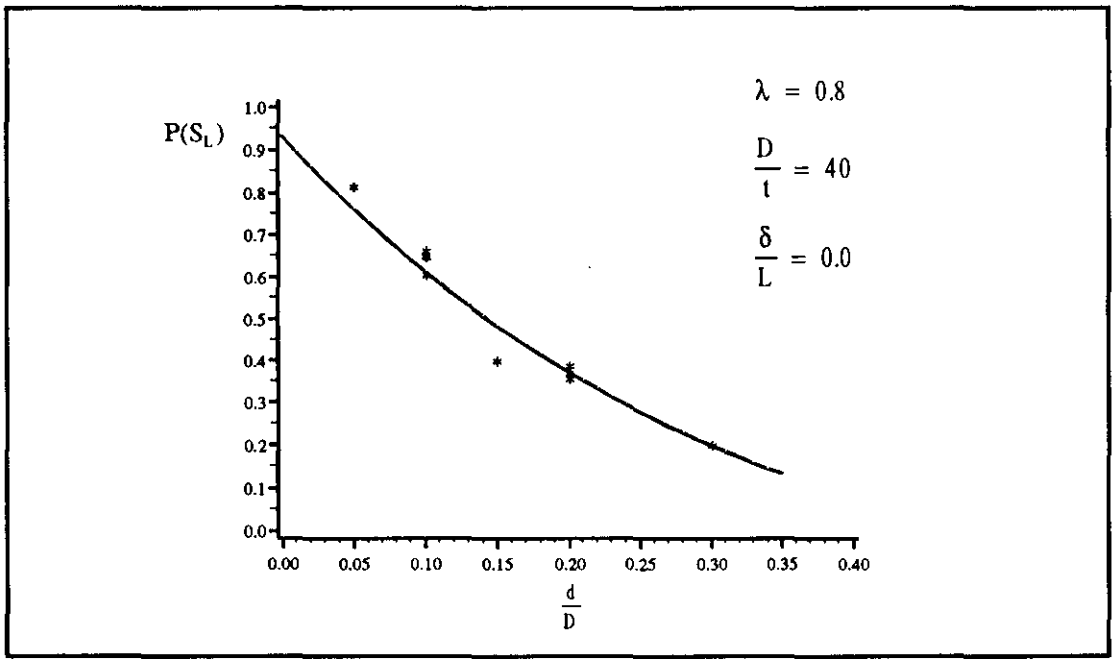

Figure 5.21 $P(S_L)$ as a function of d/D.

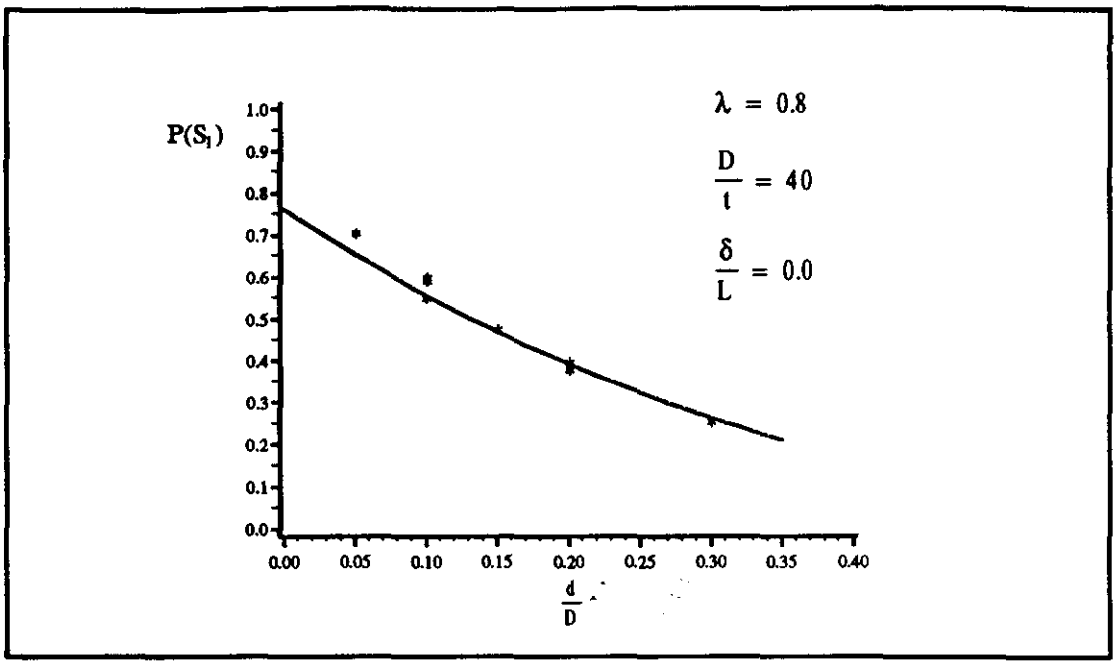

Figure 5.22 $P(S_1)$ as a function of d/D.

The coordinate function selected for $P'(S_1)$ as a function of d/D is given by Eq. 5.37 and illustrated in Fig. 5.18. The relationship described by each term of the function is, again, a monotonically decreasing function.

$$G_{d/D}^{P'(S_1)} = \left[1 - \frac{d}{D} \quad \frac{1 - \frac{d}{D}}{0.1 + \frac{d}{D}} \right] \tag{5.37}$$

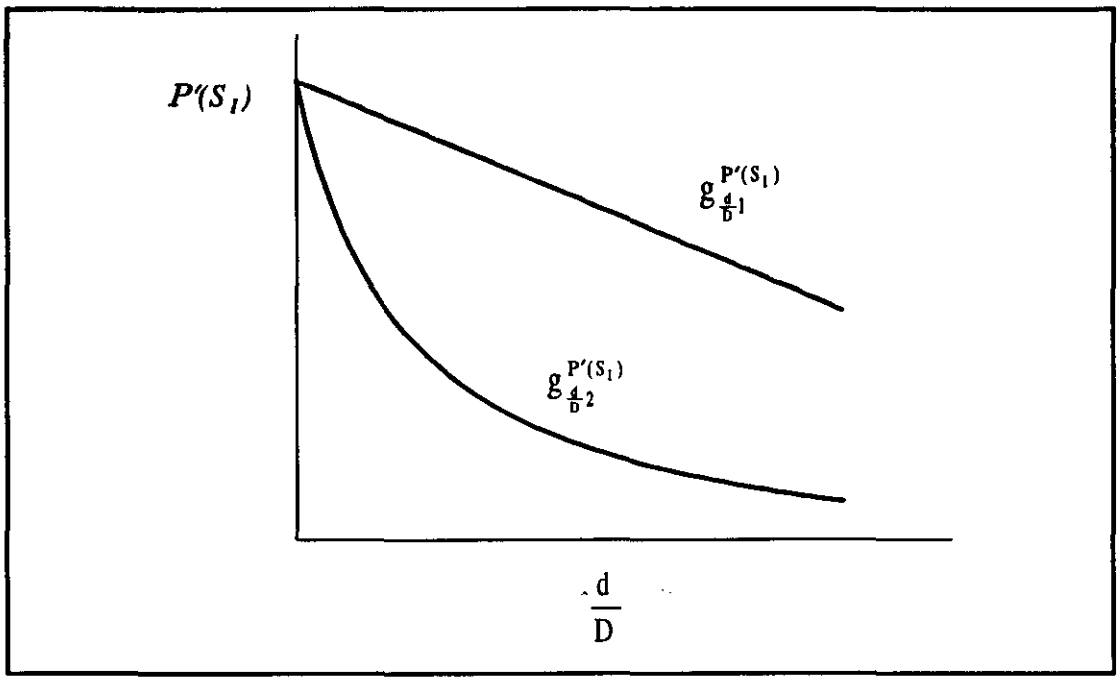

Figure 5.23 Two term coordinate function for $P'(S_1)$ as a function of d/D.

An example of the relationship between $P'(S_1)$ and d/D as provided by the data is shown in Fig. 5.24. There is correlation with the decreasing trend observed from the data and the coordinate function calculated from the product $Q_3 \cdot A_3$. Again, for large values of $P'(S_1)$, the coordinate function underestimates the data and, as previously discussed, this does not necessarily reflect on the goodness of fit to the load-shortening curves.

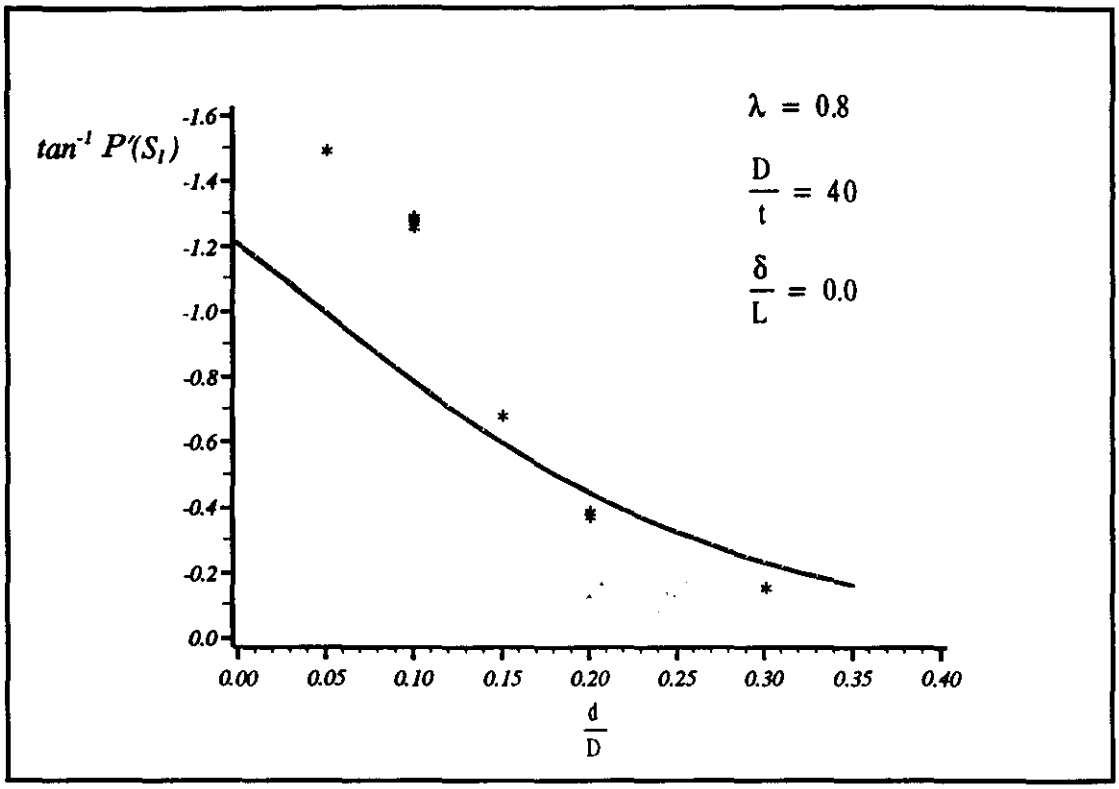

Figure 5.24 $P'(S_1)$ as a function of d/D

5.5.4 Coordinate Functions for δ/L

The coordinate function selected for $P(S_L)$ as a function of δ/L is given by Eq. 5.38. The individual terms of the coordinate function are shown in Fig. 5.25 over a range of δ/L from 0.0 to 0.02. Again as suggested by the data, the objective was a monotonically decreasing function.

$$G_{\delta/L}^{P(S_L)} = \begin{bmatrix} e^{-100\frac{\delta}{L}} & \dfrac{1}{2 + 100\dfrac{\delta}{L}} \end{bmatrix} \tag{5.38}$$

An example of the nature of the relationship between $P(S_L)$ and δ/L is shown in Fig. 5.26. Very good agreement is observed between the data and the coordinate function calculated from the regression coefficients.

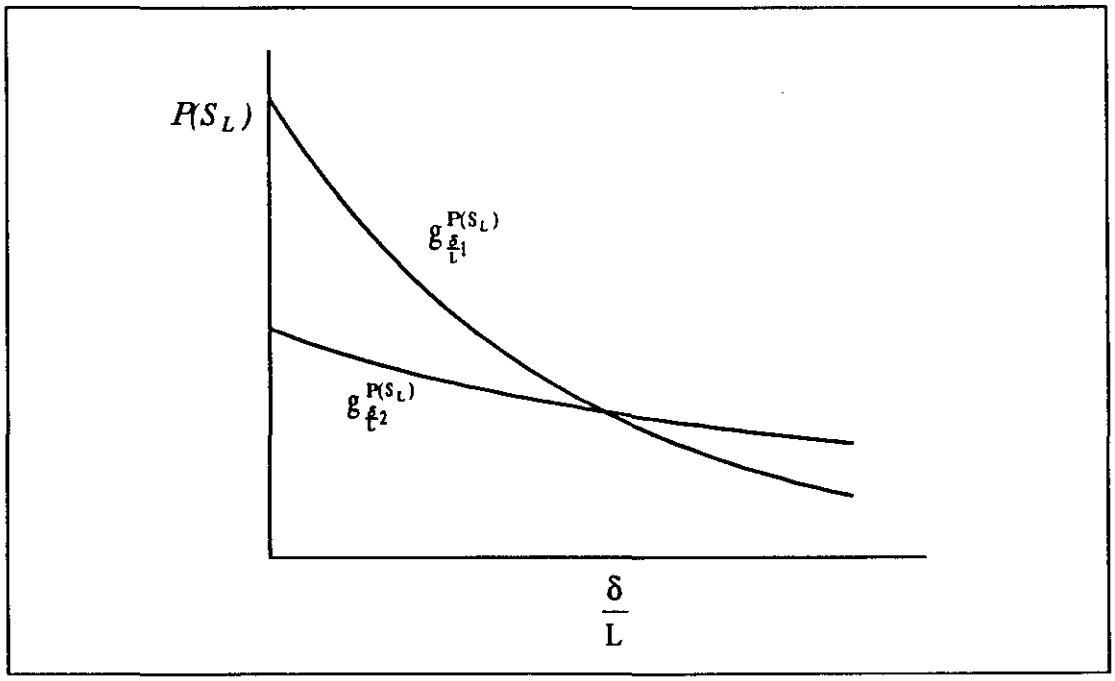

Figure 5.25 Two term coordinate function representing $P(S_L)$ as a function of δ/L.

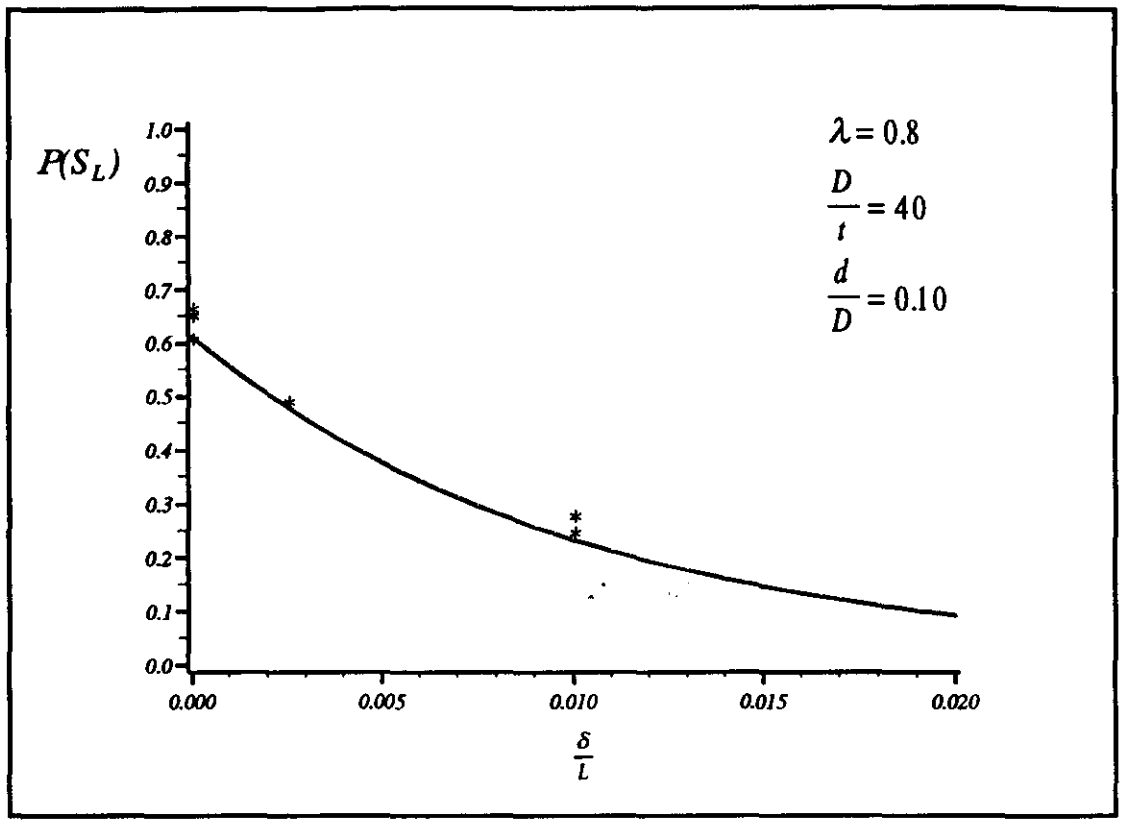

Figure 5.26 $P(S_L)$ as a function of δ/L

The coordinate function selected to represent the relationship between $P(S_I)$ and δ/L is given in Eq. 5.39 and illustrated in Fig. 5.27.

$$G_{\delta/L}^{P(S_I)} = \left[e^{-100\frac{\delta}{L}} \quad \frac{1}{1 + 15\frac{\delta}{L}} \right] \tag{5.39}$$

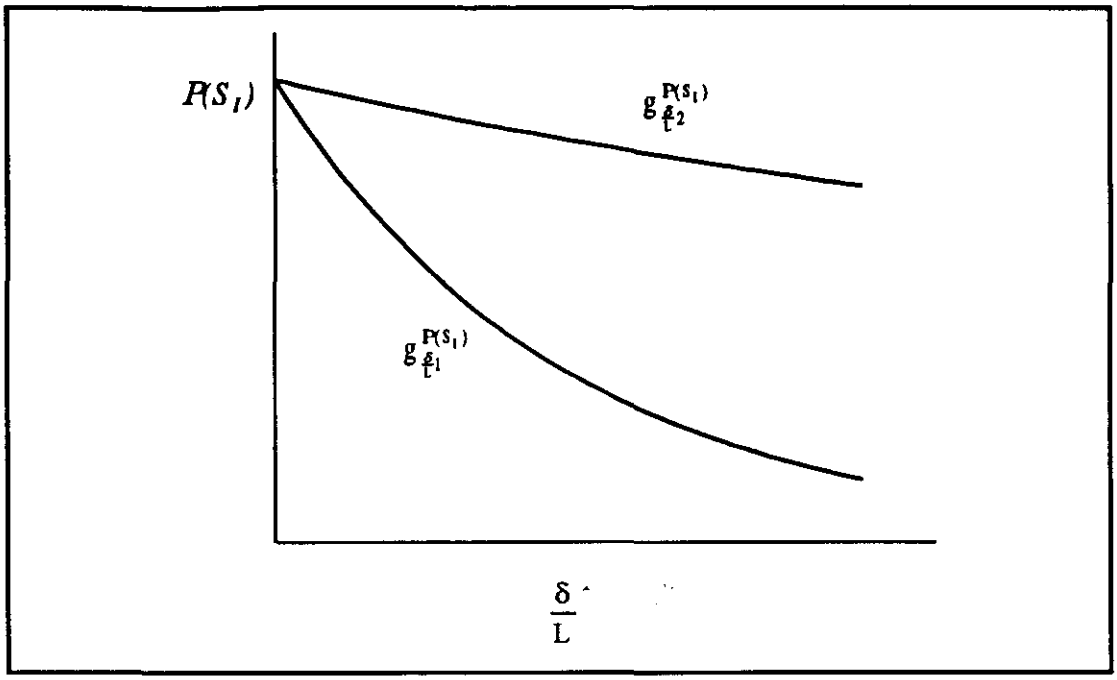

Figure 5.27 Two term coordinate function representing $P(S_1)$ as a function of δ/L.

An example of the relationship between $P(S_1)$ and δ/L defined by the data is shown in Fig. 5.28. Good agreement is observed between the data and the reuslts of the regression model.

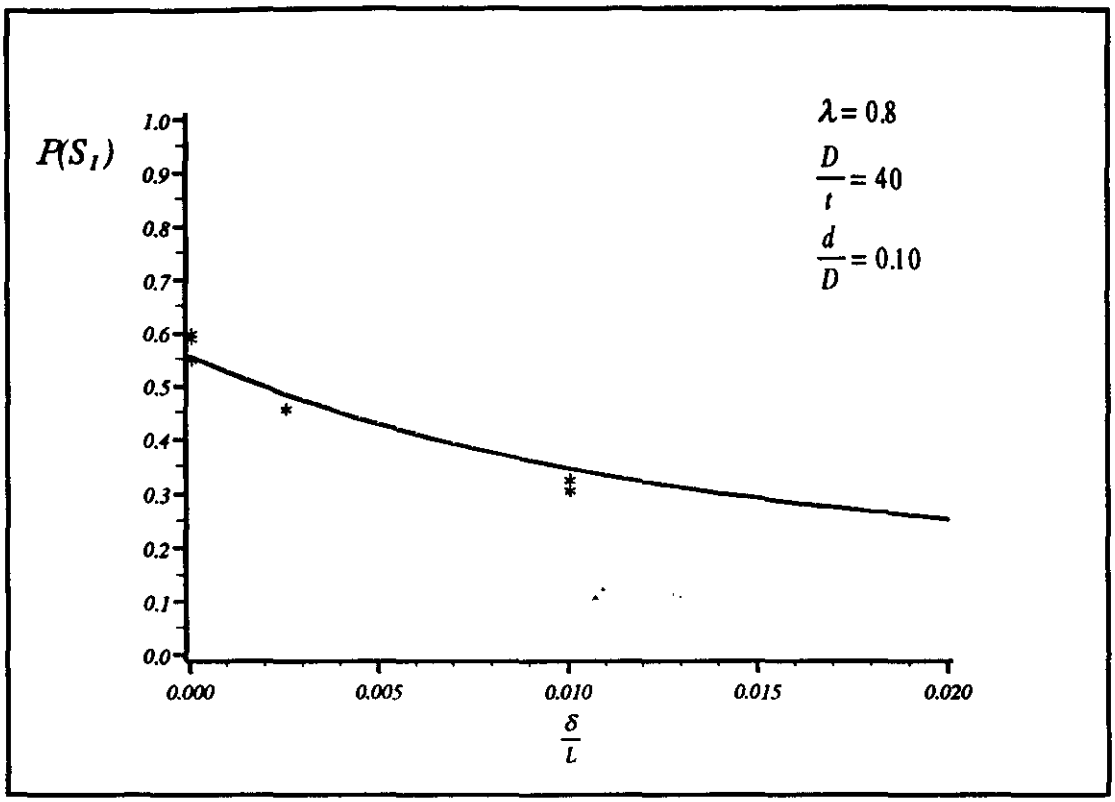

Figure 5.28 $P(S_1)$ as a function of δ/L.

The coordinate function selected for $P'(S_1)$ as a function of δ/L is given by Eq. 5.40 and is illustrated in Fig. 5.29. The two terms of the coordinate function both asymptotically approach zero for increasing out-of-straightness. The first term provides for a very rapid decrease in $P'(S_1)$ as δ/L increases from zero. This term was selected to reflect the sensitivity of the column response to small amounts of out-of-straightness compared to a straight column.

$$G_{\delta/L}^{P'(S_1)} = \left[\frac{1}{3 + 10^4 \frac{\delta}{L}} \quad \frac{1}{1 + 10 \frac{\delta}{L}} \right] \tag{5.40}$$

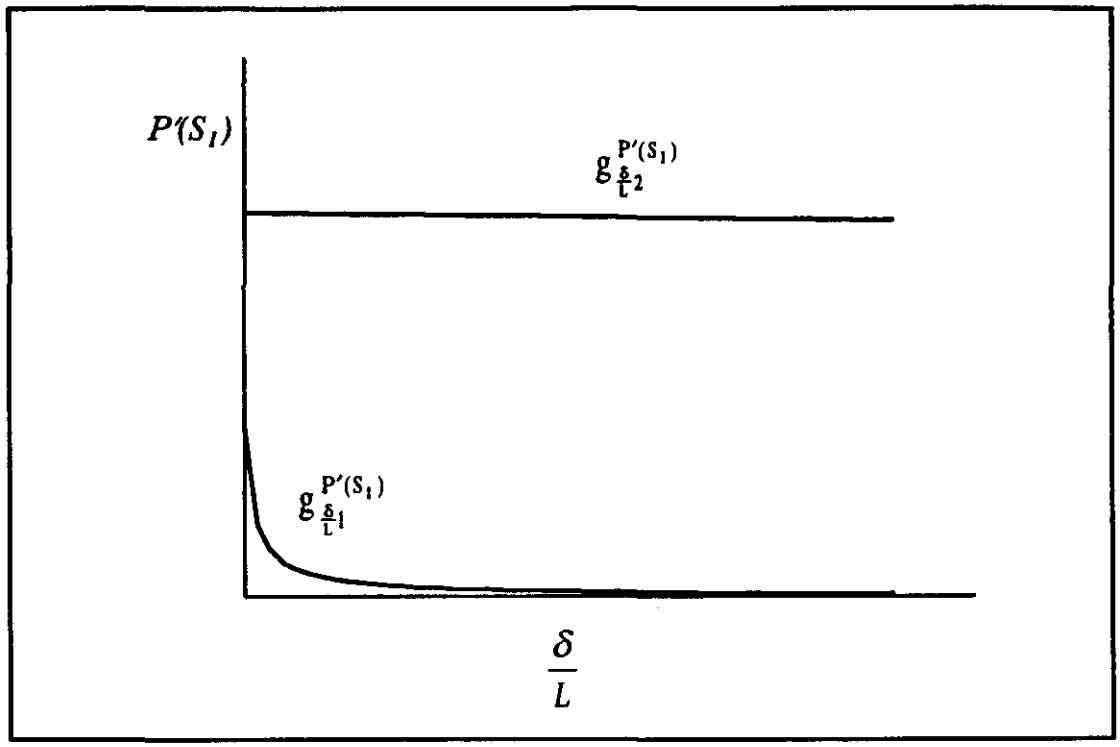

Figure 5.29 Two term coordinate function representing $P'(S_1)$ as a function of δ/L.

An example of the relationship between $P'(S_1)$ and δ/L as depicted by the data is shown in Fig. 5.30. Again, the correlation between the coordinate function for this example and the trend suggested by the data is good with the coordinate function underestimating the data for large values of $P'(S_1)$.

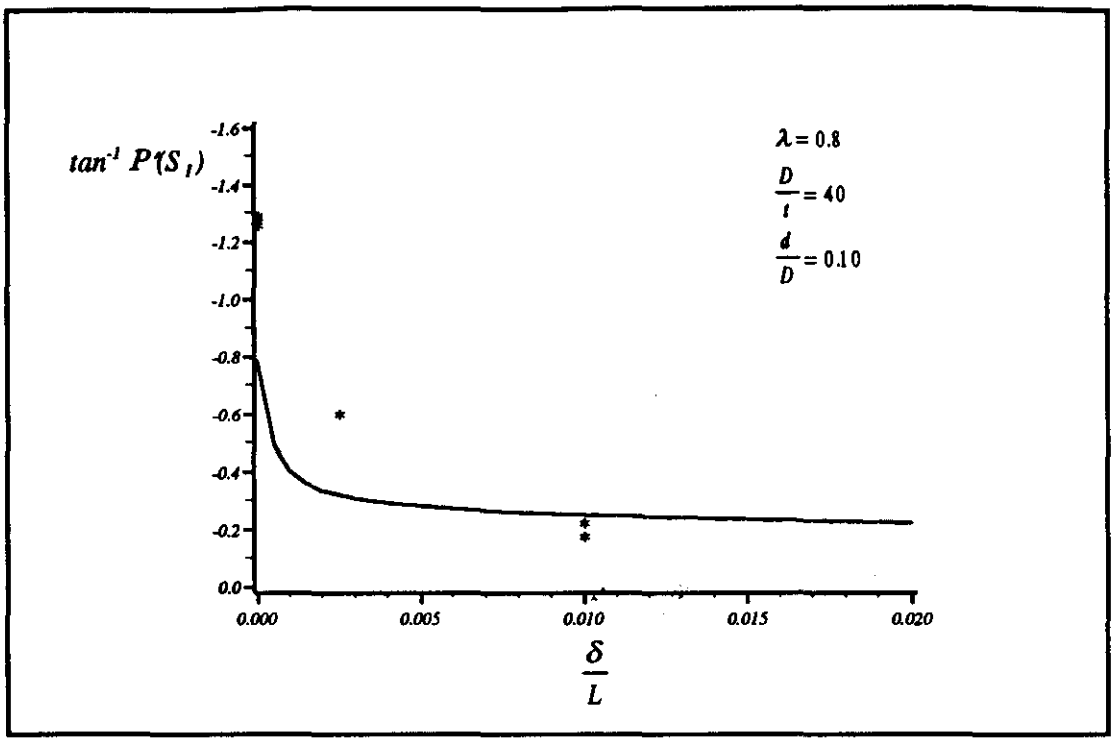

Figure 5.30 $P'(S_I)$ as a function of δ/L.

6 Results and Application

6.1 The Regression Analysis

The regression analysis was conducted in two parts. First, a linear regression analysis was performed to determine the regression coefficients for the model for S_L and S_{IL}. Then a nonlinear regression analysis was performed to determine the regression coefficients for the load-shortening response.

6.1.1 Solution of the Least Squares Equations

Solution of the regression equations was performed with the SAS/STAT[1] software. Solution of the linear regression equations was performed by a sweep algorithm with a singularity check applied to the normalized equations (See Refs. 26 or 27) . The nonlinear regression equations were solved by a Gaus-Newton procedure (See Ref. 26).

---

[1] SAS Institute, Inc.
SAS Campus Drive
Cary, NC 27513

The solution of the nonlinear regression equations requires initial values for each of the regression coefficients. These initial values were calculated from a separate linear regression analysis employing the same coordinate functions for λ, D/t, d/D and δ/L as were used in the nonlinear regression model. Unlike the complete regression model given by Eq. 5.27, the coordinate function for P as a function of S used in the linear model for the initial values was a linear combination of three terms. (The difference between the models is the nonlinearity introduced by the portion of the coordinate function for $S>S_1$ as given by Eq. 5.27 or 5.10.) The coordinate function for S used in the linear model for the initial guesses is given in Eq. 6.1.

$$G_S = \begin{bmatrix} g_{S1} & g_{S2} & g_{S3} \end{bmatrix}$$

where,

for $S \le S_L$

$$g_{S1} = \frac{S}{S_L} \qquad g_{S2} = 0 \qquad g_{S3} = 0$$

for $S_L \le S \le S_I$

$$g_{S1} = 1 + \frac{(S - S_L)}{S_L} - \frac{2S_{IL} + 3S_L}{S_L S_{IL}^2}(S - S_L)^2 + \frac{S_{IL} + 2S_L}{S_L S_{IL}^3}(S - S_L)^3 \qquad \textbf{(6.1)}$$

$$g_{S2} = \frac{3}{S_{IL}^2}(S - S_L)^2 - \frac{2}{S_{IL}^3}(S - S_L)^3$$

$$g_{S3} = \frac{-1}{S_{IL}}(S - S_L)^2 + \frac{1}{S_{IL}^2}(S - S_L)^3$$

for $S \ge S_I$

$$g_{S1} = 0 \qquad g_{S2} = \frac{S + 1}{\frac{S^2}{2} + S + 1} \qquad g_{S3} = \frac{S}{\frac{S^2}{2} + 1}$$

The linear regression model for the initial "guesses" of the regression coefficients is then given by Eq 6.2

$$\mathrm{P} = [\, Q_1 g_{S1} \quad Q_2 g_{S2} \quad Q_3 g_{S3} \,]\, \{A\} \qquad \textbf{(6.2)}$$

where the Q's are defined by Eq. 5.28 and the g's are given in Eq. 6.1. The vector A is the regression coefficients used as initial values in the nonlinear regression model for the load-shortening behavior.

6.1.2 The Regression Coefficients

The regression coefficients for the model for S_L are given in Eq. 6.3. The predicted values of S_L are given by premultipling this column vector by the row vector Q_{S_L} given by Eq. 5.17.

$$A_{S_L} = \begin{bmatrix} -4.341821 \\ 3.27389 \\ 0.24228 \\ -0.403522 \\ 5.727217 \\ -3.859998 \\ -0.297595 \\ 0.462575 \\ 1.698626 \\ -0.703155 \\ -0.179246 \\ 0.138208 \\ -2.23634 \\ 0.857564 \\ 0.210483 \\ -0.163478 \end{bmatrix} \tag{6.3}$$

The regression coefficients for the model for S_{IL} are given in Eq. 6.4. The predicted values of S_{IL} are given by premultipling this column vector by the row vector $Q_{S_{IL}}$ given by Eq. 5.22.

$$A_{S_{IL}} = \begin{bmatrix} 0.30344 \\ -0.382705 \\ -0.419944 \\ 0.682584 \\ -0.10702 \\ 0.461972 \\ 0.003252 \\ 0.267599 \\ 0.928297 \\ -0.215226 \\ -0.581171 \\ -0.110085 \\ -0.669913 \\ 0.055298 \\ 1.046916 \\ 0.077329 \end{bmatrix} \quad \textbf{(6.4)}$$

The three column vectors containing the regression coefficients for the load shortening response are given in Eq. 6.5. The value of the ordinate at $S=S_L$ and the ordinate and slope at $S=S_I$ of the nondimensionalized load-shortening curve are given

by Eq. 6.6 where each zero represents a 16x1 column vector. These values along with the coordinate function for S define the load-shortening relationship predicted by the model.

$$\begin{bmatrix} A_1 & A_2 & A_3 \end{bmatrix} = \begin{bmatrix} -96.7576688 & 2.6393317 & 6.5093733 \\ 33.8346044 & -4.6858309 & 5.0144435 \\ 86.8395019 & -0.7619274 & -152.1642763 \\ -35.8610248 & 0.8418515 & -60.3457011 \\ -10.1952749 & 3.0951957 & -0.4259591 \\ 7.1381952 & -1.0635194 & -4.1204615 \\ -0.0031403 & -1.1854643 & -51.6311469 \\ -0.927396 & 0.4652409 & 125.8307582 \\ -32.7420774 & -8.7484492 & -3.9447826 \\ 28.8206911 & 1.2345277 & 3.6585499 \\ -47.0706471 & 4.0064554 & 198.6267578 \\ 13.4244783 & -0.9345943 & -230.5340144 \\ 44.2367395 & 0.8111947 & 0.5816586 \\ -22.4094697 & 0.5335845 & -0.6080795 \\ -13.784678 & -0.0555643 & -37.2667741 \\ 7.6543422 & -0.2568981 & 40.4228052 \end{bmatrix} \quad \textbf{(6.5)}$$

$$\begin{bmatrix} \mathrm{P}(S_L) & \mathrm{P}(S_I) & \mathrm{P}'(S_I) \end{bmatrix} = \begin{bmatrix} Q_1 & Q_2 & Q_3 \end{bmatrix} \begin{bmatrix} A_1 & 0 & 0 \\ 0 & A_2 & 0 \\ 0 & 0 & A_3 \end{bmatrix} \quad \textbf{(6.6)}$$

6.1.3 Analysis of Accuracy

The agreement between the approximated load-shortening relationships and the data included in the database was very good. As a measure of the goodness of fit to the data, basic statistics for analysis of variance were calculated.

The residual sum of squares or sum of squares of the error, is defined by Eq. 6.7

$$SSE = \sum \left(y_i - \hat{y}_i\right)^2 \tag{6.7}$$

where y_i represents an observed value of the dependent variable (in this case P), $\hat{y}_i$ is a value of the dependent variable predicted by the regression model for values of the independent variables equal to those corresponding to y_i. The summation is over all points in the database. The residual sum of squares is equal to 9.92012.

The total sum of squares, SST is defined by Eq. 6.8, where y_i is as defined above.

$$SST = \sum y_i^2 \tag{6.8}$$

The sum of squares due to regression, SSR is defined by Eq. 6.9 and is a measure of the portion of SST that is attributable to the model.

$$SSR = \sum y_i \hat{y}_i \tag{6.9}$$

The mean sum of square statistics are also included in Table 6.2 and are based on 3318 data points from the 130 load-shortening curves in the database and 80 degrees of freedom for the regression model. (Degrees of freedom in this context refers to the number of regressors in the model.)

Table 6.2 Analysis of variance

	Degrees of Freedom	Sum of Squares	Mean Square
Regression	80	451.68704	5.646
Residual	3278	9.92012	0.003026
Total	3318	461.60716	

The statistic R^2 is defined as the ratio of SSR to SSE and is a measure of the "proportion of total variation about the mean explained by the regression."[28] It is often expressed as a percentage and is sometimes referred to as the multiple correlation coefficient. From the data in Table 6.2, R^2 is equal to 0.9785, indicating that the regression model captures almost 98% of the variation in the independent variable.

Another indication of the goodness of fit of the regression model is the relative error. The average of the absolute value of the relative error was calculated by

$$\bar{e}_r = \frac{1}{n} \sum \left| \frac{y_i - \hat{y}_i}{y_i} \right| \qquad (6.10)$$

The resulting value from Eq. 6.10 is 0.1297 indicating that, on average, the regression model has an error of 12.97% relative to the observed values in the database.

The fit or agreement of the model may be better, in practical terms, than indicated by the above metrics. Generally, the greatest deviation between the predicted values and the observed data occurs in the post-ultimate range of the load-shortening curve. In practice, the most important portions of the predicted load shortening curves are the slope and the extent of the initial linear portion and the portion up to the ultimate load.

6.2 Application of the method

To illustrate the application of the simplified numerical procedure, an overview of the process is given and an example calculation is presented.

6.2.1 Procedure for Calculating the Load-Shortening Response

The basic procedure for the calculation of the damaged column response is given by the following steps.

1. Determine the nondimensionalized parameters λ, D/t, d/D, δ/L and σ_y/E.

2. Calculate the terms of the coordinate functions, G.

3. Calculate the regressors, Q_{SL}, Q_{SII}, Q_1, Q_2 and Q_3 from the direct product of the coordinate functions.

4. Determine the values of S_L, S_{II}, $P(S_L)$, $P(S_I)$ and $P'(S_I)$ from the products of the corresponding regressors Q and regression coefficients A.

5. Determine the load-shortening relationship by substituting the values from step 4 above into the coordinate function for S.

6.2.2 Calculation of Ultimate Load

The estimated ultimate load for a given column can be directly calculated from the predicted values of S_L, S_{II}, $P(S_L)$, $P(S_I)$ and $P'(S_I)$. The value of S at which the ultimate load occurs, S_{ult}, is found by simply setting the first derivative of the coordinate function for S equal to zero. Solving for the roots of this equation results in the following equation for S_{ult},

$$S_{ult} = \frac{3\alpha_1 + S_{IL}(\alpha_2 + 2) \pm \sqrt{9\alpha_1^2 + 6\alpha_1 S_{IL}(\alpha_2 + 1) + S_{IL}^2(\alpha_2^2 + \alpha_2 + 1)}}{6\alpha_1 + 3S_{IL}(\alpha_2 + 1)} S_{IL} + S_L \quad \textbf{(6.11)}$$

where, α_1 and α_2 are defined in Eq. 6.12.

$$\alpha_1 = \frac{P(S_L) - P(S_I)}{\frac{P(S_L)}{S_L}} = \frac{Q_1 A_1 - Q_2 A_2}{\frac{Q_1 A_1}{Q_{S_L} A_{S_L}}}$$

$$\alpha_2 = \frac{P'(S_I)}{\frac{P(S_L)}{S_L}} = \frac{Q_3 A_3}{\frac{Q_1 A_1}{Q_{S_L} A_{S_L}}} \quad \textbf{(6.12)}$$

The ultimate load, P_{ult} is then given by substituting the appropriate value of S_{ult} into Eq. 5.25.

6.2.3 Example Calculation

The geometry and damage (λ, D/t, d/D and δ/L) of the column used in the example correspond to a finite element generated load-shortening relationship in the database. The predicted load-shortening response is then compared with the data from the database.

The example column has a slenderness ratio λ of 0.8,a D/t ratio of 40, a relative dent depth d/D of 0.10 and no initial out-of-straightness. The first step in the application of the method is to calculate the values of S_L and S_{IL}. From Eq. 5.23 repeated here,

$$\begin{Bmatrix} S_L \\ S_{IL} \end{Bmatrix} = \begin{Bmatrix} Q_{S_L} A_{S_L} \\ Q_{S_{IL}} A_{S_I} \end{Bmatrix}$$

this requires formulation of regressors Q given by Eqs. 5.17 and 5.22 and the regression coefficients A given by Eqs. 6.3 and 6.4. The coordinate functions used in the direct product formulation of Q_{SL} are given in Eq. 6.14

$$G_{\lambda}^{S_L} = \begin{bmatrix} 1 & \lambda^2 \end{bmatrix} = \begin{bmatrix} 1 & 0.8^2 \end{bmatrix} = \begin{bmatrix} 1 & 0.64 \end{bmatrix}$$

$$G_{D/t}^{S_L} = \begin{bmatrix} 1 & \frac{1}{10}\frac{D}{t} \end{bmatrix} = \begin{bmatrix} 1 & \frac{40}{10} \end{bmatrix} = \begin{bmatrix} 1 & 4 \end{bmatrix}$$

$$G_{d/D}^{S_L} = \begin{bmatrix} 1 & \frac{1}{1+\frac{d}{D}} \end{bmatrix} = \begin{bmatrix} 1 & \frac{1}{1+0.1} \end{bmatrix} = \begin{bmatrix} 1 & 0.9091 \end{bmatrix} \qquad \textbf{(6.14)}$$

$$G_{\delta/L}^{S_L} = \begin{bmatrix} 1 & \sqrt{\frac{\delta}{L}} \end{bmatrix} = \begin{bmatrix} 1 & \sqrt{0} \end{bmatrix} = \begin{bmatrix} 1 & 0 \end{bmatrix}$$

These coordinate functions are used in the direct product formulation given by Eq. 5.17 and shown here after substitution of numerical values.

$$Q_{S_L} = [1 \quad 0] \otimes [1 \quad 0.9091] \otimes [1 \quad 4] \otimes [1 \quad 0.64]$$

$$Q_{S_L}^T = \begin{bmatrix} 1 \\ 0.64 \\ 4 \\ 2.56 \\ 0.9091 \\ 0.58182 \\ 3.63636 \\ 2.32727 \\ 0 \\ 0 \\ 0 \\ 0 \\ 0 \\ 0 \\ 0 \\ 0 \end{bmatrix} \tag{6.15}$$

From Eq. 5.23, S_L is given by the product of Q_{SL} and A_{SL}. For the values given in Eqs. 6.3 and 6.15, the predicted value of S_L is 0.645.

Similarly, the calculation of S_{IL} is made from the coordinate functions in Eq. 6.16

$$G_{\lambda}^{S_{IL}} = \left[1 \quad 10\frac{\sqrt{\epsilon_y}}{\lambda}\right] = \left[1 \quad 10\frac{\sqrt{0.00125}}{0.8}\right] = [1 \quad 0.442]$$

$$G_{D/t}^{S_{IL}} = \left[1 \quad \frac{1}{10}\sqrt{\frac{D}{t}}\right] = \left[1 \quad \frac{\sqrt{40}}{10}\right] = [1 \quad 0.6325] \qquad \textbf{(6.16)}$$

$$G_{d/D}^{S_{IL}} = \left[1 \quad \frac{1}{\sqrt{\epsilon_y}}\frac{d^2}{D}\right] = \left[1 \quad \frac{0.1^2}{\sqrt{0.00125}}\right] = [1 \quad 0.2828]$$

$$G_{\delta/L}^{S_{IL}} = \left[1 \quad 100\ \frac{\delta}{L}\right] = [1 \quad 100\,(0)] = [1 \quad 0]$$

The direct product formulation for Q_{SIL} is given by

$$Q_{S_{IL}} = [1 \quad 0] \otimes [1 \quad 0.2828] \otimes [1 \quad 0.6325] \otimes [1 \quad 0.442]$$

$$Q_{S_{IL}}^{T} = \begin{bmatrix} 1 \\ 0.442 \\ 0.6325 \\ 0.2795 \\ 0.2828 \\ 0.125 \\ 0.1789 \\ 0.0791 \\ 0 \\ 0 \\ 0 \\ 0 \\ 0 \\ 0 \\ 0 \\ 0 \end{bmatrix} \tag{6.17}$$

From Eq. 5.23, S_{IL} is given by the product of Q_{SIL} and A_{SIL}. For the values given in Eqs. 6.4 and 6.17, the predicted value of S_{IL} is 0.109.

With the predicted values of S_L and S_{IL} determined, the next step is to calculate the predicted values of $P(S_L)$, $P(S_{IL})$ and $P'(S_{IL})$ from Eq. 6.6. The coordinate functions used in the direct product formulation for Q_1, Q_2 and Q_3 are given in Eqs. 5.29 through 5.40. The coordinate functions used in the direct product formulation of

Q_1 are given in Eq. 6.18 incorporating the values of the example column geometry and damage.

$$G_{\lambda}^{P(S_L)} = \left[\frac{1}{1.5+\lambda} \quad \text{sech}\left(\frac{\lambda^2}{2}\right)\right] = \left[\frac{1}{1.5+0.8} \quad \text{sech}\left(\frac{0.8^2}{2}\right)\right]$$
$$= [0.4348 \quad 0.9509]$$

$$G_{D/t}^{P(S_L)} = \left[1 \quad \log_{10}\frac{D}{t}\right] = [1 \quad \log_{10}40]$$
$$= [1 \quad 1.6021]$$

$$G_{d/D}^{P(S_L)} = \left[\frac{d}{D} - 2\left(\frac{d}{D}\right)^2 + \left(\frac{d}{D}\right)^3 \quad 1 - 3\left(\frac{d}{D}\right)^2 + 2\left(\frac{d}{D}\right)^3\right] \tag{6.18}$$
$$= [0.10 - 2(0.10)^2 + (0.10)^3 \quad 1 - 3(0.10)^2 + 2(0.10)^3]$$
$$= [0.081 \quad 0.972]$$

$$G_{\delta/L}^{P(S_L)} = \left[e^{-100\frac{\delta}{L}} \quad \frac{1}{2+100\frac{\delta}{L}}\right] = \left[e^{-100(0)} \quad \frac{1}{2+100(0)}\right]$$
$$= [1 \quad 0.5]$$

From Eq. 5.28 the regressors Q_i are given by the direct product formulation as illustrated in Eq. 6.19.

$$Q_1 = [1 \quad 0.5] \otimes [0.081 \quad 0.972] \otimes [1 \quad 1.6021] \otimes [0.4348 \quad 0.9509]$$

$$Q_1^T = \begin{bmatrix} 0.035217 \\ 0.077023 \\ 0.056420 \\ 0.12339 \\ 0.42261 \\ 0.92427 \\ 0.67704 \\ 1.48074 \\ 0.017609 \\ 0.038511 \\ 0.028210 \\ 0.061697 \\ 0.21130 \\ 0.46214 \\ 0.33852 \\ 0.74037 \end{bmatrix} \tag{6.19}$$

From Eq. 6.6, $P(S_L)$ is given by the product $Q_1 \cdot A_1$. For the values given in Eqs. 6.19 and 6.5, the calculated value of $P(S_L)$ is 0.612.

Similarly, the value of $P(S_I)$ is calculated from the direct product of the coordinate functions and the regression coefficients. As defined by Eqs. 5.30, 5.33, 5.36 and 5.39 , the coordinate functions for this example column are given by Eq. 6.20

$$G_{\lambda}^{P(S_1)} = \left[e^{-\lambda} \quad \operatorname{sech}\left(2\lambda^2\right)\right] = \left[e^{-0.8} \quad \operatorname{sech}\left(2\,(0.8)^2\right)\right]$$

$$= [0.4493 \quad 0.5162]$$

$$G_{D/t}^{P(S_1)} = \left[1 \quad \log_{10}\frac{D}{t}\right] = \left[1 \quad \log_{10}40\right]$$

$$= [1 \quad 1.6021]$$

$$G_{d/D}^{P(S_1)} = \left[\frac{d}{D} - 2\left(\frac{d}{D}\right)^2 + \left(\frac{d}{D}\right)^3 \quad 1 - 3\left(\frac{d}{D}\right)^2 + 2\left(\frac{d}{D}\right)^3\right] \tag{6.20}$$

$$= \left[0.10 - 2(0.10)^2 + (0.10)^3 \quad 1 - 3(0.10)^2 + 2(0.10)^3\right]$$

$$= [0.081 \quad 0.972]$$

$$G_{\delta/L}^{P(S_1)} = \left[e^{-100\frac{\delta}{L}} \quad \frac{1}{1 + 15\frac{\delta}{L}}\right] = \left[e^{-100\,(0)} \quad \frac{1}{1 + 15\,(0)}\right]$$

$$= [1 \quad 1]$$

As defined by Eq. 5.28, the direct product formulation of Q_2 for the example column is given by Eq. 6.21.

$$Q_2 = [1 \quad 1] \otimes [0.081 \quad 0.972] \otimes [1 \quad 1.6021] \otimes [0.4493 \quad 0.5162]$$

$$Q_2^T = \begin{bmatrix} 0.036396 \\ 0.041810 \\ 0.058308 \\ 0.066982 \\ 0.43675 \\ 0.50172 \\ 0.69970 \\ 0.80378 \\ 0.036396 \\ 0.041810 \\ 0.058308 \\ 0.066982 \\ 0.43675 \\ 0.50172 \\ 0.69970 \\ 0.80378 \end{bmatrix} \tag{6.21}$$

From Eq. 6.6, $P(S_1)$ is given by the product $Q_2 \cdot A_2$. For the values given in Eqs. 6.21 and 6.5, the predicted value of $P(S_1)$ is 0.5557.

Similarly, the value of $P'(S_1)$ is calculated from the direct product of the coordinate functions and the regression coefficients. As defined by Eqs. 5.31, 5.34, 5.37 and 5.40 , the coordinate functions for the example column are given in Eq. 6.22

$$G_{\lambda}^{P'(S_I)} = \left[\lambda e^{-\lambda} \quad \lambda^3 e^{-\lambda^2}\right] = \left[0.8 e^{-0.8} \quad 0.8^3 e^{-0.8^2}\right]$$

$$= [0.3595 \quad 0.2700]$$

$$G_{D/t}^{P'(S_I)} = \begin{bmatrix} 1 & \frac{1}{\frac{D}{t}} \end{bmatrix} = \begin{bmatrix} 1 & \frac{1}{40} \end{bmatrix}$$

$$= [1 \quad 0.025]$$

$$G_{d/D}^{P'(S_I)} = \begin{bmatrix} 1 - \frac{d}{D} & \frac{1 - \frac{d}{D}}{0.1 + \frac{d}{D}} \end{bmatrix} \qquad \textbf{(6.22)}$$

$$= \begin{bmatrix} 1 - 0.10 & \frac{1 - 0.10}{0.1 + 0.10} \end{bmatrix}$$

$$= [0.90 \quad 4.50]$$

$$G_{\delta/L}^{P'(S_I)} = \begin{bmatrix} \frac{1}{3 + \frac{\delta}{L} 10^4} & \frac{1}{1 + 10\frac{\delta}{L}} \end{bmatrix} = \begin{bmatrix} \frac{1}{3 + (0)\, 10^4} & \frac{1}{1 + 10\,(0)} \end{bmatrix}$$

$$= [0.3333 \quad 1]$$

As defined by Eq. 5.28, the direct product formulation of Q_3 for the example column is given by Eq. 6.23.

$$Q_3 = [0.3333 \quad 1] \otimes [0.90 \quad 4.50] \otimes [1 \quad 0.025] \otimes [0.3595 \quad 0.2700]$$

$$Q_3^T = \begin{bmatrix} 0.10784 \\ 0.080992 \\ 0.0026960 \\ 0.0020248 \\ 0.53919 \\ 0.40496 \\ 0.013480 \\ 0.010124 \\ 0.32352 \\ 0.24298 \\ 0.0080879 \\ 0.0060744 \\ 1.61758 \\ 1.21488 \\ 0.040440 \\ 0.030372 \end{bmatrix} \tag{6.23}$$

From Eq. 6.6, $P'(S_I)$ is given by the product $Q_3 \cdot A_3$. For the values given in Eqs. 6.23 and 6.5, the predicted value of $P'(S_I)$ is -1.003.

With the predicted values of S_L, S_{IL}, $P(S_L)$, $P(S_{IL})$ and $P'(S_{IL})$ and the coordinate function for S as given in Eq. 5.25., the final step is to calculate the load-shortening relationship. The result is given by Eq. 6.24, where the computed values are incorporated into the coordinate function for S.

for $0 \le S \le S_L \rightarrow 0 \le S \le 0.645$

$$P(S) = \frac{P(S_L)}{S_L} S = \frac{0.612}{0.645} S$$

$$= 0.949\, S$$

for $S_L \le S \le S_I \rightarrow 0.645 \le S \le 0.754$

$$P(S) = P(S_L)\left[1 + \frac{S - S_L}{S_L} - \frac{2S_{IL} + 3S_L}{S_L S_{IL}^2}(S - S_L)^2 + \frac{S_{IL} + 2S_L}{S_L S_{IL}^3}(S - S_L)^3\right]$$

$$+ P(S_I)\left[\frac{3}{S_{IL}^2}(S - S_L)^2 - \frac{2}{S_{IL}^3}(S - S_L)^3\right]$$

$$+ P'(S_I)\left[\frac{-1}{S_{IL}}(S - S_L)^2 + \frac{1}{S_{IL}^2}(S - S_L)^3\right] \qquad \textbf{(6.24)}$$

$$P(S) = 0.612\left[1 + \frac{S - 0.645}{0.645} - 281\,(S - 0.645)^2 + 1675\,(S - 0.645)^3\right]$$

$$+ 0.556\left[252\,(S - 0.645)^2 - 1544\,(S - 0.645)^3\right]$$

$$- 1.00\left[9.17\,(S - 0.645)^2 + 84.2\,(S - 0.645)^3\right]$$

for $S \ge S_I \rightarrow S \ge 0.754$

$$P(S) = \frac{P(S_I)}{1 - \frac{P'(S_I)}{P(S_I)}(S - S_I)}$$

$$P(S) = \frac{0.556}{1 + 1.80\,(S - S_I)}$$

Finally, the load-shortening relationship resulting from Eq. 6.24 can be plotted. Figure 6.1. illustrates the predicted load-shortening relationship from the regression analysis and the analytical relationship from the finite element model that was included in the database.

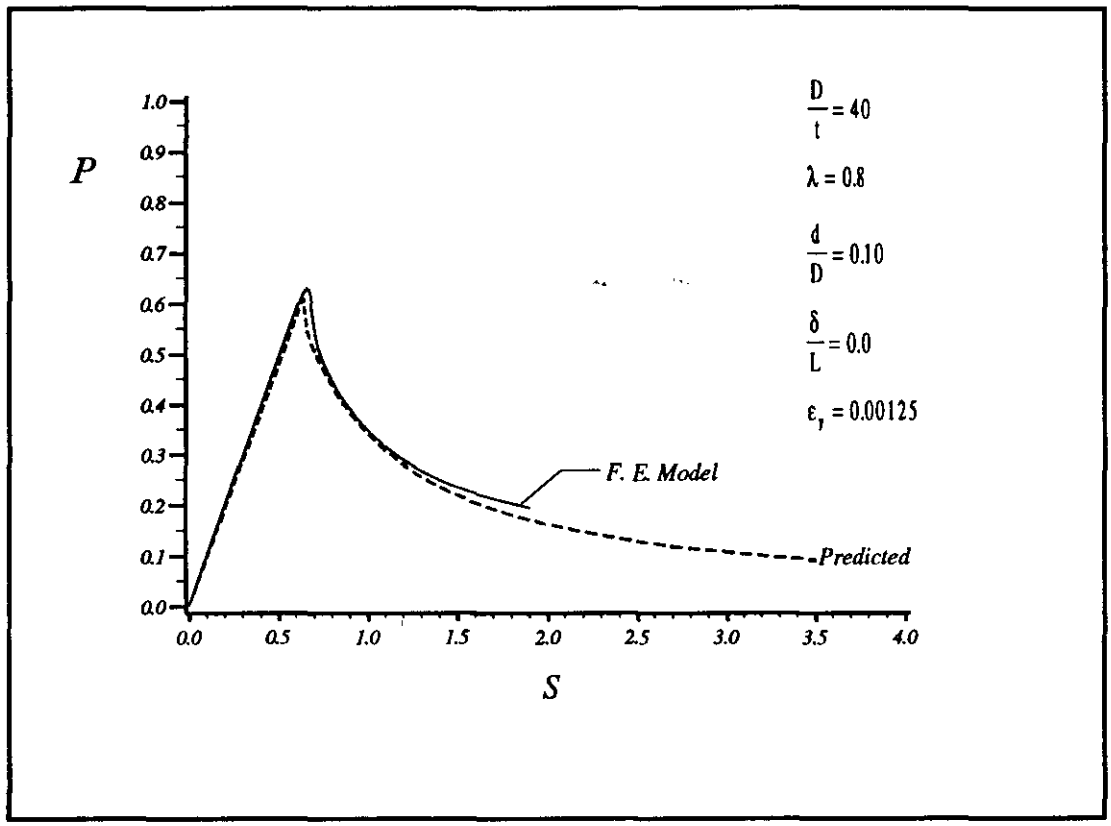

Figure 6.1 Predicted and analytical (from database) load-shortening curves.

The ordinate of the ultimate load S_{ult}, calculated from Eq.6.11, is 0.67. Substituting this value into Eq. 5.25 gives the ultimate load $P_{ult} = 0.612$.

6.2.4 Range of Applicability

The simplified method is valid over the range of values of column parameters covered by the data included in the database. These include the range of values typically found in fixed offshore structures. Generally the method is applicable over the range of the parameters given in Eq. 6.25.

$$
\begin{aligned}
20 < \frac{D}{t} < 95 \\
0.4 < \lambda < 1.2 \\
0.0 < \frac{d}{D} < 0.30 \\
0.0 < \frac{\delta}{L} < 0.02 \\
0.00125 < \epsilon_y < 0.00250
\end{aligned}
\qquad \textbf{(6.25)}
$$

6.3 Predicted Load-Shortening Relationships

To illustrate the validity of the regression model, predicted results are compared with some analytical and experimental load-shortening relationships from the database.

6.3.1 Comparison with Analytical Data from the Database

In Figs. 6.2 through 6.7, predicted load-shortening relationships are compared with curves generated from the finite element model and included in the database. The comparisons shown are for a range of column geometries, dent depth and out-of-straightness and are representative of the "goodness" of fit to the analytically generated curves in the database. Comparisons are shown for columns with D/t ratios of 25, 40, 60 and 80 and slenderness ratios λ of 0.4, 0.8 and 1.2. The examples with a D/t ratio of 25 (Figs. 6.2 and 6.3) include a "short" (λ=0.4) column with moderate damage (d/D=0.10 and δ/L=0.002) and a more slender column (λ=1.2) with heavy damage (d/D=0.05 and δ/L=0.02) largely in the form of initial out-of-straightness which might be expected in long columns with low D/t ratio. Figures 6.4 and 6.5 show examples with a D/t ratio of 40, slenderness ratios λ of 0.8 and 1.2, moderate dent depth and moderate and no out-of-straightness. The predicted and analytical relationships are shown for a column with D/t ratio of 60 in Fig. 6.6. Finally, in Fig. 6.7,. a comparison is given for a relatively short (λ=0.4) column with high D/t ratio (D/t=80) and having damage in the form of a significant dent (d/D=0.20) as might be expected to occur in a short column with high D/t ratio.

In general, these comparisons indicate reasonably good agreement with the analytical data over a fairly broad range of column geometries and damage.

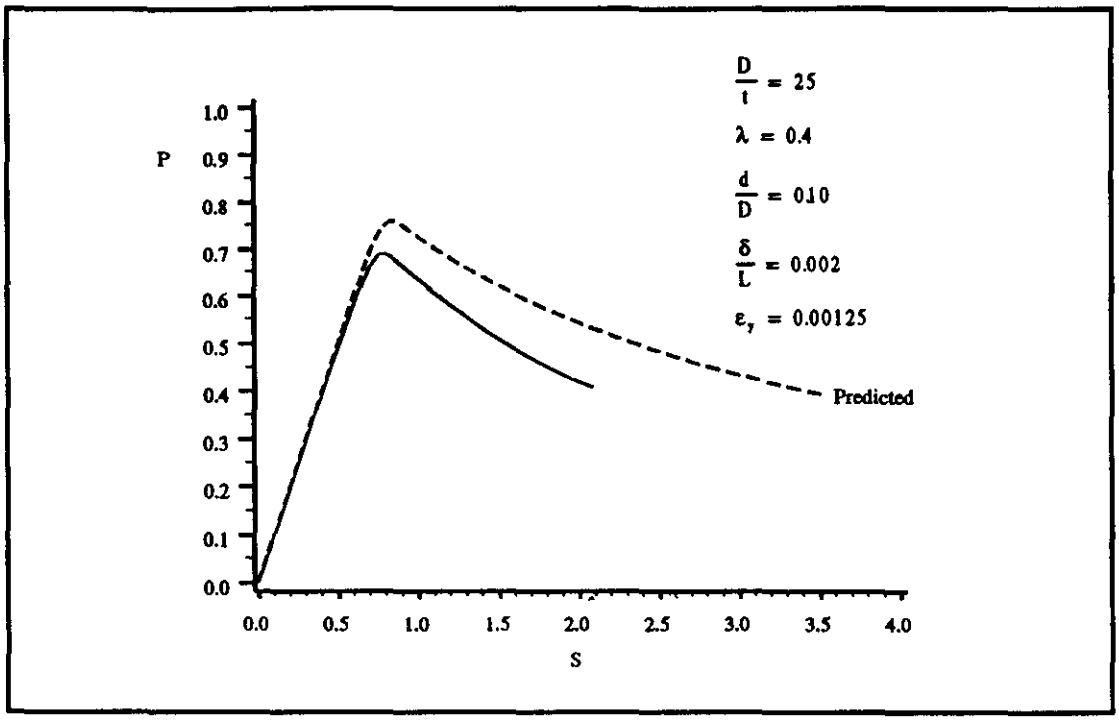

Figure 6.2 Comparison of predicted and calculated (F.E.) load-shortening responses.

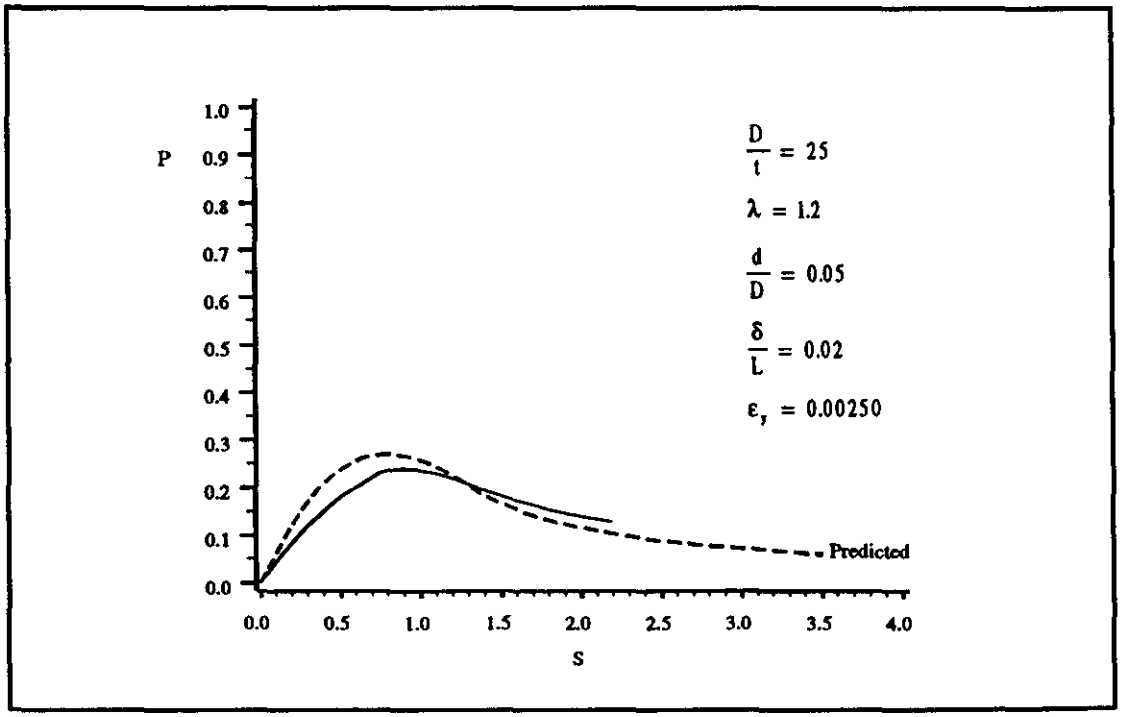

Figure 6.3 Comparison of predicted and calculated (F.E.) load-shortening responses.

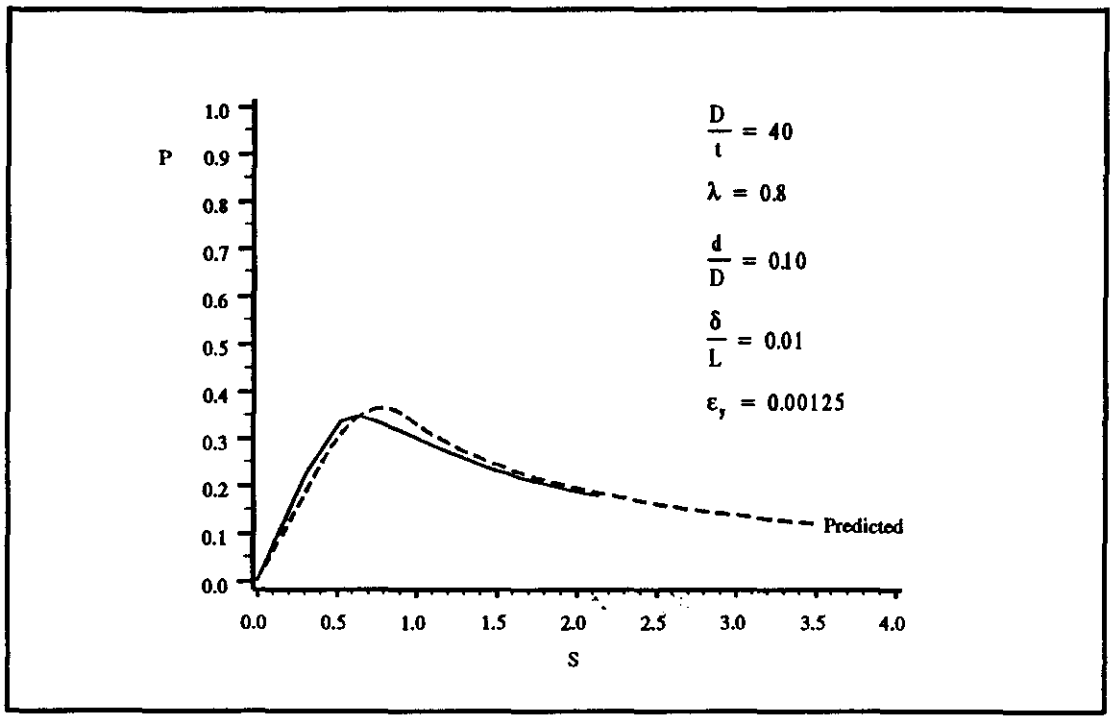

Figure 6.4 Comparison of predicted and analytical (F.E.) load-shortening responses.

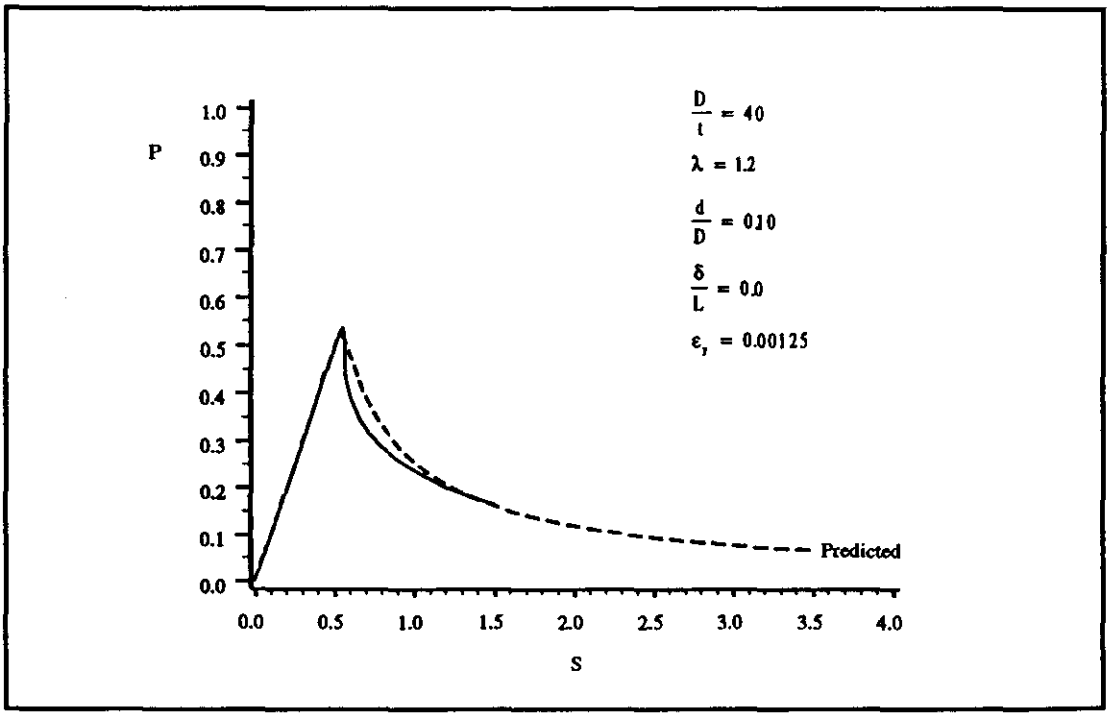

Figure 6.5 Comparison of predicted and analytical (F.E.) load-shortening responses.

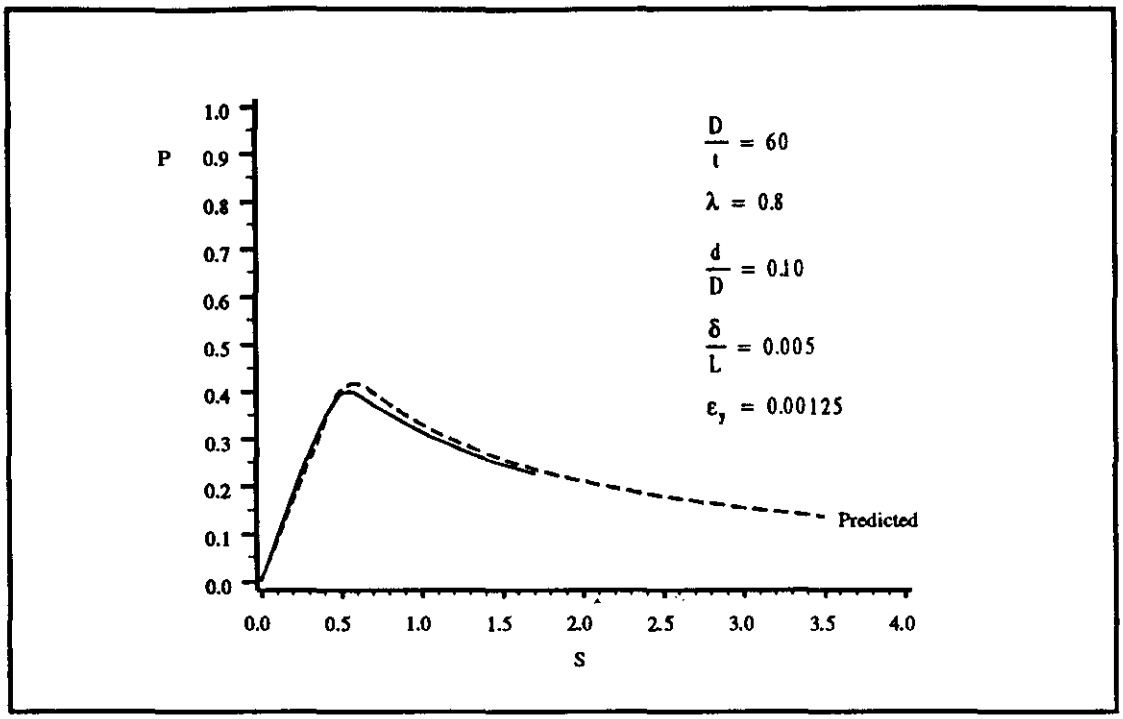

Figure 6.6 Comparison of predicted and analytical (F.E.) load-shortening responses.

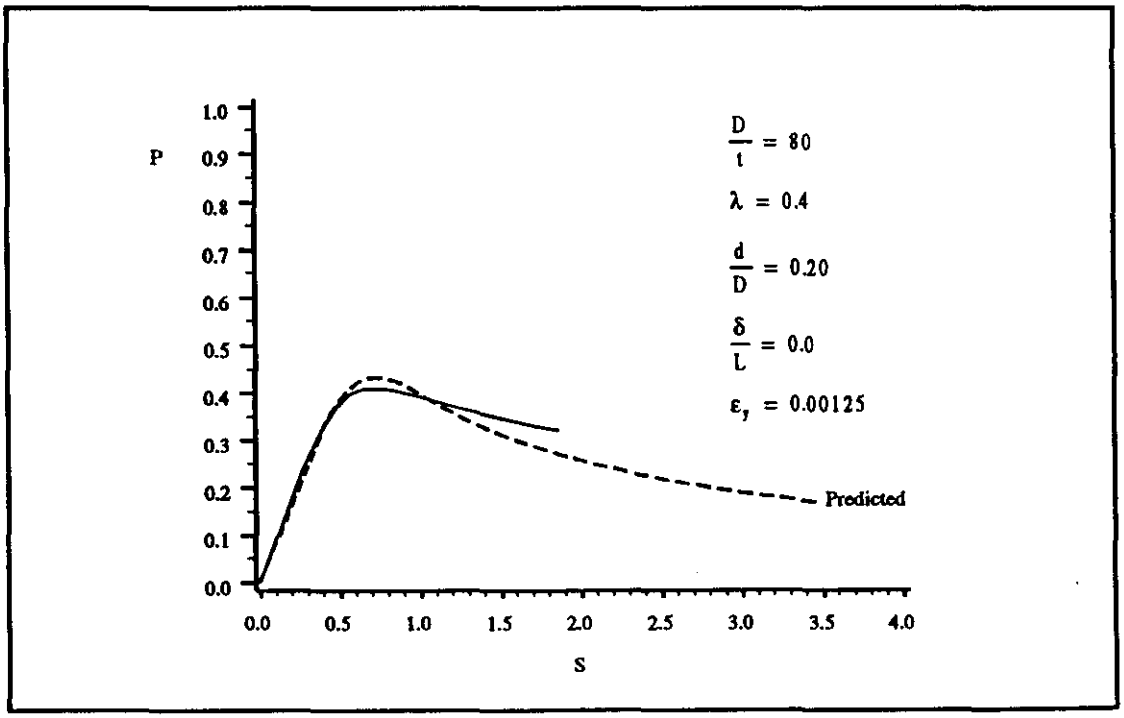

Figure 6.7 Comparison of predicted and analytical (F.E,) load-shortening responses.

The example comparisons illustrate reasonably good agreement between the predicted load-shortening relationships and those generated from the finite element analysis. In the worst case, the relative error between the predicted and analytical ultimate load is approximately 12%. The agreement in the post-ultimate range is not as good on average. Typically, as shown in Fig. 6.2, when there is deviation at the ultimate load it is maintained through the post-ultimate range resulting in larger relative error (due to the decreasing value of load).

6.3.2 Comparison with Experimental Data from the Database

In addition to the analytical results, comparisons are provided between predicted load-shortening relationships and experimental results included in the database. The test data in the database were taken from published reports from Smith[2,3,13], Taby[5,6,7,8] and Ostapenko[30]. From each series of tests published by these researchers, an example comparison between the empirical and predicted load-shortening relationships is given in Figs. 6.8 through 6.13. Additional comparisons with experimental data from the database are provided in Figs. 6.14 through 6.18. These comparisons are representative of the "goodness" of fit to the data.

Because the published results from Ref. 30 included comparison with results by others, comparisons for these specimens are provided in the following section. This permits comparison between the method presented here and those by others.

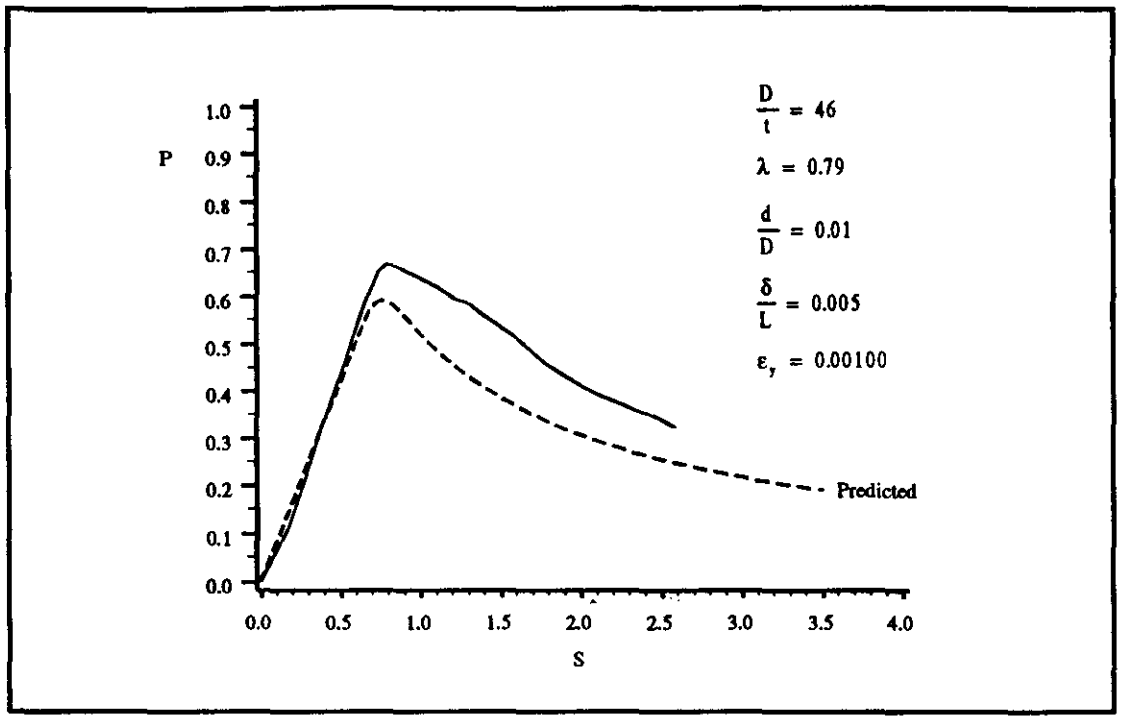

Figure 6.8 Predicted and experimental load-shortening response (B4 Ref. 2).

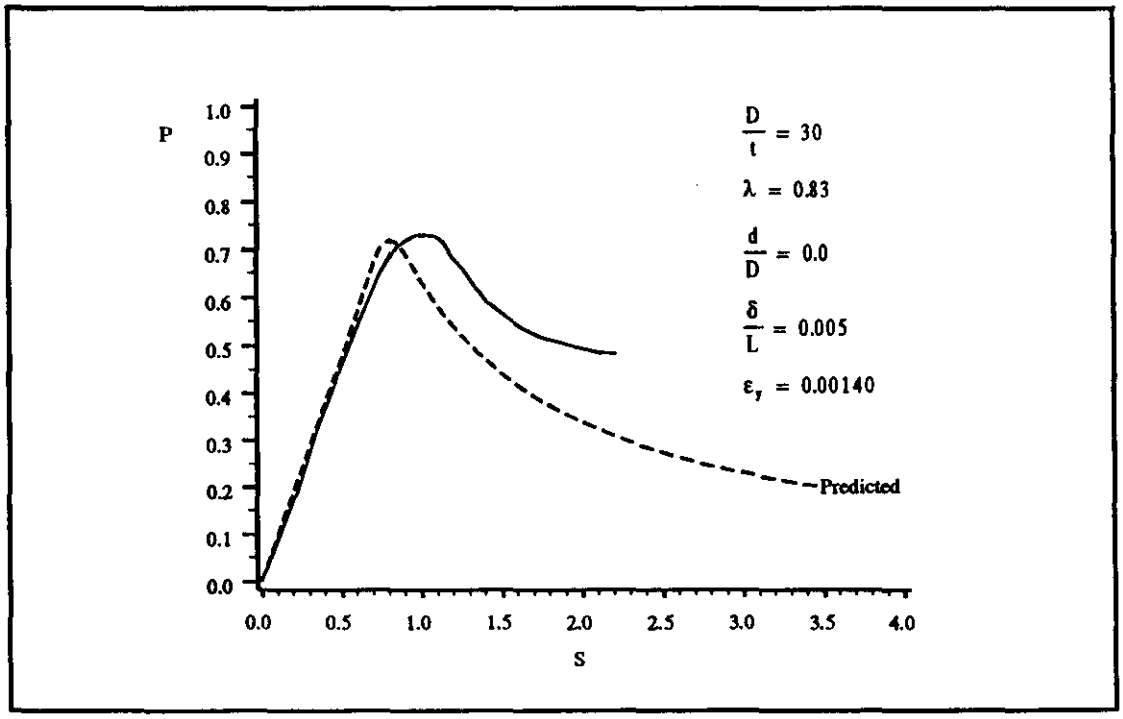

Figure 6.9 Predicted and experimental load-shortening response (E2 Ref.13).

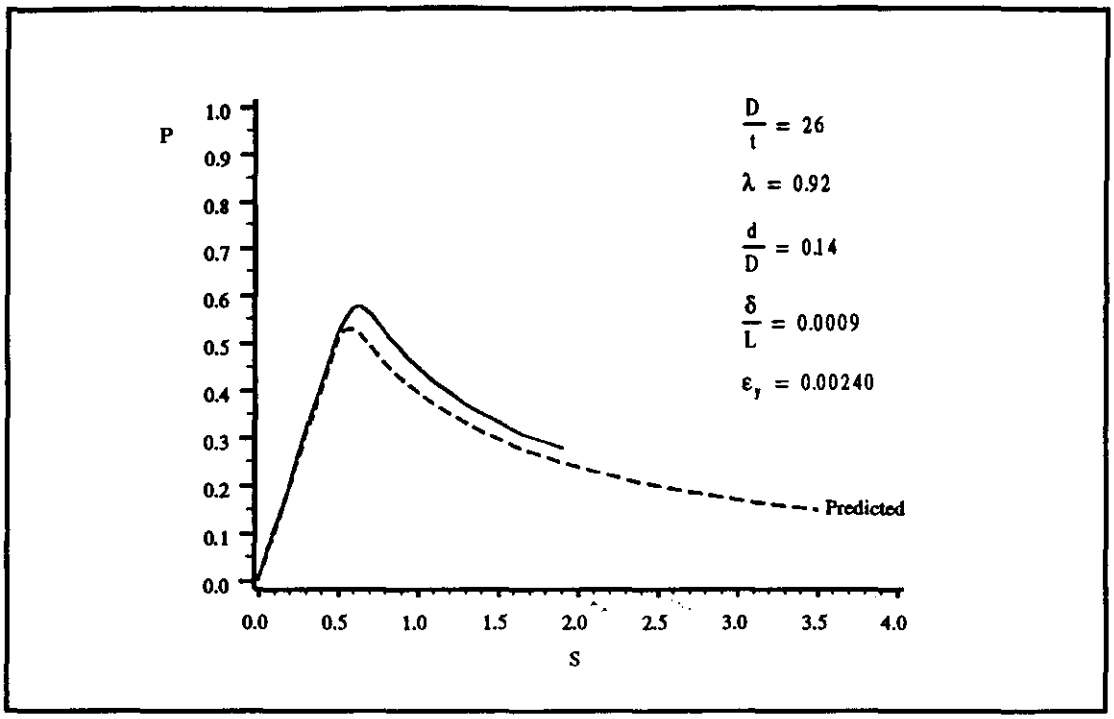

Figure 6.10 Predicted and experimental load-shortening response (R1C Ref. 3).

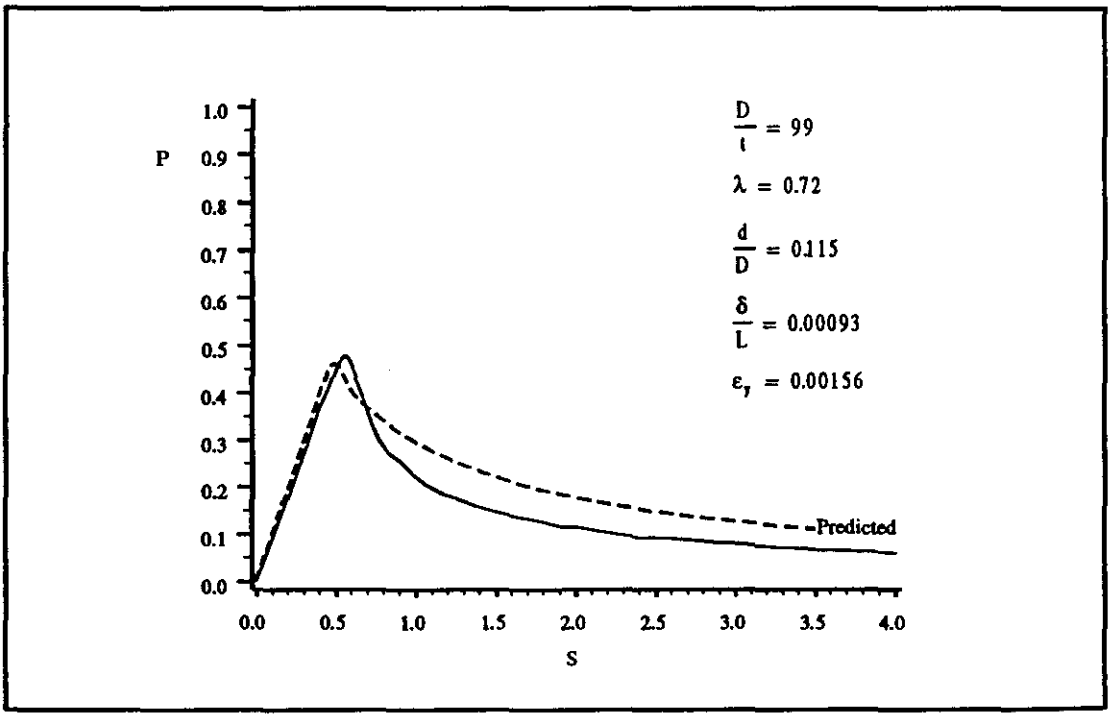

Figure 6.11 Predicted and experimental load-shortening response (1BDB Ref. 8)

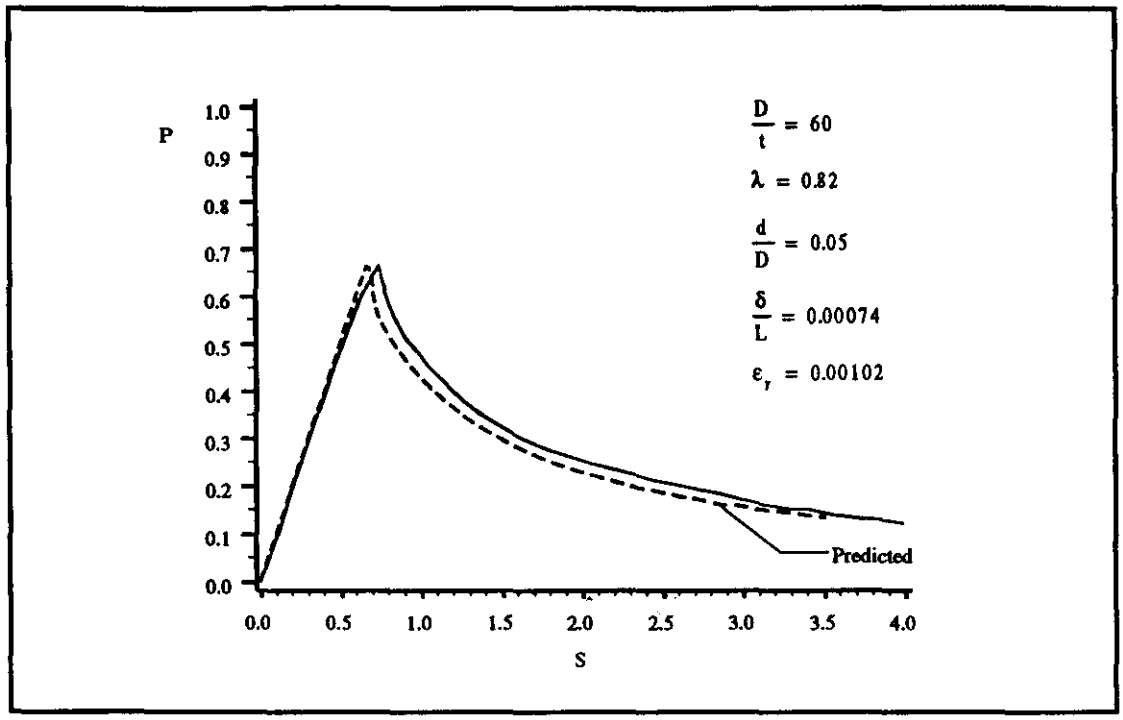

Figure 6.12 Predicted and experimental load-shortening response (IAI Ref. 5).

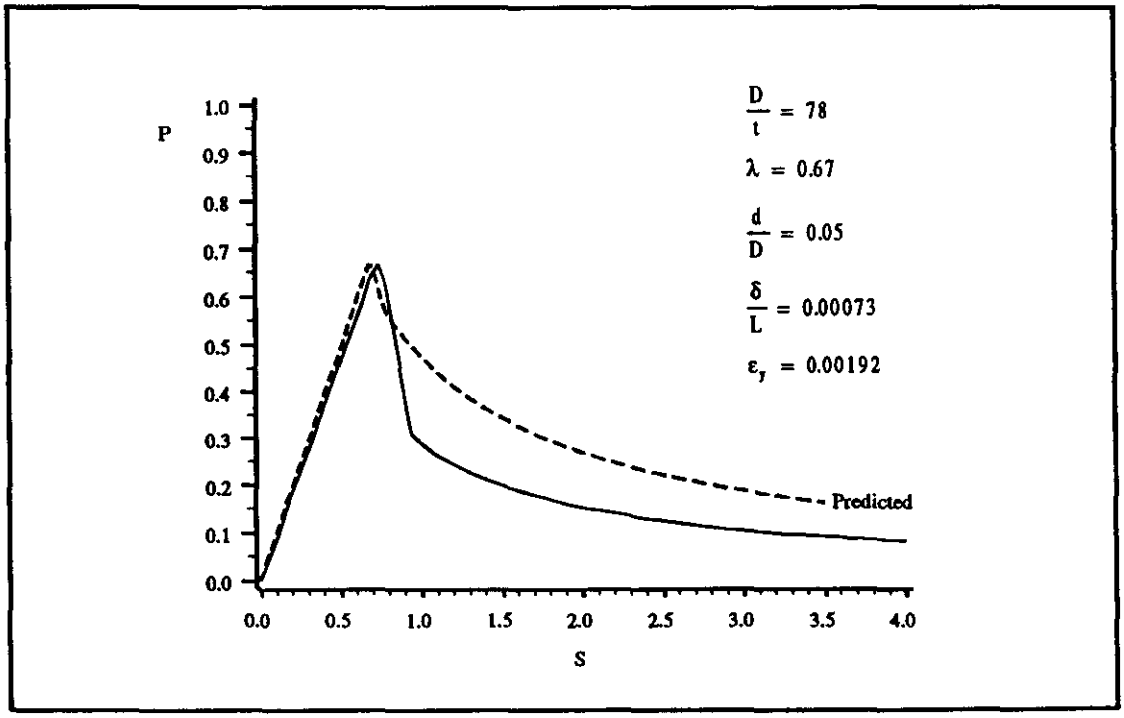

Figure 6.13 Predicted and experimental load-shortening response (IAS Ref. 6).

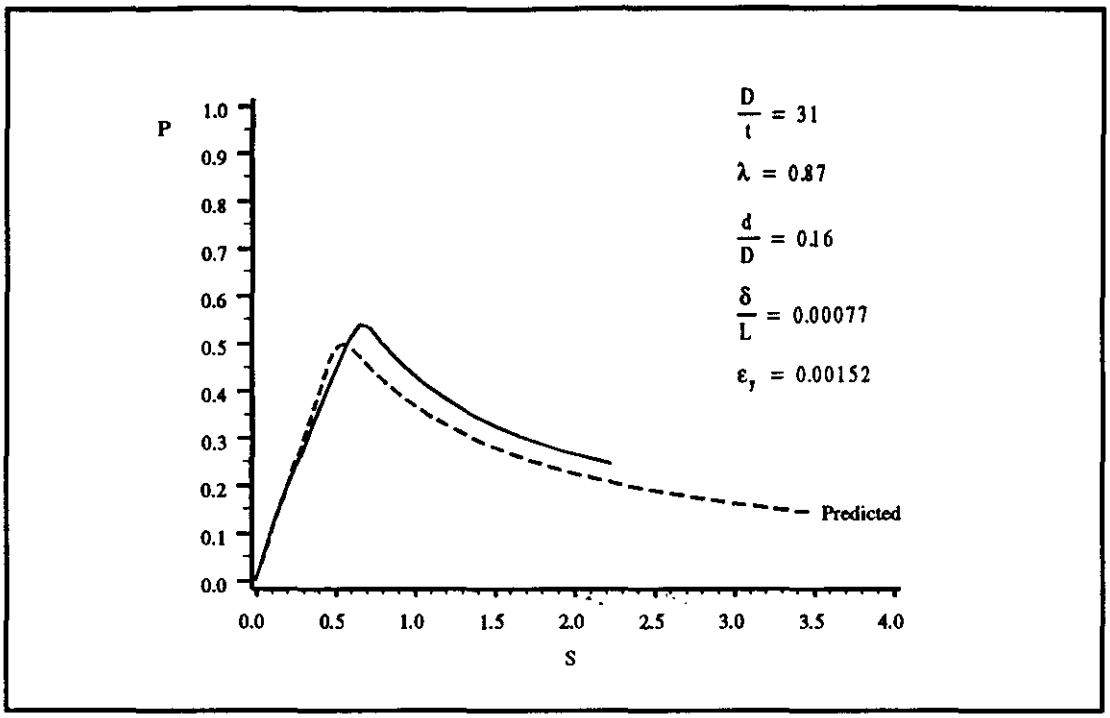

Figure 6.14 Predicted and experimental load-shortening relationships (D3 Ref. 30).

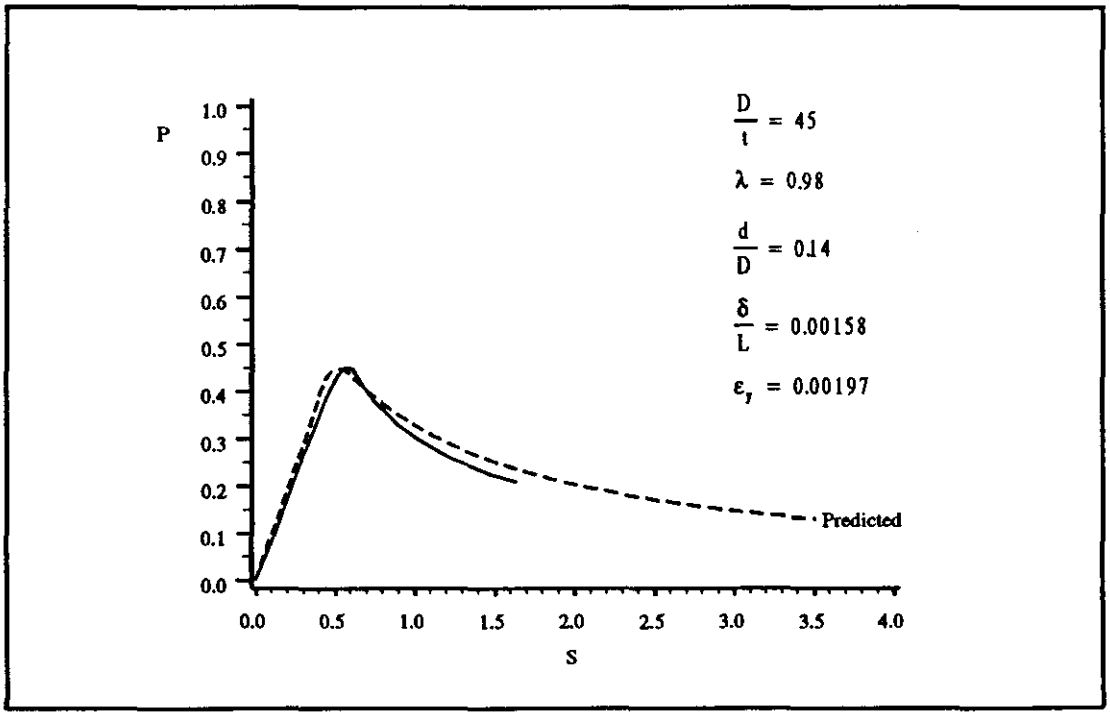

Figure 6.15 Predicted and experimental load-shortening relationships (P2P Ref. 30)

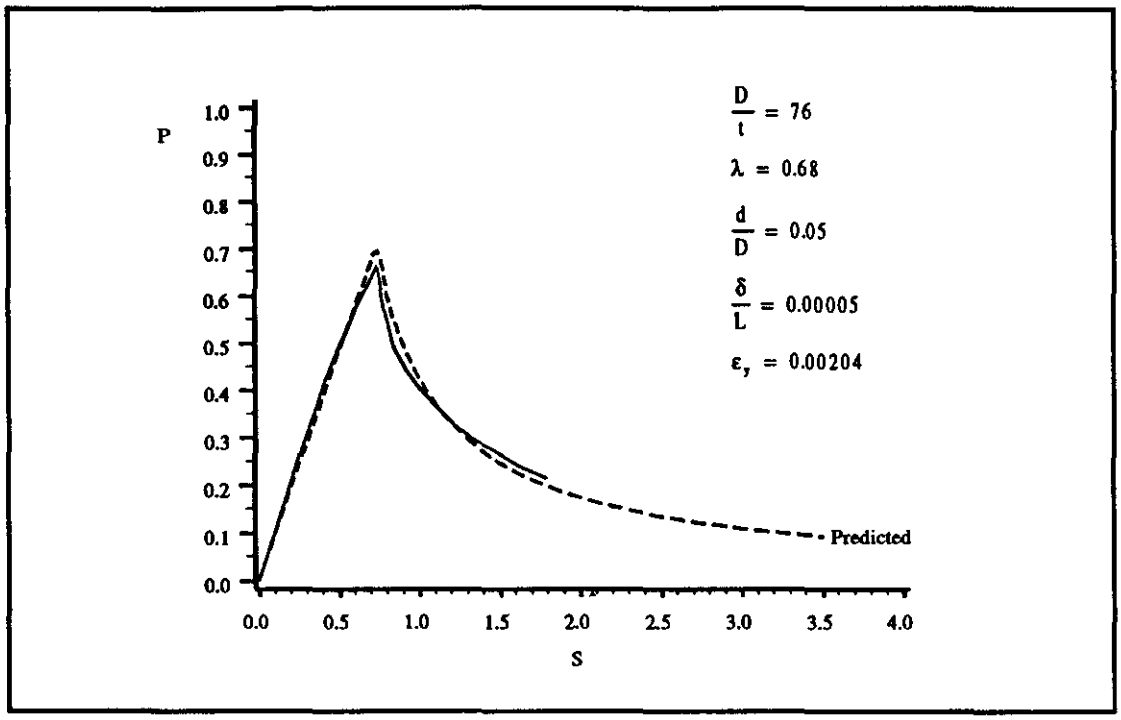

Figure 6.16 Predicted and experimental load-shortening relationships (P3PA Ref. 30)

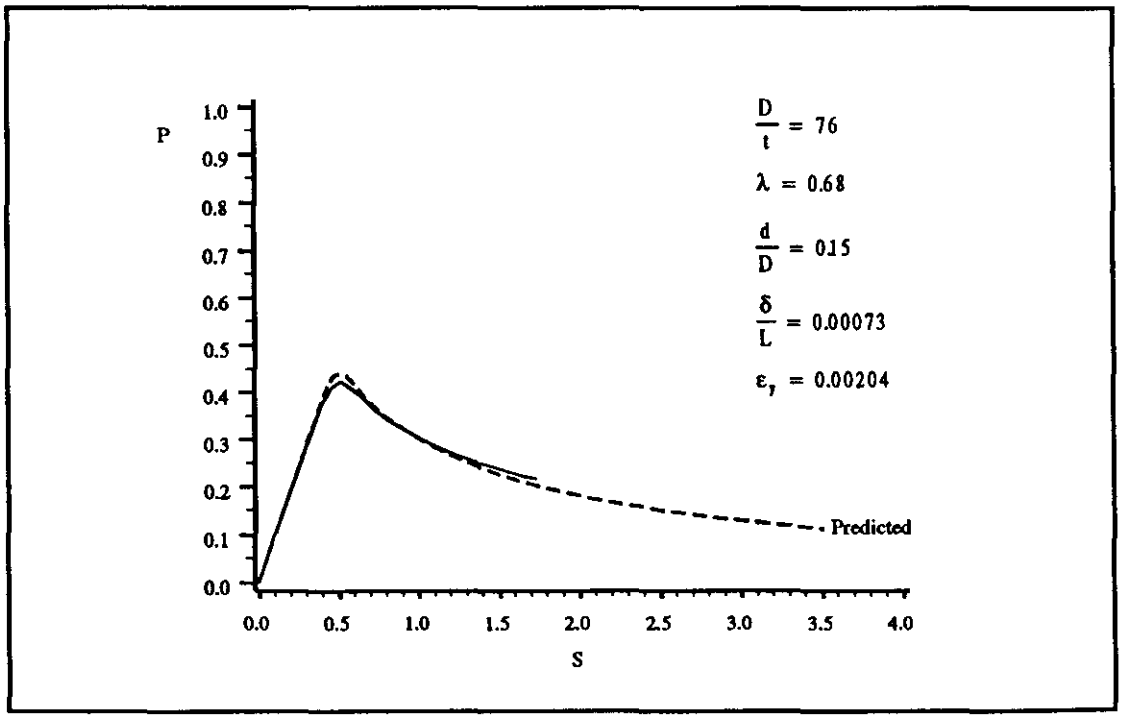

Figure 6.17 Predicted and experimental load-shortening relationships (P3PB Ref. 30)

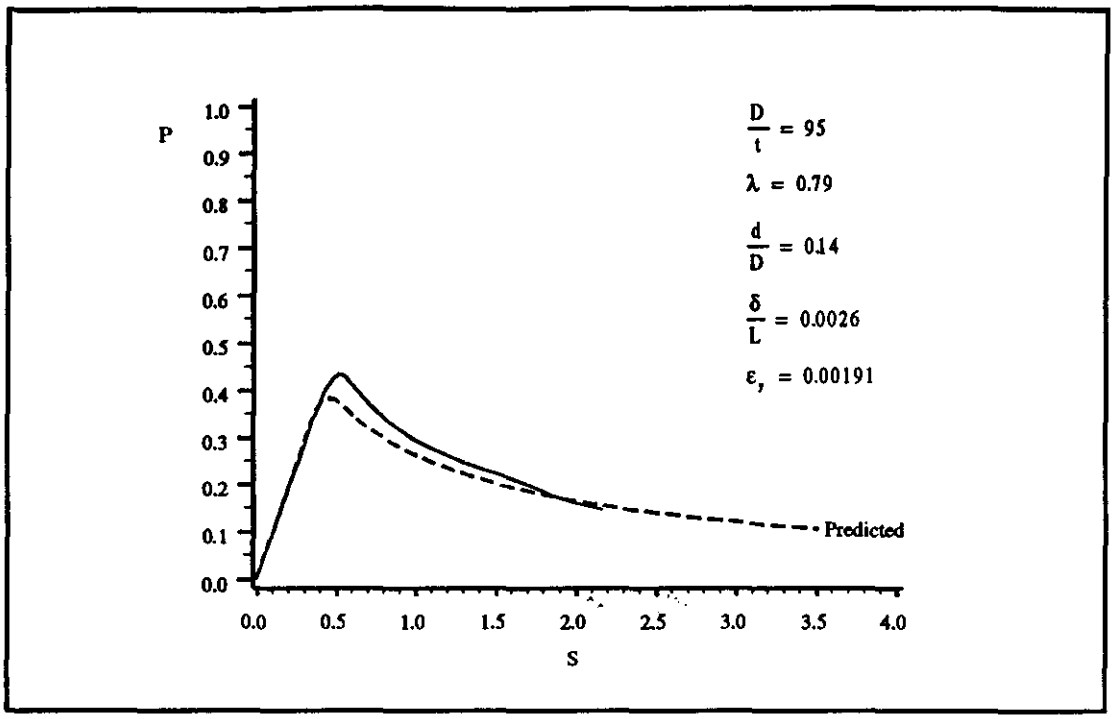

Figure 6.18 Predicted and experimental load-shortening relationships (P4P Ref. 30).

6.3.3 Comparison with Results by Others

The experimental load-shortening curves from the work by Ostapenko, et al, (Ref. 30) include comparisons with finite element analysis, the analytical method (program WBK) developed by Kim (Ref. 15), and results from the programs DENTA [10] and BCDENT [29]. (The finite element model used in the analysis presented in Ref. 30 is virtually the same as presented in Chapter 3.) The figures from Ref. 30 illustrated the load-shortening relationship as the nondimensionalized load as a function of the axial shortening in inches. The predicted and experimental load-shortening relationship for the five specimens are repeated in Figs. 6.19, 6.22, 6.25, 6.28 and 6.31 with the nondimensionalized load plotted as a function of axial shortening to permit comparison with plots from Ref. 30 which are also included here.

Comparison of the results for specimen D3 shown in Figs. 6.19, 6.20 and 6.21 show that all the analyses except for BCDENT underestimate the ultimate load. However, the results from the current procedure provide reasonable agreement with the ultimate load and perhaps the best agreement among the methods in the post-ultimate range.

The results for specimen P2P are shown in Figs. 6.22, 6.23 and 6.24. The results from the current procedure arguably provide the best approximation of the test data.

The results for specimen P3PA are shown in Figs.6.25, 6.26 and 6.27. The program DENTA and the current procedure provide similar and reasonably good agreement with the test data.

The results for specimen P3PB are shown in Figs. 6.28, 6.29 and 6.30. Again the current procedure provides very good agreement with the test data which is only better approximated by the finite element results. Program DENTA also provides reasonably good results for this specimen.

Finally, the results for specimen P4P are shown in Figs. 6.31, 6.32 and 6.33. All of the methods underestimate, in varying degrees, the ultimate load and the load over most if not all of the post-ultimate range. However, the current procedure provides reasonably good agreement with the test data and is arguably the best approximation of the five methods shown.

In general, these examples have demonstrated reasonably good approximation to test data. Comparisons to the other approximate methods (finite element, WBK, DENTA and BCDENT) indicate that the current procedure provides results that are comparable, or better, to the best results provided by any of the other procedures. It should be noted in this context that the proposed method involves only matrix multiplication and calculation of simple functions that can be readily performed in a spreadsheet or programmable calculator whereas the other methods all require a copy of the specific computer program.

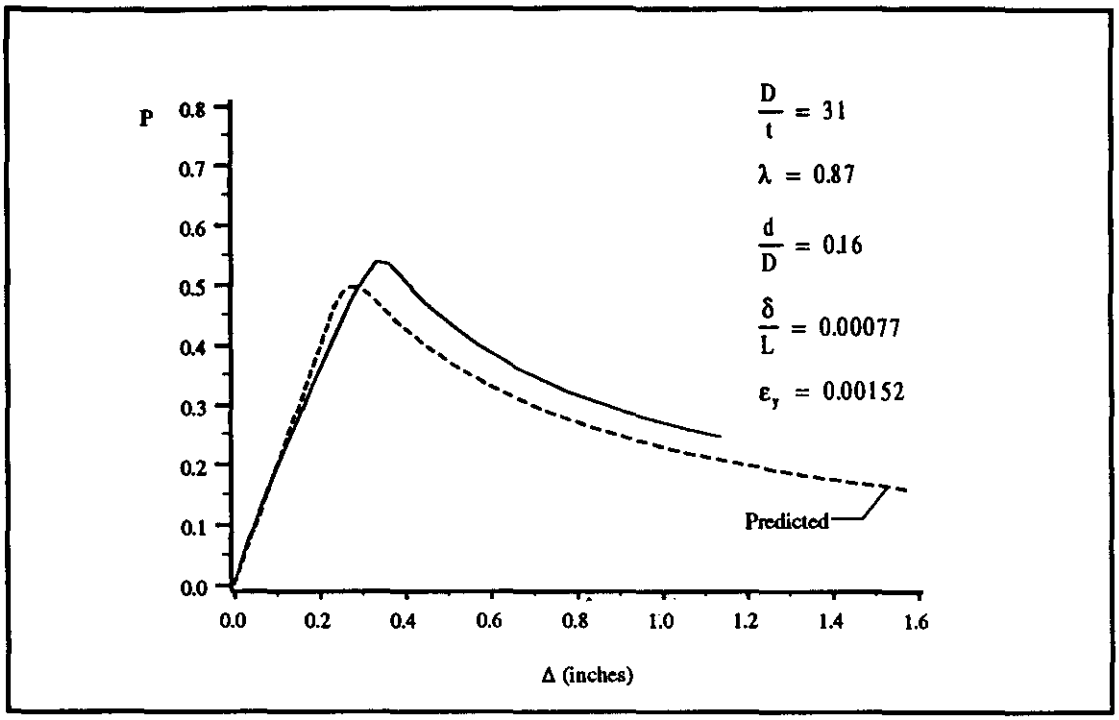

Figure 6.19 Predicted and observed load vs. axial shortening (D3 Ref. 30).

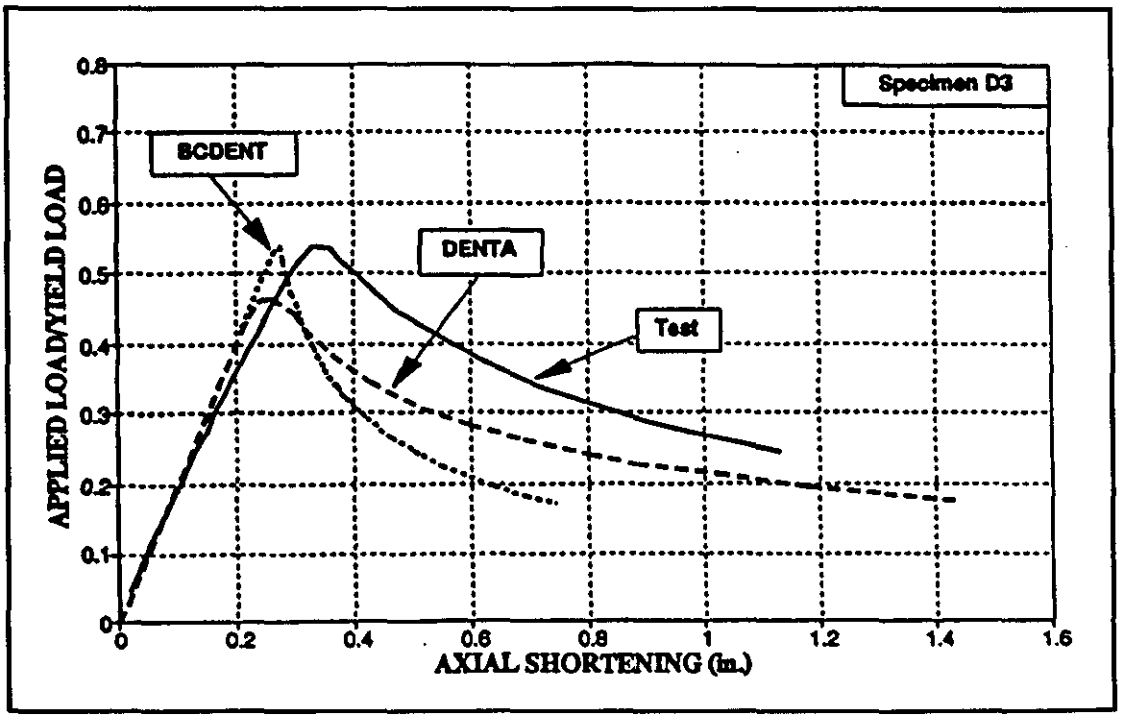

Figure 6.20 Comparison of specimen D3, BCDENT and DENTA (Ref. 30)

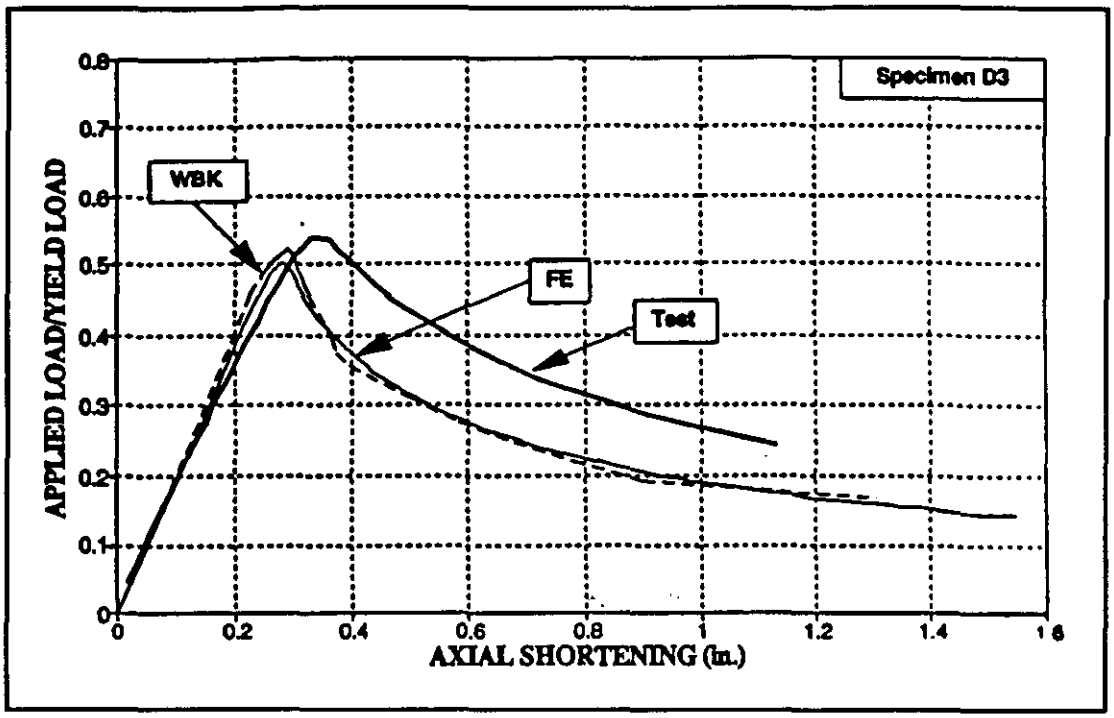

Figure 6.21 Comparison of specimen D3, finite element and WBK (Ref. 30)

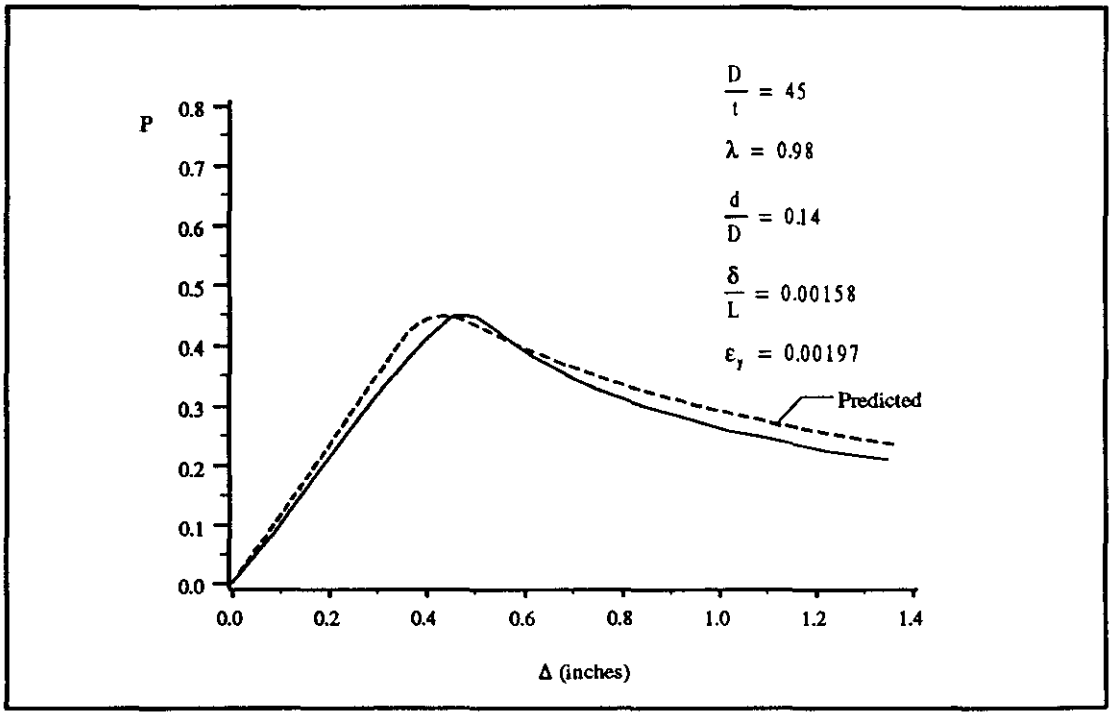

Figure 6.22 Predicted and observed load vs. axial shortening (P2P Ref. 30)

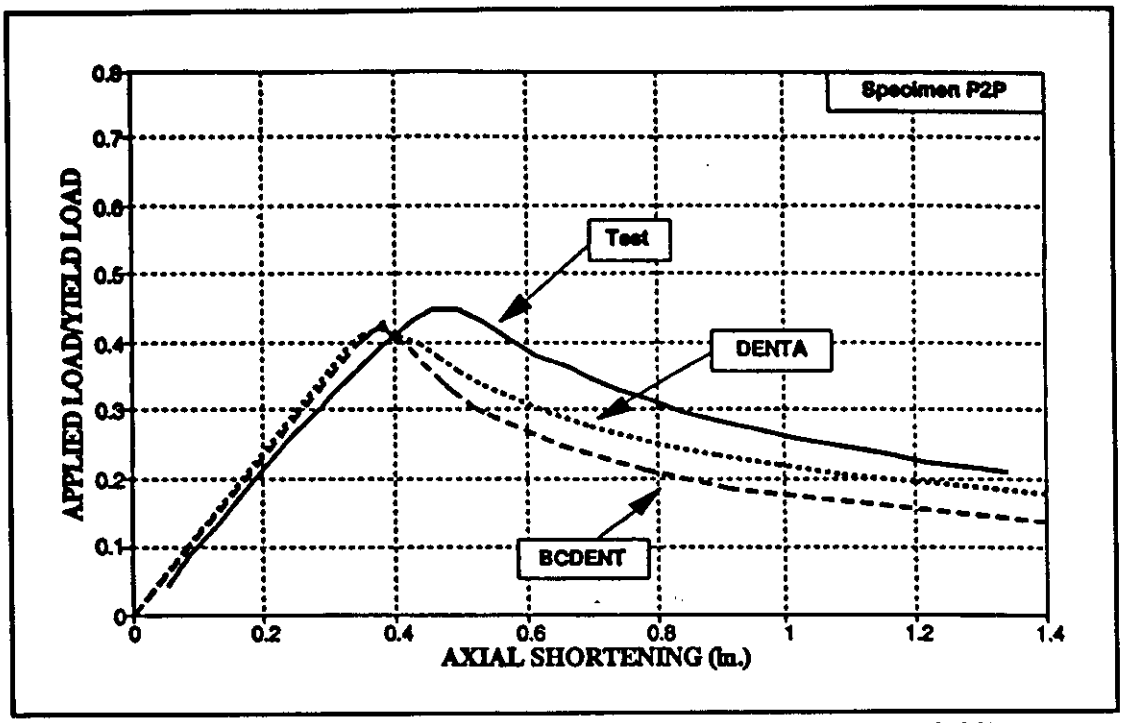

Figure 6.23 Comparison of specimen P2P, BCDENT and DENTA (Ref. 30)

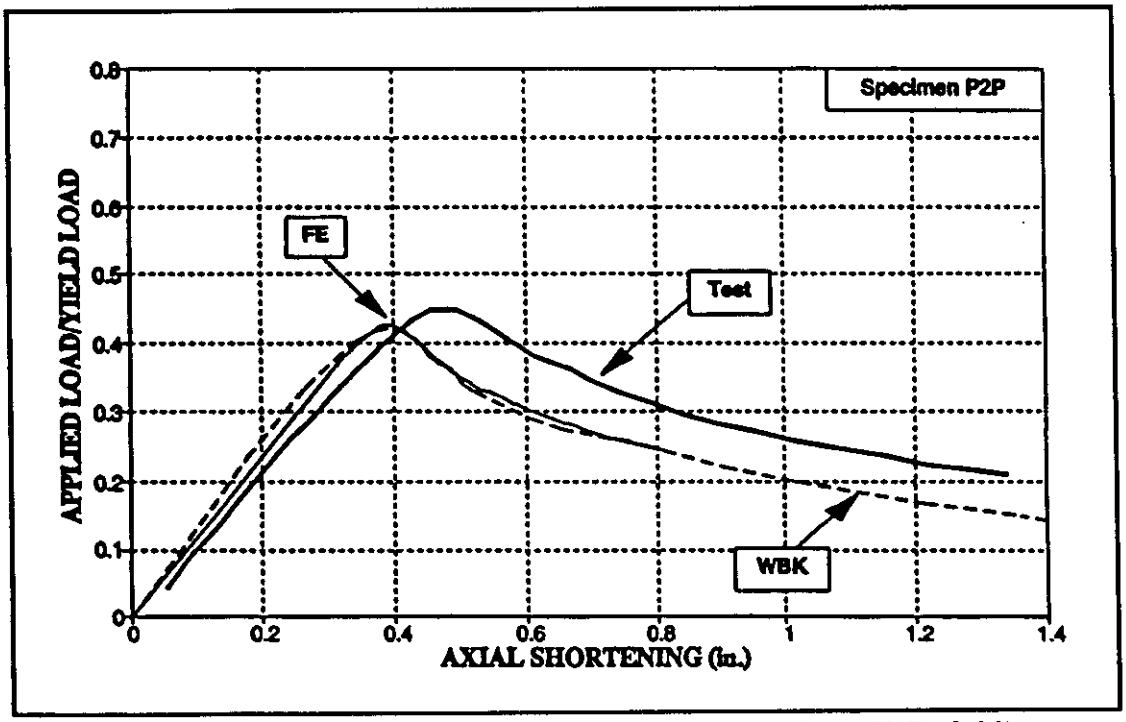

Figure 6.24 Comparison of specimen P2P, finite element and WBK (Ref. 30)

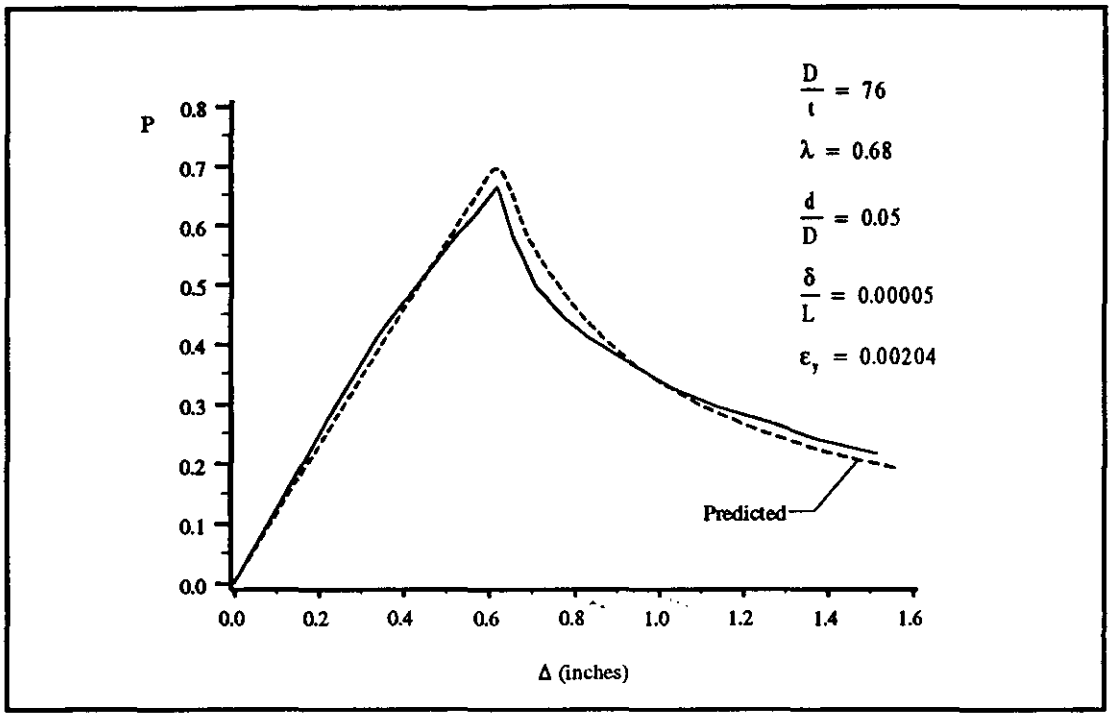

Figure 6.25 Predicted and observed load vs. axial shortening (P3PA Ref. 30)

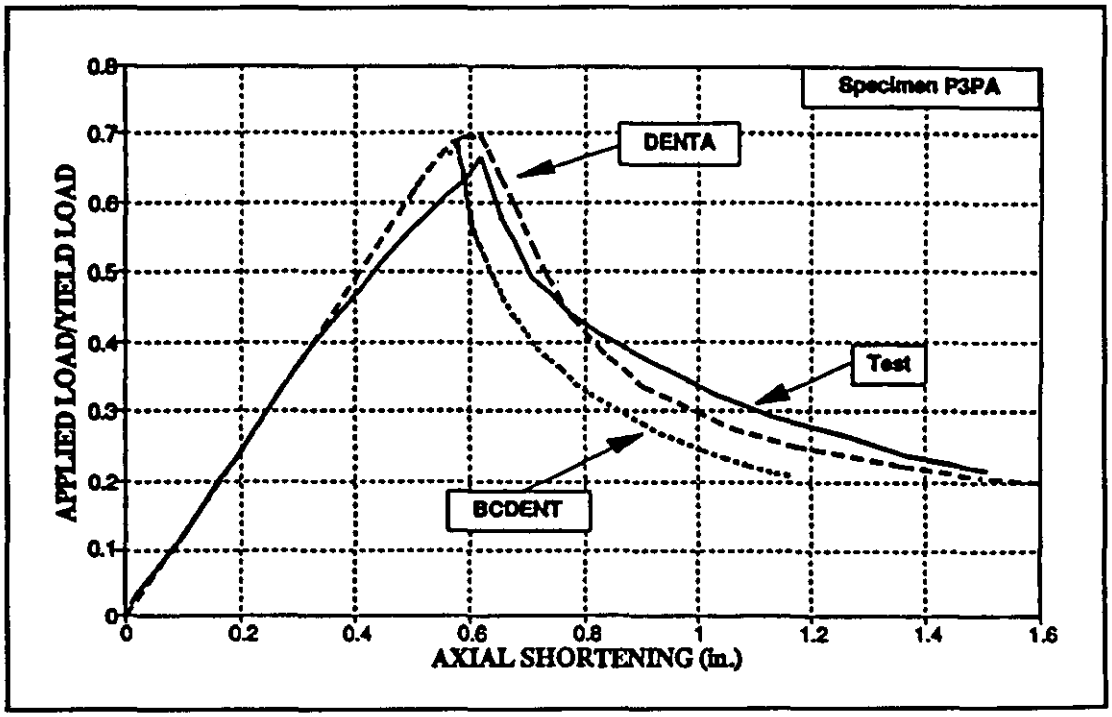

Figure 6.26 Comparison of specimen P3PA, BCDENT and DENTA (Ref. 30)

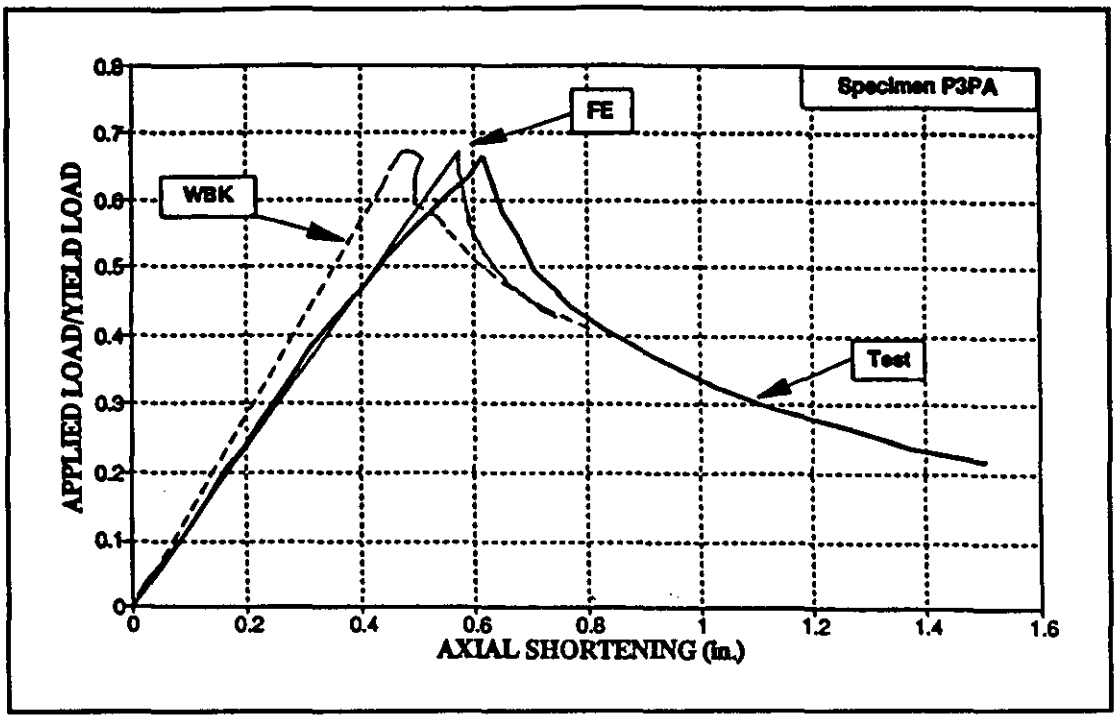

Figure 6.27 Comparison of specimen P3PA, finite element and WBK (Ref. 30)

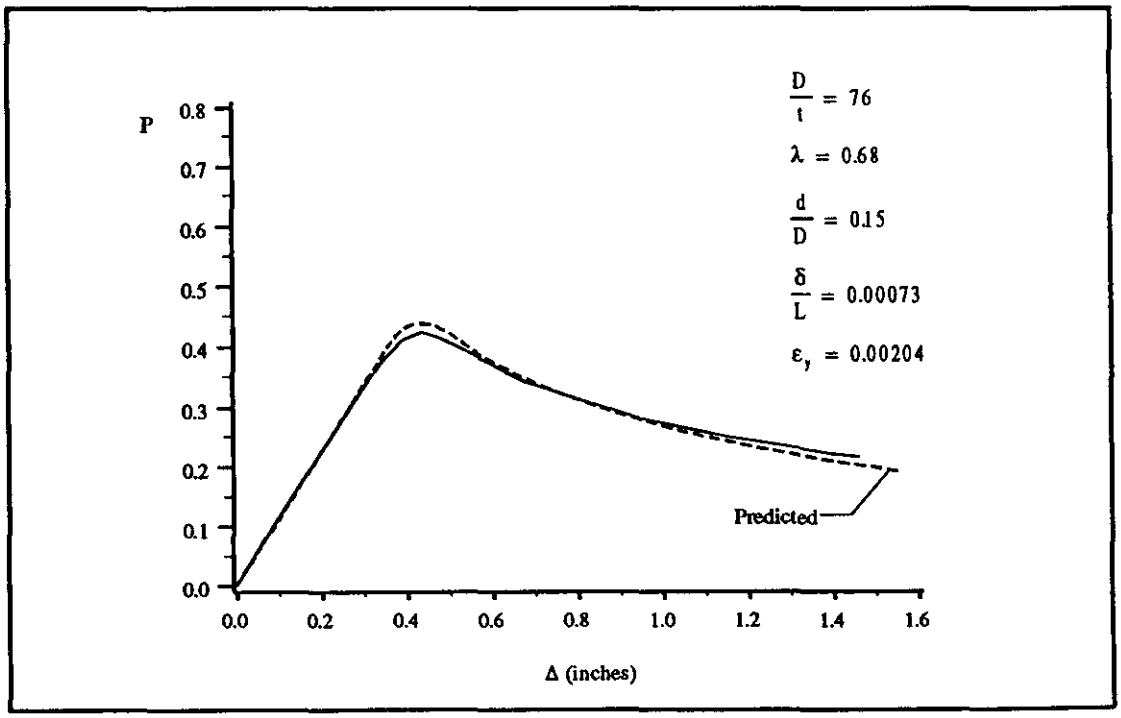

Figure 6.28 Predicted and observed load vs. axial shortening (P3PB Ref. 30)

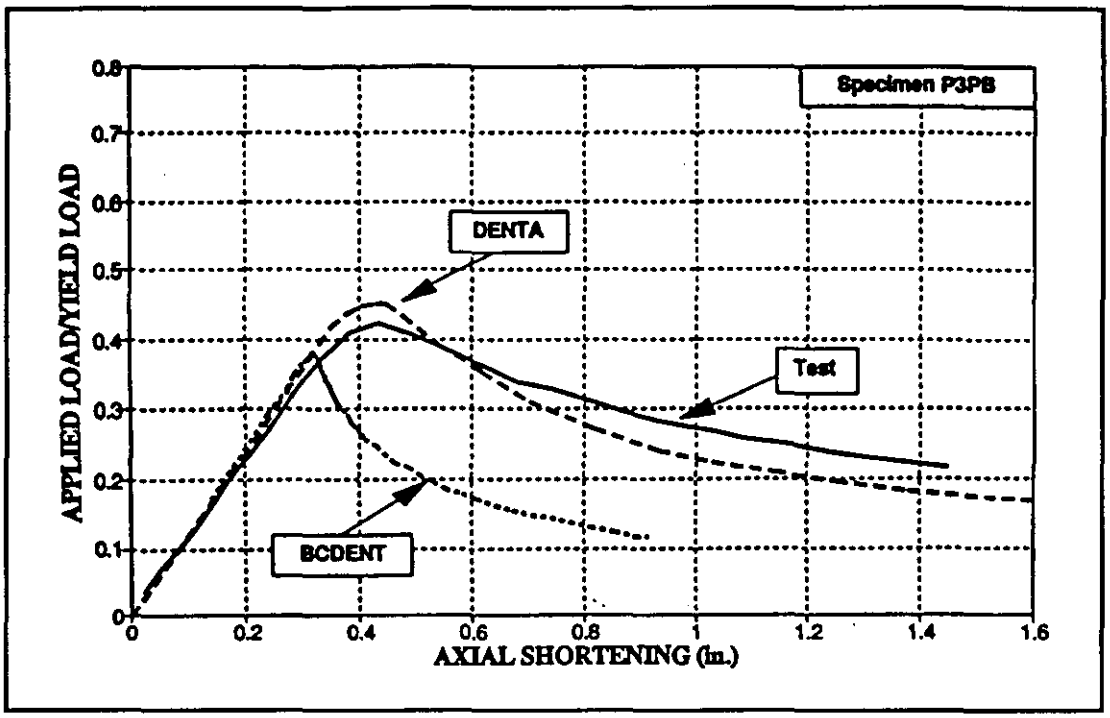

Figure 6.29 Comparison of specimen P3PB, BCDENT and DENTA (Ref. 30).

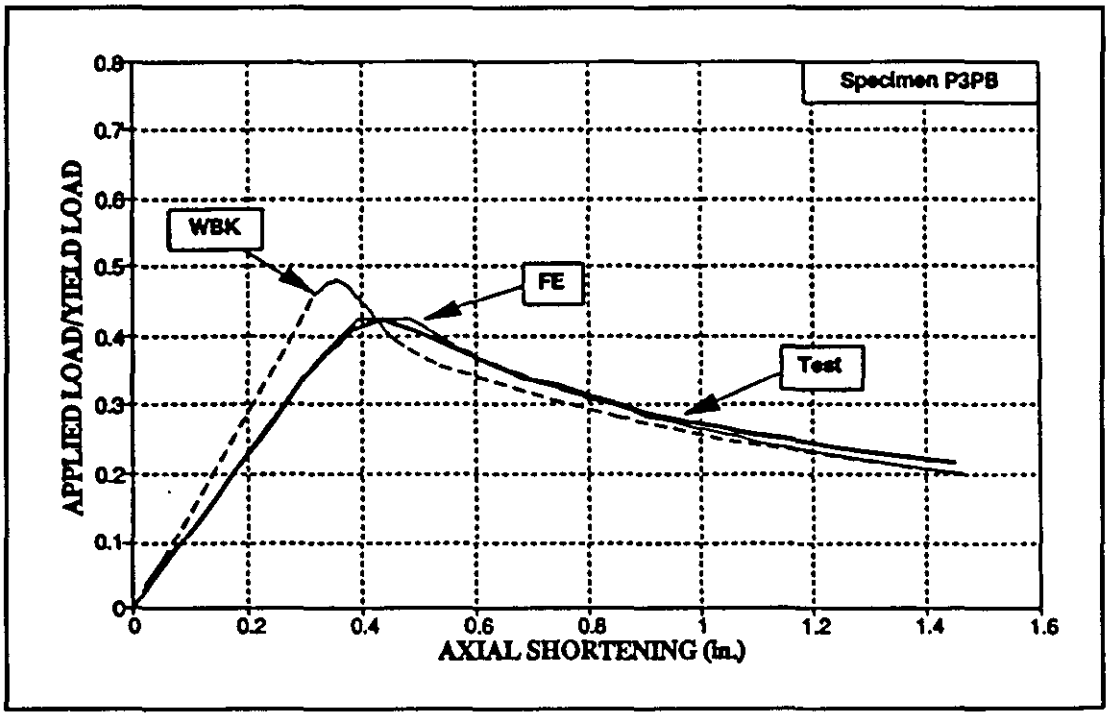

Figure 6.30 Comparison of specimen P3PB, finite element and WBK (Ref. 30).

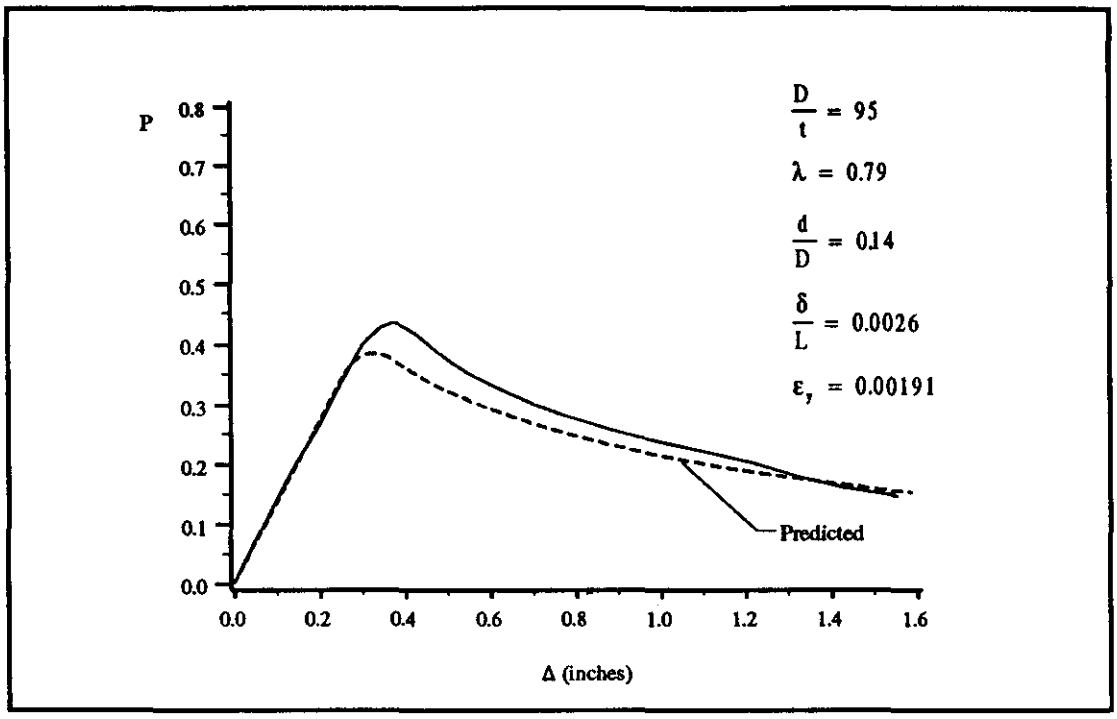

Figure 6.31 Predicted and observed load vs. axial shortening (P4P Ref. 30).

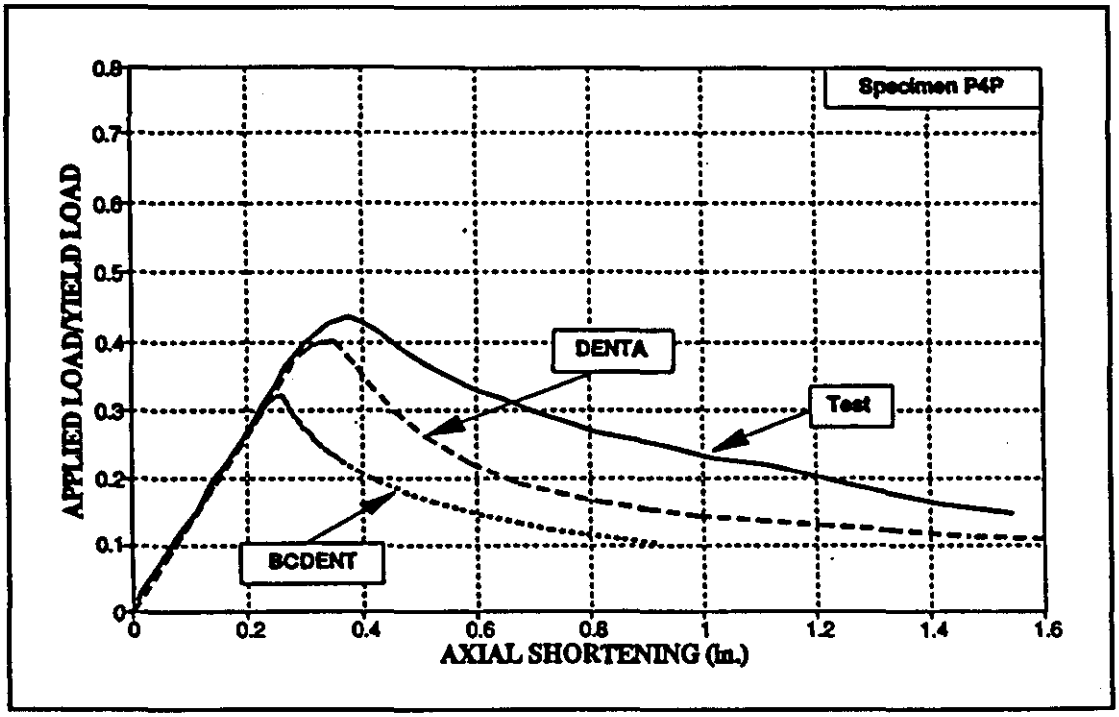

Figure 6.32 Comparison of specimen P4P, BCDENT and DENTA (Ref. 30).

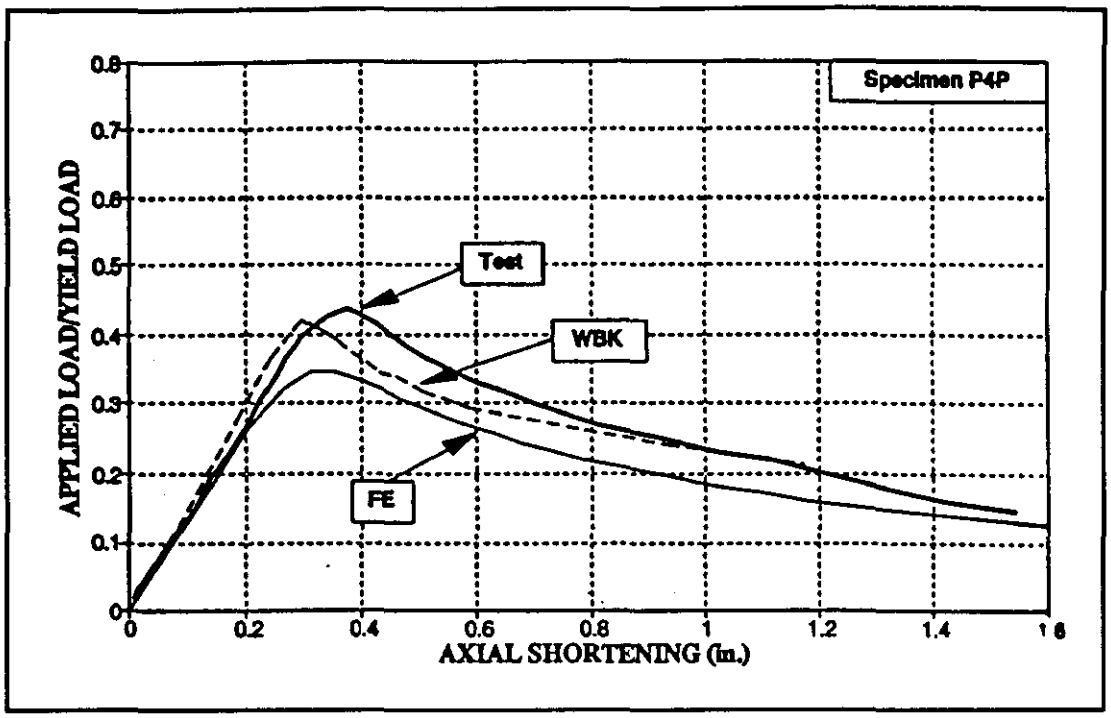

Figure 6.33 Comparison of specimen P4P, finite element and WBK (Ref. 30).

6.4 Application to the Study of Damage Effects

Ultimately, the regression model can be used to predict the load shortening behavior of damaged tubular columns. Because of its formulation and simplicity in use, the procedure can be easily used to examine the influence of the column geometry and damage parameters. Obviously the influence of damage on a given column is of interest.

To illustrate the capability of the procedure and to further illustrate its results, the load-shortening relationships are provided for varying amounts of damage. These are shown for four column geometries based on the four combinations of D/t=30, D/t=60, λ=0.6 and λ=1.2. In Figs.6.34 through 6.37, the influence of dent-depth is illustrated for the four column geometries and an initial out-of-straightness, δ/L=0.005. The primary effect of increasing dent damage is a reduction in the ultimate strength of the column and a gradual reduction in load for a given amount of shortening in the post-ultimate range.

Figures 6.38 through 6.41 illustrate the influence of out-of-straightness on the load-shortening behavior. These examples consist of the four combinations of column geometries listed in the previous paragraph with a dent-depth, d/D=0.15. As shown in these figures, the primary effects of increasing initial out-of-straightness are a reduction in ultimate strength and a reduction in initial stiffness of the column.

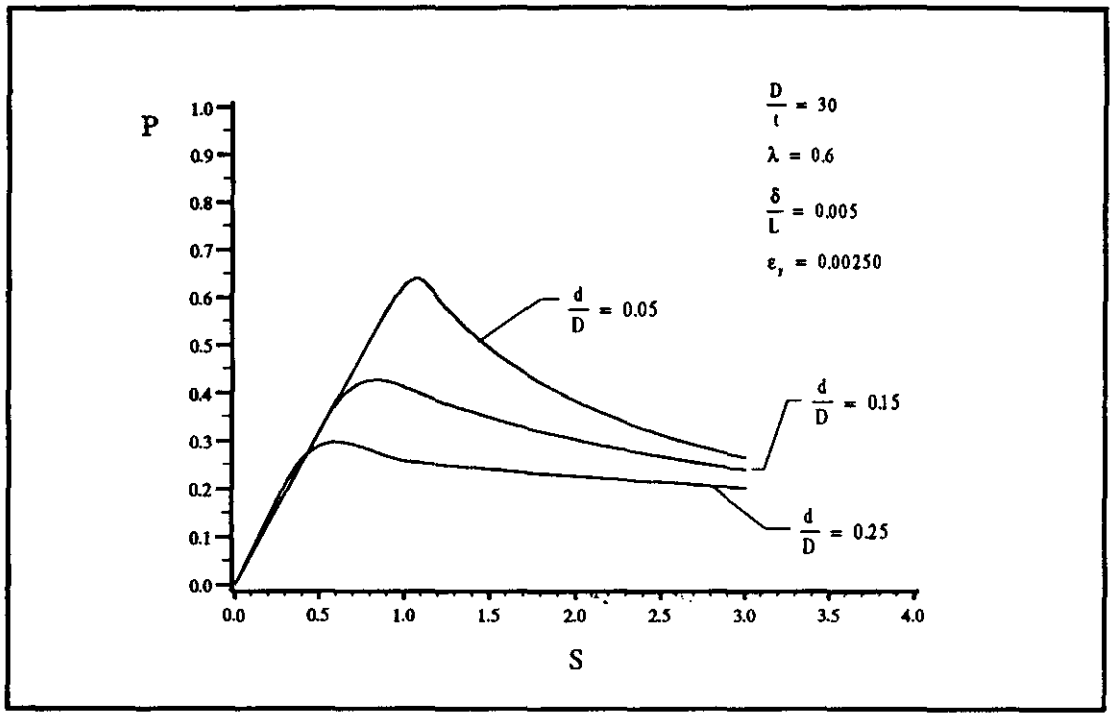

Figure 6.34 Influence of dent-depth for D/t=30 and λ=0.6.

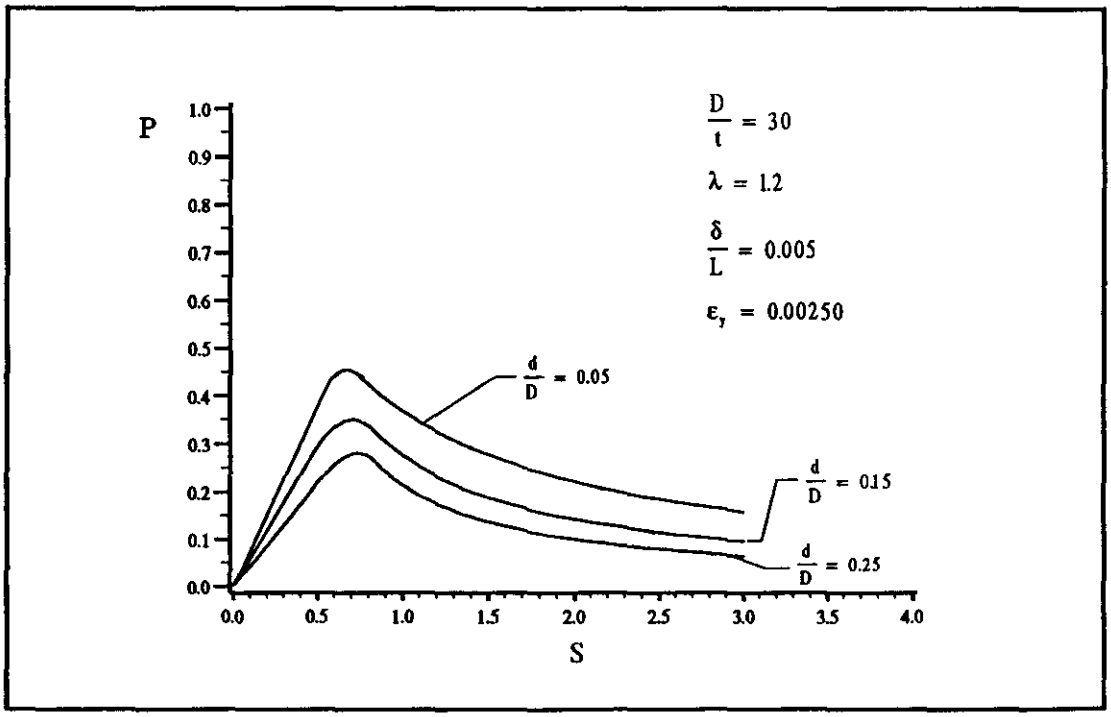

Figure 6.35 Influence of dent-depth for D/t=30 and λ=1.2.

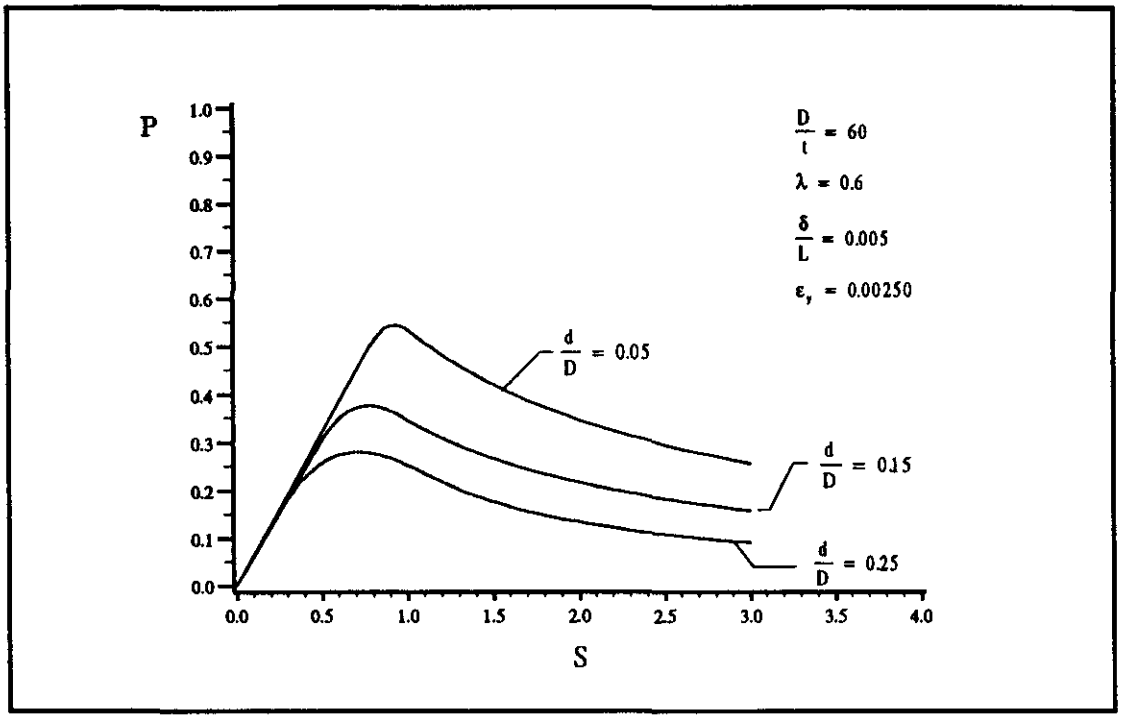

Figure 6.36 Influence of dent-depth for D/t=60 and λ=0.6.

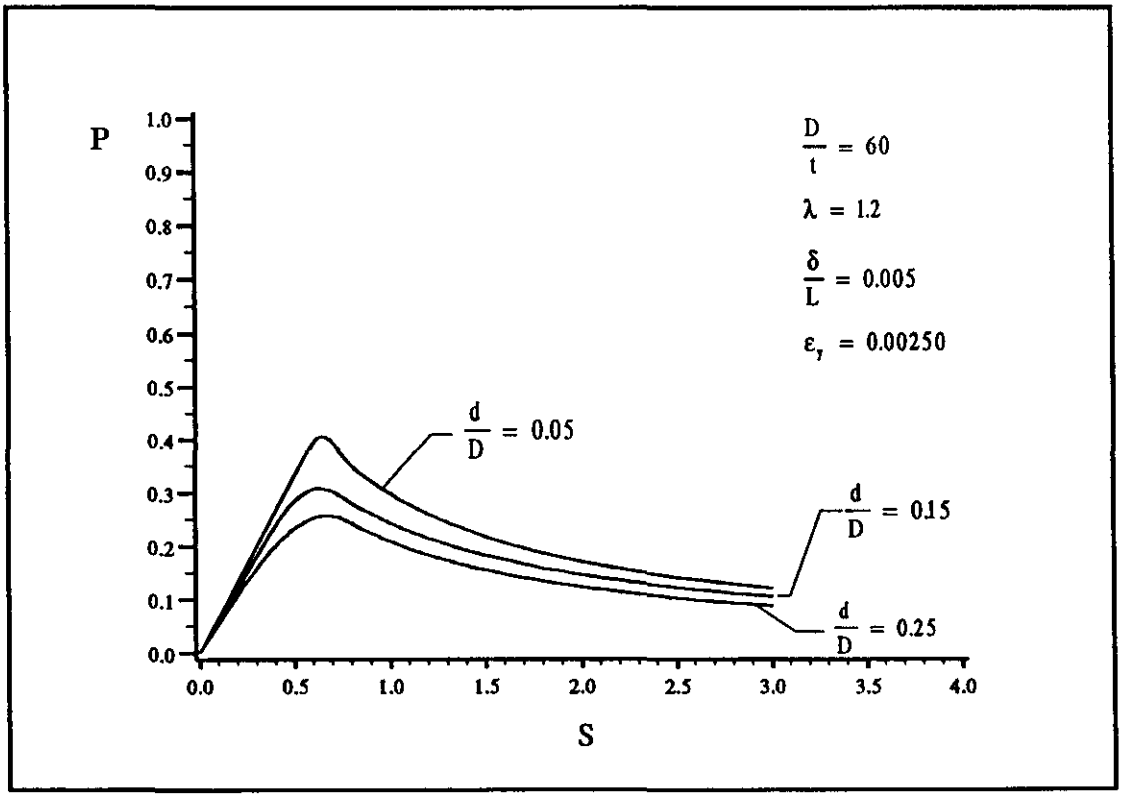

Figure 6.37 Influence of dent-depth for D/t=60 and λ=1.2.

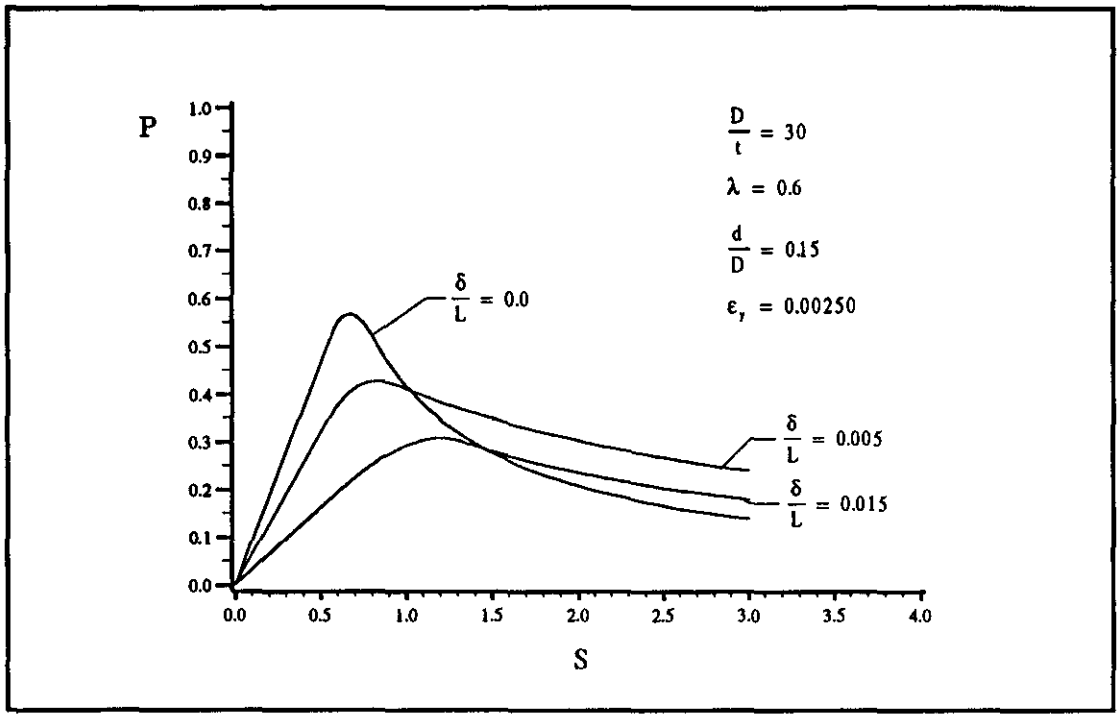

Figure 6.38 Influence of out-of-straightness for D/t=30 and λ=0.6.

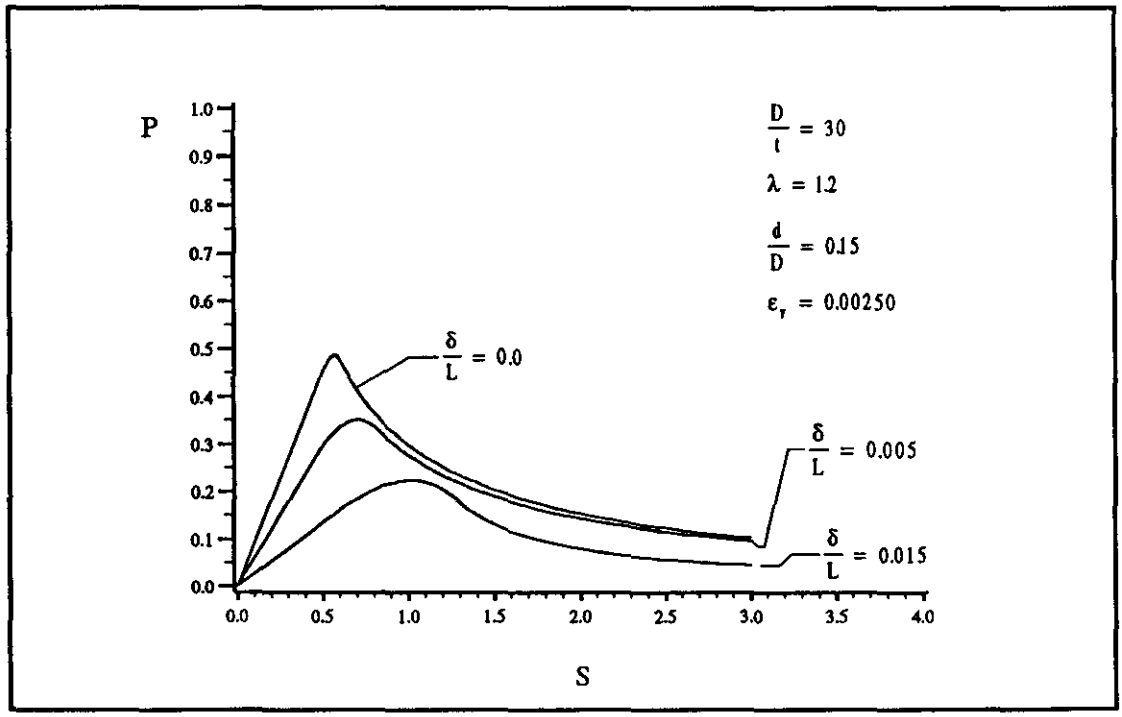

Figure 6.39 Influence of out-of-straightness for D/t=30 and λ=1.2.

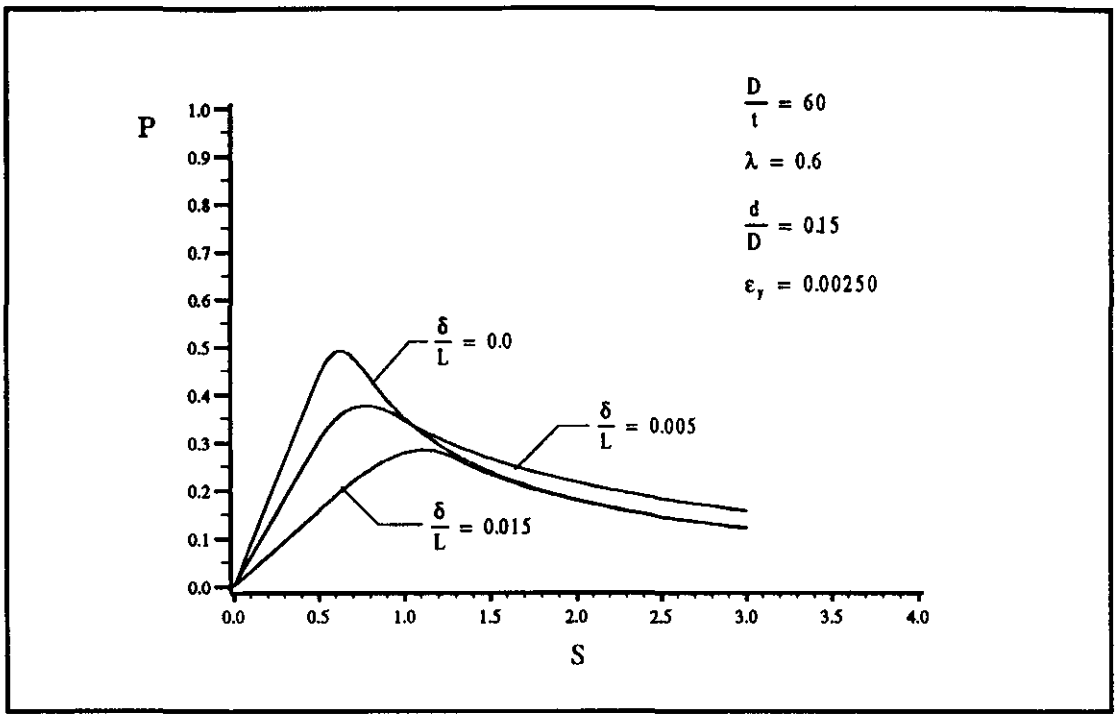

Figure 6.40 Influence of out-of-straightness for D/t=60 and λ=0.6.

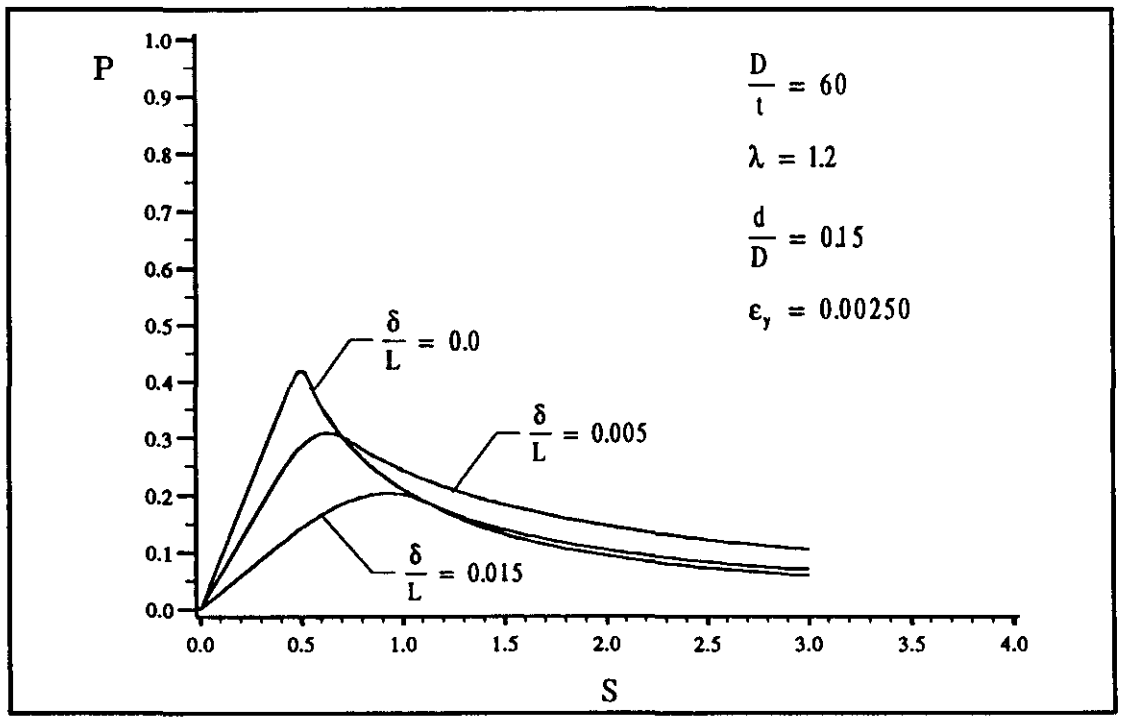

Figure 6.41 Influence of out-of-straightness for D/t=60 and λ=1.2

7 Summary and Conclusions

7.1 Summary

A simplified engineering method was developed to predict the load-shortening response of damaged (dented and crooked), pin-ended, tubular columns. The method is based on a parametric study of column behavior and a regression analysis of data from a finite element analysis and published experimental results. The resulting procedure is a simple numerical relationship describing the load as a function of column geometry, material and damage.

7.1.1 Finite Element Analysis

In order to conduct the parametric study and develop the relationship for axial load as a function of column geometry and damage, 93 column load-shortening curves were generated in addition to the data available in the literature.

The finite element program ADINA was used to generate the load-shortening data since it has capabilities for nonlinear material behavior and suitable shell elements for large-displacement analysis. After considerable experimentation, a discretization

model that took advantage of the double symmetry of the problem was developed. The model had 32 shell elements, 4 beam elements and 268 nodal points (1162 degrees of freedom) and gave reasonably good correlation with the experimental data. The program was then used to generate load-shortening relationships to be included in the database to supplement the curves available from previous experimental research. A total of 93 load-shortening curves were generated from the finite element analysis.

7.1.2 Database of Damaged Column Behavior

All experimental data available in published literature on the axial behavior of dented and crooked tubular members under concentrically applied axial load was collected and put into a database (Total of 37 curves). Information for each specimen covers the following items: Source, identification, data on material, geometry, location and amount of damage, and the load vs. axial shortening relationship described by a series of discrete coordinate pairs. Computer generated results were used to fill in and supplement the experimental data mainly to cover sparsely populated ranges of parameters. The data can be readily retrieved, manipulated and analyzed with the SAS software selected for this purpose.

7.1.3 Parametric Study

The axial load, nondimensionalized with respect to the yield or squash load, was defined as a function of five parameters; D/t, λ (slenderness), d/D (relative dent-depth), δ/L (out-of-straightness), and S (average axial strain divided by yield strain).

The relationships between the axial load and each of these parameters were studied to find a simple yet accurate expression to approximate the relationship.

7.1.4 Development and Application of the Procedure

The procedure was based on a nonlinear piecewise regression analysis. This approach consists of segmentation of the characteristic shape of load-shortening relationships observed for tubular columns. Once the load-shortening relationship was described by three segments, the effect of column geometry and damage were established. The numerical procedure is then based on a regression model incorporating column geometry and damage parameters.

The procedure developed here allows a rapid computation of the load-shortening relationship for a given column geometry and damage. The method employs a set of 80 constants and can be easily programmed requiring only minimal computational resources such as a programmable calculator or a spreadsheet program. The resultant relationship which covers the elastic pre-ultimate, ultimate and post-ultimate ranges, can be used for practical application within the ranges of parameters specified..

Obviously, the procedure can be used to predict damaged column behavior and to observe the effects of varying amounts of damage or variations of other column parameters. Because the procedure provides a complete load-shortening response, it can be used as a subroutine/subprogram in a structural analysis of framed structures containing damaged members.

7.2 Conclusions

The method presented here provides a simple procedure that reasonably predicts the complete load-shortening response of pin-ended damaged tubular columns. The accuracy of the model based on comparison to experimental data is comparable or better than other more complex, approximate methods. This procedure has the advantage of not requiring any specialized program or computer. It can be readily incorporated into a portable/handheld or other type of computer.

The primary limitation of the method is its restriction to pin-ended columns. This limitation is not shared by some other methods [15, 10]. With additional work, the current procedure could be expanded to include end effects.

7.3 Recommendations for Future Work

The solution to the problem of damaged and deteriorated member behavior as it relates to offshore structures is far from complete. Additional work related to the proposed method should include incorporation of end effects, a study of the influence of dents significant distance away from mid-length of the column. Further work is needed to quantify the effects of other types of damage including corrosion and fatigue cracking. Ultimately, there is a need for procedures to account for damaged member behavior including dent-damage, out-of-straightness, corrosion and fatigue considering the complete three dimensional beam-column.

Nomenclature

A	Column matrix of regression coefficients
B	Matrix of regressors evaluated for each data point
D	Diameter of tubular member
d	Dent-depth
E	Modulus of elasticity
e	Error function for regression, sum of squares of the error
F	Column matrix of values of dependent variable
f	Individual values of dependent variable (an element of F)
f	Approximating function
G	Coordinate function matrix
g	Individual term of coordinate function (an element of G)
i	Index for number of data points
j	Index for number of regressors

k	Index for number of independent variables
L	Length of column
l_d	Length of dent
l	Total number of data points
m	Total number of regressors
n	Total number of independent variables
P	Axial load nondimensionalized with respect to the yield load
P_{ult}	Ultimate nondimensionalized axial load
Q	Row matrix of regressors
Q_C	Row matrix of regressors consolidated into coefficients of the set of retained regressors
Q_R	Row matrix of regressors retained as variables in the consolidation of the model
q	Individual regressor (an element of Q)
R	Radius of tubular member
r	Radius of gyration of cross section
S	Axial shortening nondimensionalized with respect to $\epsilon_y \cdot L$

S_I Abscissa of inflection point in the load-shortening curve

S_{IL} Distance between S_L and S_I

S_L Abscissa of the point defining the end of the linear portion of the load-shortening curve

S_{ult} Value of nondimensionalized axial shortening at which the ultimate load occurs

t Thickness of tube wall

α_1 Parameter used in calculating S_{ult}, defined in Eq. 6.12

α_2 Parameter used in calculating S_{ult}, defined in Eq. 6.12

γ Coordinate function expressed as a linear combination of the elements of G

Δ Axial shortening

δ Initial out-of-straightness

ϵ Residual or error in approximation to a data point

ϵ_y Material yield strain

λ Column slenderness defined by $\frac{L}{\pi r}\sqrt{\varepsilon_y}$

σ_y Material yield stress

References

[1] Moan, T.J., *Advances in the Design of Offshore Structures for Damage-Tolerance*, In *Advances in Marine Structures*, Smith, C.S. and Clarke, J.D. (editors), Elsevier Applied Science, London and New York, 1986, Proceedings of an International Conference held at the Admiralty Research Establishment, Dumferline, 20-23 May 1986.

[2] Smith, C.S., Kirkwood, W. and Swan, J.W., *Residual Strength and Stiffness of Damaged Steel Bracing Members*, In *Proceedings of the Second International Conference on the Behavior of Off-Shore Structures*, Stephens, H.S (editor), BHRA Fluid Engineering, London, England, 1979.

[3] Smith, C.S., *Assessment of Damage in Offshore Steel Platforms*, In *Proceedings of International Conference on Marine Safety*, Glasgow, England, 1983.

[4] Taby, J. and Rashed, S.M.H., *Experimental Investigation of the Behaviour of Damaged Tubular Members*, Technical Report MK/R93, Department of Naval Architecture and Marine Engineering, The Norwegian Institute of Technology, Trondheim, Norway, 1980.

[5] Taby, J., Moan, T. and Rashed, S.M.H., *Theoretical and Experimental Study of the Behaviour of Damaged Tubular Members in Offshore Structures*, Norwegian Maritime Research 9(2):26-33, 1981.

[6] Taby, J. and Moan, T., *Collapse and Residual Strength of Damaged Tubular Members*, Behavior of Offshore Structures, Elsevier Science Publishers B.V., Amsterdam, 1985.

[7] Taby, J., *Experiments with Damaged Tubulars*, Technical Report 6.07, SINTEF, Norwegian Institute of Technology, Trondheim, Norway, October, 1986.

[8] Taby, J., *Residual Strength of Damaged Tubulars*, Final Report 6.10, SINTEF, Norwegian Institute of Technology, Trondheim, Norway, October,

1986.

[9] Taby, J., *DENTA User's Manual (VAX Version)*, Technical Report MK/R 93/86, Department of Marine Technology, The Norwegian Institute of Technology, Trondheim, Norway, November, 1986.

[10] Taby, J., *DENTA II -- User's Manual (VAX - version 1.01)*, Department of Marine Technology, The Norwegian Institute of Technology, The University of Trondheim, March 1988.

[11] van Aanhold, J.E. and Taby, J., *Analysis of Structures with Damaged Structural Members*, Det Norske Veritas Research Division, Offshore Technology Testing and Research Report No. STF A83002, Trondheim, Norway, October, 1983. (Available from National Technical Information Service, Springfield, VA 22161)

[12] Ellinas, C.P., *Ultimate Strength of Damaged Tubular Bracing Members*, Journal of Structural Engineering, ASCE, 110(2):245-259, February, 1984.

[13] Smith, C.S., Sommerville, W.L. and Swan, J.W., *Residual Strength and Stiffness of Damaged Steel Bracing Members*, In Proceedings of the 13th Offshore Technology Conference, Offshore Technology Conference, Houston, May, 1981, (Paper OTC 3981).

[14] Richards, D.M. and Andronicou, A., *Residual Strength of Dented Tubulars: Impact Energy Correlation*, Journal of Energy Resources Technology, December, 1985.

[15] Kim, W., *Behavior and Strength of Damaged Tubular Columns with End Restraints*, Ph.D. Dissertation, Lehigh University, September, 1992.

[16] Ricles, J., Gillum, T. and Lamport, W., *Grout Repair of Dented Offshore Tubular Bracing - Experimental Behavior*, J. of Structural Engineering, ASCE, 1120(7), 1994.

[17] Ricles, J. and Gillum, T., *Grout Repair of Dent-Damaged Steel Marine Tubulars*, J. of Waterway, Port, Coastal and Ocean Engineering, ASCE, 122(3), May/June, 1996.

[18] Ostapenko, A. and Surahman, A., *Structural Element Models for Hull Strength Analysis*, Fritz Engineering Laboratory Report No. 480.6, Lehigh University, Bethlehem, PA, September, 1982.

[19] Ostapenko, A., *Computational Model for Load-Shortening of Plates*, Proceedings of the Structural Stability Research Council, Structural Stability

Research Council, 1985.

[20] Padula, J.A. and Ostapenko, A., *Indentation Behavior of Tubular Members*, Fritz Engineering Laboratory Report No. 508.8, Lehigh University, Bethlehem, PA, June, 1988.

[21] Timoshenko, S. and Woinowsky-Krieger, S., *Theory of Plates and Shells*, Second Edition, McGraw-Hill, New York, 1959.

[22] Wierzbicki, T. and Suh, M.S., *Denting Analysis of Tubes Under Combined Loading*, Technical Report MITSG 86-5, MIT Sea Grant College Program, Massachusetts Institute of Technology, Cambridge, MA, March, 1986

[23] Searle, S.R., *Matrix Algebra Useful for Statistics*, 1982, John Wiley and Sons, New York, NY.

[24] Padula, J.A. and Ostapenko, A., *Axial Behavior of Damaged Tubular Columns*, Fritz Engineering Lab Report No. 508.11, Lehigh University, Bethlehem, PA, September 1989.

[25] Padula, J.A. and Ostapenko, A., *Load-Shortening Behavior of Damaged Tubular Columns*, Paper 6382, Proceedings of the 1990 Offshore Technology Conference. Houston, TX, May, 1990.

[26] SAS Institute Inc., SAS/STAT User's Guide, Version 6, Fourth Edition, Volume 2, SAS Institute Inc., Cary, NC, 1989.

[27] Goodnight, J. H., *A Tutorial on the SWEEP Operatror, The American Statistician, 33, 1979.*

[28] Draper, N.R. and Smith, H., *Applied Regression Analysis*, 2nd Edition, John Wiley and Sons, New York, NY, 1981.

[29] Duan, L., Loh, J.T. and Chen, W.F., *Analysis of Dented Tubular Members Using Moment Curvature Approach*, Exxon Report 1992.

[30] Ostapenko, A., Wood, B. A., Chowdhury, A. and Hebor, M. F., *Residual Strength of Damaged and Deteriorated Tubular Members in Offshore Structures*, ATLSS Report No. 93-03, Lehigh University, Bethlehem, PA, January, 1993.

Appendix A. Column Geometry, Material and Damage Parameters

The nondimensional geometry, material and damage parameters from the columns included in the database are shown in Table A.1.

Table A.1 Geometry, material and damage parameters for columns in the database

D/t	d/D	δ/L	λ	ϵ_y
20	0.100	0.0000	0.80	0.00125
20	0.200	0.0000	0.80	0.00125
25	0.050	0.0020	0.80	0.00125
25	0.150	0.0020	0.80	0.00125
25	0.250	0.0020	0.80	0.00125
25	0.050	0.0030	0.80	0.00125
25	0.050	0.0040	0.80	0.00125
25	0.050	0.0060	0.80	0.00125
25	0.050	0.0200	0.40	0.00250
25	0.250	0.0200	0.40	0.00250
25	0.050	0.0200	0.40	0.00125
25	0.300	0.0200	0.40	0.00125
25	0.050	0.0200	0.80	0.00250
25	0.200	0.0200	0.40	0.00250
25	0.050	0.0200	1.19	0.00250
25	0.050	0.0200	0.80	0.00125
25	0.200	0.0200	0.80	0.00125
25	0.050	0.0200	1.19	0.00125

25	0.100	0.0020	0.40	0.00125
25	0.100	0.0020	1.19	0.00250
26	0.142	0.0009	0.92	0.00240
26	0.147	0.0028	0.92	0.00240
26	0.138	0.0014	0.92	0.00240
27	0.107	0.0011	1.10	0.00238
27	0.143	0.0021	0.92	0.00238
29	0.154	0.0027	1.10	0.00187
29	0.000	0.0050	1.04	0.00109
29	0.048	0.0055	1.06	0.00113
30	0.000	0.0032	0.83	0.00140
30	0.050	0.0100	0.94	0.00175
30	0.100	0.0100	0.94	0.00175
30	0.000	0.0034	0.84	0.00142
31	0.156	0.0008	0.87	0.00152
40	0.050	0.0000	0.80	0.00125
40	0.100	0.0000	0.80	0.00125
40	0.200	0.0000	0.80	0.00125
40	0.300	0.0000	0.80	0.00125
40	0.150	0.0000	0.80	0.00125
40	0.100	0.0000	0.40	0.00125
40	0.200	0.0000	0.40	0.00125
40	0.100	0.0000	0.80	0.00125
40	0.200	0.0000	0.80	0.00125
40	0.050	0.0000	1.19	0.00125
40	0.100	0.0000	1.19	0.00125
40	0.200	0.0000	1.19	0.00125
40	0.100	0.0000	0.80	0.00125
40	0.200	0.0000	0.80	0.00125
40	0.100	0.0000	0.80	0.00125
40	0.200	0.0000	0.80	0.00125
40	0.100	0.0000	0.40	0.00125
40	0.200	0.0000	0.40	0.00125
40	0.100	0.0000	1.59	0.00125
40	0.200	0.0000	1.59	0.00125
40	0.100	0.0000	0.53	0.00225
40	0.200	0.0000	0.53	0.00225
40	0.100	0.0000	0.47	0.00175

40	0.050	0.0200	1.19	0.00125
40	0.050	0.0100	0.80	0.00125
40	0.100	0.0100	0.80	0.00125
40	0.050	0.0100	0.40	0.00125
40	0.200	0.0100	0.40	0.00125
40	0.050	0.0200	1.19	0.00250
40	0.200	0.0200	1.19	0.00250
40	0.100	0.0100	0.80	0.00250
40	0.050	0.0100	0.40	0.00250
40	0.200	0.0100	0.40	0.00250
40	0.128	0.0018	0.67	0.00146
40	0.128	0.0018	0.67	0.00146
41	0.102	0.0018	0.62	0.00232
41	0.127	0.0050	0.68	0.00137
42	0.100	0.0025	0.80	0.00250
45	0.082	0.0050	0.87	0.00122
45	0.082	0.0050	0.78	0.00099
45	0.096	0.0019	0.93	0.00175
45	0.139	0.0016	0.98	0.00197
45	0.096	0.0019	0.94	0.00177
45	0.181	0.0010	0.91	0.00167
45	0.094	0.0013	0.45	0.00167
45	0.122	0.0020	0.45	0.00167
46	0.094	0.0010	0.47	0.00175
46	0.011	0.0050	0.79	0.00100
46	0.092	0.0019	0.94	0.00177
46	0.094	0.0005	0.91	0.00167
46	0.181	0.0037	0.94	0.00177
51	0.020	0.0005	0.72	0.00129
58	0.016	0.0005	0.69	0.00126
58	0.034	0.0004	0.66	0.00116
60	0.100	0.0000	0.80	0.00125
60	0.200	0.0000	0.80	0.00125
60	0.051	0.0007	0.90	0.00125
60	0.100	0.0025	0.80	0.00125
60	0.100	0.0050	0.80	0.00125
60	0.100	0.0025	0.80	0.00250
60	0.051	0.0007	0.90	0.00125

60	0.051	0.0007	0.82	0.00102
76	0.051	0.0000	0.68	0.00204
76	0.149	0.0007	0.68	0.00204
78	0.048	0.0007	0.64	0.00175
78	0.150	0.0007	0.64	0.00175
78	0.048	0.0007	0.67	0.00192
80	0.050	0.0000	0.80	0.00125
80	0.100	0.0000	0.80	0.00125
80	0.150	0.0000	0.80	0.00125
80	0.200	0.0000	0.80	0.00125
80	0.300	0.0000	0.80	0.00125
80	0.100	0.0000	1.19	0.00125
80	0.200	0.0000	1.19	0.00125
80	0.100	0.0000	0.40	0.00125
80	0.200	0.0000	0.40	0.00125
80	0.200	0.0000	0.94	0.00175
80	0.200	0.0000	1.13	0.00250
80	0.050	0.0200	1.19	0.00250
80	0.200	0.0200	1.19	0.00250
80	0.050	0.0200	0.80	0.00250
80	0.200	0.0200	0.80	0.00250
80	0.050	0.0200	0.40	0.00250
80	0.200	0.0200	0.40	0.00250
80	0.050	0.0200	0.40	0.00125
80	0.200	0.0200	0.40	0.00125
85	0.022	0.0010	1.06	0.00238
86	0.037	0.0003	1.05	0.00234
88	0.077	0.0008	0.65	0.00148
91	0.141	0.0024	0.65	0.00148
95	0.138	0.0026	0.79	0.00191
99	0.115	0.0009	0.72	0.00156
100	0.115	0.0010	0.76	0.00175
100	0.100	0.0000	0.40	0.00125
100	0.100	0.0000	0.80	0.00125
100	0.100	0.0000	1.19	0.00125
121	0.095	0.0010	0.63	0.00175

Vita

Joseph A. Padula was born on March 8, 1955 in San Diego, California. He is the son of Helen A. and Joseph A. Padula. Having attended several elementary schools in various parts of the United States, Mr. Padula graduated from Lake Taylor Senior High School in Norfolk, Virginia in 1971. A Bachelor's Degree in civil engineering from Old Dominion University was awarded to Mr. Padula in 1985. A Master of Science degree in civil engineering from Lehigh University was awarded in 1987.

Mr. Padula is currently employed as a research civil engineer at the U.S. Army Engineer Waterways Experiment Station, Information Technology Laboratory in Vicksburg, Mississippi. He has also held positions with construction contractors and a consulting engineering firm.